Modulation of lymphatic function during sepsis

Uzma Reem

**This thesis is submitted for the degree of
Doctor of Philosophy**

Department of Cardiovascular Science

University of Sheffield

October 2015

بسم الله الرحمن الرحيم

In the loving memory of a most special person in my life,

my grandma

Acknowledgement

Abstract

Rationale & Hypothesis: Lymphatic vessel function becomes impaired during sepsis; with stagnation of lymphatic flow and dysfunction of the mechanisms regulating contractility, which contribute to tissue oedema. Angiopoietin-1 (Ang-1) is a growth hormone that regulates vascular permeability via Tie-2 and is known to have anti-inflammatory effects on the blood vasculature, however, any effects on lymphatics have not yet been characterised. We hypothesised that inflammatory mediators released during sepsis compromise lymphatic function which is improved by Ang-1.

Methodology: Mesenteric collecting lymphatics (80-200 μm) were dissected from male Sprague Dawley rats (150-200g) and mounted on a pressurised myograph system at 3cm H_2O. Responses to inflammatory stimuli were measured up to 2.5h following exposure to LPS (50 μg/ml), TNF-α (10-500ng/ml) and IL-1β (10-100ng/ml). Role of NO in mediating effects of TNF-α was assessed by measuring contractility of TNF-α treated vessels in the presence of L-NAME (1mM). To determine the effects of Ang-1 on vessel function, changes in spontaneous contractions were measured for 2.5h in response to 250 ng/ml recombinant human Ang-1 in the absence and presence of 10ng/ml TNF-α.

Findings & Conclusions: There was minimal change in frequency of contractions from baseline at the end of 2.5h with Ang-1 alone (1.33±0.66) and in combination with TNF-α (0.66±1.76) compared to the reduced contractions induced by TNF-α alone (-9±1.87), suggesting a protective effect of Ang-1. Ang-1 alone slightly decreased amplitude (10±16%) with minimal change in combination with TNF-α (2±5%) compared to increased amplitude induced by TNF-α alone (15±23%). TNF-α did not alter frequency in presence of L-NAME, suggesting that effects may be NO mediated. Ang-1 does not alter spontaneous contractions but improves contraction frequency and amplitude in inflamed lymphatic vessels. Our study elucidates the effects of potent inflammatory mediators on lymphatic vessel function and demonstrates a protective role of Ang-1 in vessel function during sepsis.

Publications arising from this work

Reem U, Zawieja D, Brown NJ, Kammerer R, Brookes ZLS (2009). Lipolysaccharide reduces the function of mesenteric lymphatic vessels, *Winter Scientific Meeting of Anaesthetic Research Society.*

Reem U, Zawieja D, Brown NJ, Kammerer R, Brookes ZLS (2010). Lipolysaccharide alters the function of rat mesenteric lymphatic vessels. *Microcirculation (Abstracts of 60th meeting of BMS)* 17(6): 458-493. (Oral presentation)

Reem U, Zawieja D, Brown NJ, Kammerer R, Brookes ZLS, Hellewell PG (2010). Lipolysaccharide alters the function of rat mesenteric lymphatic vessels, *The Medical School 6th Annual Research Meeting.* (Poster presentation)

Reem U, Brown NJ, Hellewell PG (2012). Investigation into the effects of nitric oxide and TNF-α on lymphatic vessel function, *The Medical School 8th Annual Research Meeting.* (Poster presentation)

Reem U, Brown NJ, Hellewell PG (2012). Effects of nitric oxide and TNF-α on lymphatic vessel function. *Microcirculation (Abstracts of the 2nd joint meeting of the BMS and AMS 62nd meeting of the BMS)* 20(1): 58. (Oral presentation)

Reem U, Hellewell PG, Brown NJ (2013). Effects of angiopoietin-1 on lymphatic vessel function. *Microcirculation (Abstracts of BMS Young Investigator Symposium)* 20(6): 565-578. (Poster presentation)

Reem U, Brown NJ, Hellewell PG (2013). Effects of angiopoietin-1 on lymphatic vessel function, *The Medical School 9th Annual Research Meeting.* (Poster presentation)

Abbreviations

ABIN-2	A20 Binding Inhibitor of NF-kB Activation-2
Ach	Acetylcholine
AJs	Adherens Junctions
Ang	Angiopoietin
AOI	Area of Interest
APC	Antigen Presenting Cell
APSS	Albumin-physiological salt solution
BSA	Bovine albumin serum
CGRP	Calcitonin Gene Related Peptide
COMP.Ang-1	Cartilage Oligomeric Matrix Protein Ang-1
COX	Cyclo-Oxygenase
DAMPs	Damage-Associated Molecular Patterns
DCs	Dendritic Cells
DIC	Disseminated Intravascular Coagulation
DPBS	Dulbecco's Phosphate Buffered Saline
DMEM-F12	Dulbecco's Modified Eagle Medium F12
ECM	Extra Cellular Matrix
ECs	Endothelial Cells
EDD	End diastolic diameter
ESD	End systolic diameter
NO	Nitric Oxide
ERK	Extra-cellular Signal Regulated Kinase

ESAM	Endothelial cell-Selective Adhesion Molecule
FITC	Fluorescein Isothiocyanate
HR.Ang-1	Human Recombinant Ang-1
ICAM-1	Inter-Cellular Adhesion Molecule-1
IKK	Iκb Kinase
IL	Interleukin
IRAK-1	IL-1 Receptor Associated Kinase-1
TRAF6	TNF receptor-aasociated factor 6
JAM	Junctional Adhesion Molecule
JNK	c-Jun-N-Terminal Kinase
L-NAME	Nω-Nitro-L-Arginine Methyl Ester
L-NMMA	L-N^{G}-Monomethyl Arginine
LECs	Lymphatic Endothelial Cells
LPS	Lipopolysaccharide
LT	Leukotrienes
LYVE-1	Lymphatic Vessel Endothelial Hyaluronan receptor-1
MAPK	Mitogen-Activated Protein Kinase
MAT.Ang-1	Matrillin Ang-1
MD2	Myeloid Differentiation protein-2
MLCK	Myosin Light Chain Kinase
MODS	Multiple Organ Dysfunction Syndrome
MOF	Multiple Organ Failure
MyD88	Myeloid Differentiation Factor 88
Mal	MyD88 adaptor-like protein
NIFR	Non-invasive near-Infrared Fluorescence

NLRP3	NOD-Like Receptor Family Pyrin-domain-containing 3
NOD	Nucleotide-binding Oligomerization Domain
NOS	NO-Synthase
PAF	Platelet Activating Factor
PAMPs	Pathogen Associated Molecular Patterns
PECAM	Platelet Endothelial Cell Adhesion Molecule
PG	Prostaglandins
PGI1	Prostacyclin
PI3K	Phosphatidylinositol 3-Kinase
PKG	Protein Kinase G
PRR	Pathogen Recognition Receptor
PTFC	Photo Thermal Flow Cytometry
RIP1	Receptor-Interacting Protein 1
RMLV	Rat Mesenteric Lymphatic Vessel
RNS	Reactive Nitrogen Species
ROS	Reactive Oxygen Species
SAPK	Stress Activated Potein Kinase
SIRS	Systemic Inflammatory Response Syndrome
SMCs	Smooth Muscle Cells
SNP	Sodium Nitroprusside
STDs	Spontaneous Transient Depolarizations
TAK1	TGF-β-Activated Kinase 1
TJs	Tight Junctions
TLR4	Toll-Like Receptor 4

TNBS	2,4,6-Trinitrobenzenesulfonic Acid
TNF	Tumor Necrosis Factor
TRAM	TRIF-Related Adaptor Molecule
TREM	Triggering Receptors Expressed on Myeloid cells
TRIF	TIR-containing adaptor Inducing IFN-β
TGF-β	Transforming Growth Factor-beta
TXA$_2$	Thromboxane A$_2$
VCAM-1	Vascular Cell Adhesion Molecule-1
VDA	Video Dimension Analyser
VE-PTP	Vascular Endothelial Phosphotyrosine Phosphatase
VEGFR-3	Vascular Endothelial Growth Factor Receptor-3
VIP	Vasoactive Intestinal Polypeptide
ZO	Zona Occludins

Table of contents

List of Figures

List of Tables

Chapter One

Introduction

1.1 Sepsis

Sepsis yearly affects over 18 million people worldwide. It is the leading cause of death in noncoronary intensive care units and is expected to rise by 1 % per year (Kumar and Sharma 2008; Schulte *et al* 2013). It continues to remain a major healthcare problem associated with 30-50 % mortality, with severe sepsis claiming between 36 000 and 64 000 lives annually in the UK alone (Daniels 2011; McPherson *et al* 2013; Weber and Swirski 2014). Sepsis develops when a normal host response to an infection intensifies and then becomes dysregulated, leading to an imbalance between proinflammatory and anti-inflammatory responses (Silva *et al* 2008; Schulte *et al* 2013). The commonest sites of infection are the lungs, abdominal cavity, the urinary tract and primary infections of the blood stream (Cohen 2002). Sepsis is marked by an initial hyper-inflammatory host response that can progress to its sequelea termed as severe sepsis, septic shock and multiple organ failure (MOF). Severe sepsis is characterised by rapidly progressing cellular and tissue failure, microvascular perfusion deficiencies, coagulation, tissue oedema followed by organ failure, with septic shock representing a type of severe sepsis exhibiting hypotension despite fluid resuscitation. Septic shock can ultimately result in Multiple Organ Dysfunction Syndrome (MODS) (Remick 2007; Pinheiro da Silva and Nizet 2009). Sepsis can be triggered not only directly through the presence of pathogens into the bloodstream but also indirectly as a result of non-infectious conditions, such as post-surgical complications, traumas, burns, haemorrhages, and other disease states. A broader term Systemic Inflammatory Response Syndrome (SIRS) is used to the define host response resulting from infectious and non-infectious processes (Nathens and Marshall 1996). Hence, the diagnosis of sepsis requires existence of an underlying infection along with a SIRS disease state (Aziz *et al* 2013; Schulte *et al* 2013).

1.1.1 Pathogenesis

Gram-negative bacteria have been reputed to be the most common identified in septic patients amongst other pathogens like gram-positive bacteria, viruses or fungi, but more recently this has been disputed with studies demonstrating gram-positive as more frequent (van der Poll and Opal 2008). However, fundamentally the pathogenesis is similar and gram-negative bacteria induced sepsis will be used in this study as it has been more widely studied and the molecular signaling events are well characterised.

The host's innate immune system recognises molecular bacterial motifs known as Pathogen Associated Molecular Patterns (PAMPs). PAMPs include diverse microbial products like lipopolysaccharide (LPS) from Gram-negative bacteria, lipotechoic acid and peptidoglycan from the Gram-positive bacteria as well as CpG DNA (bacterial DNA rich in cytosine-phosphate diesterguanosine), bacterial flagellin and double-stranded RNA from viruses (Alexopoulou *et al* 2001). Additionally, intracellular proteins released from dying cells known as 'alarmins' mediate the immunological recognition of damaged tissue and, along with PAMPs, are referred to as damage-associated molecular patterns (DAMPs) (Yang *et al* 2009). Gram-negative bacteria exert their effects through LPS, an endotoxin which is a highly potent activator of innate immune responses and is responsible for endotoxic shock (Bryant *et al* 2010). LPS directly activates monocytes, macrophages, neutrophils, complement components and non-immune cells like endothelial, epithelial and vascular smooth muscle cells (SMCs) (Remick 1995). Some of these cell types (monocytes and macrophages) express CD14 (a 55kDa cell-surface molecule) and an additional co-receptor myeloid differentiation protein-2 (MD2), required for LPS activity. CD14/MD2 bind LPS in conjunction with a plasma protein, LBP (LPS binding protein) to ultimately relay the signal via a transmembrane Pathogen Recognition Receptor (PRR) known as Toll-like receptor 4 (TLR4), one of the 10 TLRs identified in the human genome. All TLRs are single-spanning transmembrane proteins with extracellular domains containing leucine-rich repeats and a highly conserved cytoplasmic domain known as Toll interleukin-1 receptor resistance (TIR) domain (van der Poll and Opal 2008). Many cells that do not express CD14 (dentritic cells (DCs), fibroblasts, SMCs, and vascular endothelium) respond to LPS by interacting with soluble CD14 (sCD14) (Cohen 2002). However, CD14-TLR4-MD2 pathway is only one of the pathways that maybe involved in LPS recognition as several studies have shown CD14 independent activation of TLR4 receptors in innate immune cells (Kumar and Sharma 2008). For example in one study, the inability of monoclonal antibodies blocking CD14 to inhibit LPS-induced TNF-α secretion, implies the existence of some alternative pathways of LPS recognition by TLR4 (Gessani *et al* 1993). A more recent study reported that LPS activated platelets that do not express CD14 but express TLR4 receptors, stimulated the release of pro-inflammatory IL-1β rich microparticles (Brown and McIntyre 2011). Thus, there is increasing evidence to suggest that the CD14-MD2-TLR4 model is a simplistic portrayal of LPS recognition by innate immune cells (Kumar 2008). Various

other PRRs are involved in LPS recognition including the intracellular nucleotide-binding oligomerization domain (NOD) receptors NOD-1 and NOD-2, the triggering receptors expressed on myeloid cells (TREM) family, the Sialic acid binding Ig-like Lectins (Siglec) molecules, the C-type lectin receptors and NOD-like receptor family pyrin-domain-containing 3 (NLRP3) inflammasome resulting in activation of an overwhelming innate immune response (Marshall 2008). PRRs also recognise other conserved PAMPs expressed by invading microorganisms in the cytosol mentioned above (Triantafilou and Triantafilou 2004; Kumar and Sharma 2008). PAMPs recognised by TLRs are listed in table 1.1.

TLRs	PAMPs
TLR2	Lipoproteins, peptidoglycan, lipotechoic acid
TLR4	LPS
TLR5	Flagellin
TLR9	CpG elements in bacterial DNA

Table 1.1 TLRs recognising conserved bacterial structures called PAMPs (van der Poll and Opal 2008)**.**

Antibody-mediated blockade of TLR4 and MD2 confered protection against polymicrobial sepsis (Daubeuf *et al* 2007), TLR4$^{-/-}$ mice are sepsis resistant (Roger *et al* 2009) , and recent clinical trials with a TLR4 antagonist show promise as reduced mortality has been observed in patients with severe sepsis (Tidswell *et al* 2010). Thus, TLR4 pathway appears central to triggering the innate immune response mounted by the host. Activation of this pathway triggers nuclear translocation of NF-κB through a series of phosphorylation cascades triggered by mitogen-activated protein kinase (MAPK) family (p38 MAPK, c-Jun-N-terminal kinase/stress activated potein kinase (JNK/SAPK) and extra-cellular signal regulated kinase (ERK)) (Jean-Baptiste 2007). Phosphatidylinositol 3-kinase (PI3K), through association with myeloid differentiation factor 88 (MyD88) or TNF receptor-associated factor 6 (TRAF6), also participates in NF-κB activation through an Akt-dependent mechanism (Dauphinee and Karsan 2006).

NF-κB/rel transcription factors are held by inhibitory IκB-α proteins, in the cellular cytoplasm as inactive dimers. Inflammatory stimuli including LPS, peptidoglycan, and pro-inflammatory cytokines result in the phosphorylation of IκB-α by kinases IKKα and IKKβ, which are catalytically active components of the IκB kinase complex (IKK) inducing the release of NF-κB which then targets genes for synthesis of other inflammatory mediators like cytokines, chemokines and adhesion molecules. Other upstream kinases like IL-1 receptor associated kinases (IRAK-1) and IRAK-4 directly activated by TLRs, as well as kinases like p38 and Akt that are associated with TLRs or other G-protein-coupled receptors, also participate in IKK phosphorylation and activation. Studies have shown that NF-κB activation contributes to the severity of cellular and organ dysfunction (Abraham 2005) (Figure 1.1).
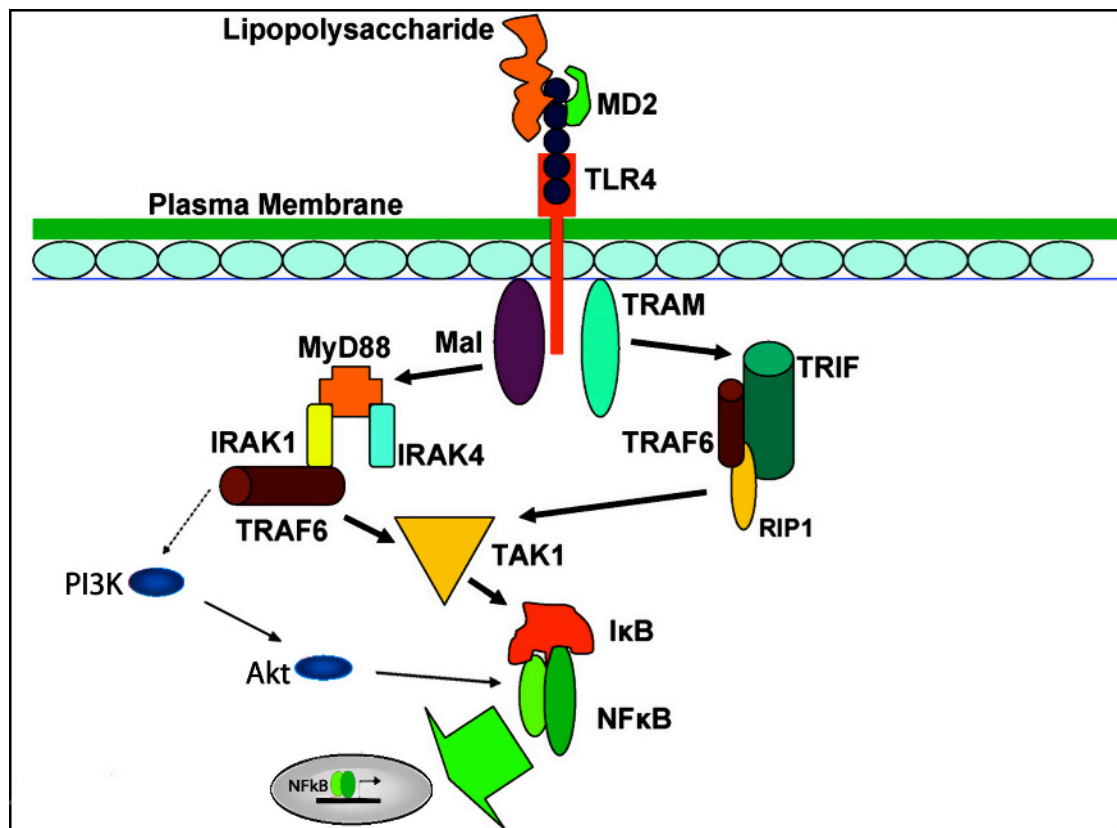
Figure 1.1 A simplified schematic representation of events following LPS binding to TLR4. Homodimerization of TLR4 leads to subsequent recruitment of TIR domain containing adaptor molecules such as MyD88, MyD88 adaptor-like protein (Mal), also called TIRAP, TIR-containing adaptor inducing IFN-β (TRIF), and TRIF-related adaptor molecule (TRAM), to the cytoplasmic tail of the receptor. MyD88 engages IRAK1 and 4 to the TLR4 receptor complex via interactions between the death domains of MyD88 and IRAKs. TRAF6 is recruited by IRAK1 and this complex, in turn, activates transforming growth factor-β (TGF-β)-activated kinase 1 (TAK1), leading to the phosphorylation of IκB and the translocation of NF-κB to the nucleus, where it triggers the transcription of various pro-inflammatory cytokines. A MyD88-independent pathway initiated by the engagement of TRAM by TLR4 leading to the recruitment of TRIF, receptor-interacting protein 1 (RIP1), and TRAF6, also activates TAK-1. Activation of TRAF6 also triggers inflammation via activation of PI3K and Akt. Adapted from (Dauphinee and Karsan 2006; Marshall 2008).

1.1.2 Immune response and inflammatory mediators

The inflammatory response at the onset of sepsis involves the innate (cellular and humoral) and adaptive immune system. Endothelial, epithelial cells as well as inflammatory cells produce inflammatory mediators (Table 1.2; Figure 1.2). Inflammatory cells comprise circulating leukocytes (neutrophils, monocytes and lymphocytes), tissue macrophages, DCs, mast cells and eosinophils. As part of the cellular innate immune system, neutrophils and monocytes are activated by invading bacteria, their components described above and endogenous mediators from the host (cytokines, chemokines, complement-activation products and intracellular alarmins) to release secondary mediators [lipid mediators, granular enzymes, Reactive Oxygen Species (ROS) (e.g., superoxide, hydrogen peroxide) and Reactive Nitrogen species (RNS) (e.g., nitric oxide (NO))]. These cells are then directed towards sites of infection by chemotaxis and upregulation of adhesion molecules eg. selectins, Inter-Cellular Adhesion Molecule 1 (ICAM-1), Vascular Cell Adhesion Molecule 1 (VCAM-1) on endothelial cells (ECs) leading to leukocyte adhesion and transmigration (Bellingan 1999; Riedemann *et al* 2003; Hoesel *et al* 2006; Cepinskas and Wilson 2008). Leukocyte adhesion involves three main stages as described classically-rolling, firm adhesion and transmigration. Vascular selectins (E and P-selectin) and L-selectin expressed by leukocytes mediate the tethering of neutrophils and monocytes to the endothelium allowing rolling. Integrins (leukocyte β_2 integrins and VLA-4 (Cd29)) and Platelet Endothelial Cell Adhesion Molecule (PECAM) (CD31) further allow for firm adhesion interactions via endothelial ligands ICAM-1, ICAM-2 and VCAM-1 leading to transmigration of neutrophils across the vessel wall. This causes an efflux of a significant amount of intravascular fluid partly explaining the prevailing tissue oedema in severe sepsis (Sriskandan and Altmann 2008).

Complement	Effects
TLR-4 mediated complement activation C3a, C5a	Activates coagulation cascade, apoptosis, release of MIF and HMGB1, chemotaxis, granular enzymes and ROS from polymorphonuclear leukocytes (PMN) (Hoesel *et al* 2006; Rittirsch *et al* 2008)
Pro-inflammatory cytokines	**Effects**
TNF-α from activated macrophages, lymphocytes within 30-90 min of stimulation	Activates genes for complement components, NO-synthase (NOS), cell-adhesion molecules, Platelet Activating Factor (PAF), IL-1, IL-6, IL-8 and IL-10 (Jean-Baptiste 2007).
IL-1 from monocytes, macrophages, lymphocytes, astrocytes and ECs, PMN within 180 min of stimulation	Effects similar to those induced by TNF-α, proliferation of B and T-cells, lymphokine stimulation (Jean-Baptiste 2007).
IL-6 from T cells, fibroblasts, ECs, lymphocytes within 6 h of stimulation	T-cells, B-cells proliferation and production of acute phase proteins (Jean-Baptiste 2007).
Late release- HMGB1 from macrophages, monocytes and neutrophils necrotic cells in damaged tissue or from activated macrophages at sites of infection within 16 h of stimulation with C5a, PAMPs, pro-inflammatory cytokines	Activates TLR-4, increases activity of pro-inflammatory cytokines TNF-α by activating macrophages (Shimaoka and Park 2008).
MIF released immediately after macrophages, monocytes stimulation by endotoxins, C5a, TNF-α, IFN-γ	TLR-4 expression, amplifies production of pro-inflammatory cytokines like TNF-α (Jean-Baptiste 2007).
Chemokine	**Effects**
IL-8 from monocytes, macrophages, Kupffer cells within 60-90 min of stimulation	Induces IFN-γ production and acts as a chemotatic agent for neutrophils and T-cells (Jean-Baptiste 2007).

Table 1.2 Pro-inflammatory mediators released during sepsis. MIF-Macrophage migration inhibitory factor; HMGB1- High-mobility group protein B1
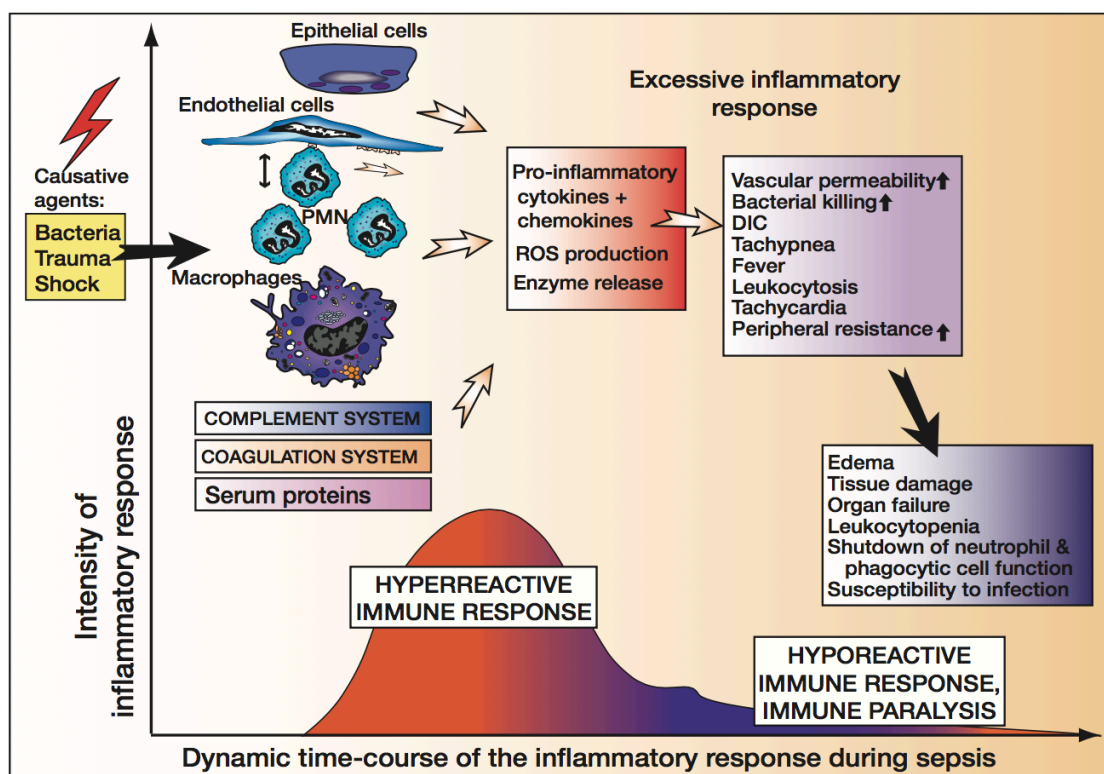
Figure 1.2 Effects of inflammatory mediators during sepsis. Epithelial cells, ECs, inflammatory cells such as PMNs and macrophages as well as the complement and coagulation systems produce pro-inflammatory cytokines and chemokines on activation by invading bacteria and other stimuli. Neutrophils, monocytes and other phagocytes release secondary mediators such as granular enzymes and ROS in response to the primary mediators during the hyperactive phase of sepsis. The excessive pro-inflammatory environment leads to increased vascular permeability, bacterial killing and peripheral resistance resulting in tissue damage, organ failure and impaired innate immune function. This ultimately increases susceptibility to infection in the hyporeactive phase of the immune response accompanied by immune paralysis. Image from (Riedemann *et al* 2003).

1.1.2.1 Cytokines

Among the various cytokine mediators released in sepsis, the prototypic inflammatory cytokines TNF-α and IL-1β released by mononuclear cells that mainly mediate the microvascular dysfunction of LPS-induced shock will be used in this study. Their main features are elaborated in the section below.

1.1.2.1.1 TNF-α

Tumor necrosis factor (TNF)-α is expressed as a 17 kDa polypeptide that induces transmembrane signaling through two types of TNF receptors, TNF-R1 (present on most cells) and TNF-R2 (present on membrane of immune cells). TNF is derived mainly from activated immune cells like macrophages and non-immune cells like fibroblasts in response to infectious or inflammatory stimuli. NF-κB is activated by these receptors via TNF-associated factor, which leads to downstream activation of genes synthesising NOS, cell adhesion molecules, PAF, IL-1, IL-6, IL-8, IL-10. TNF-α is released in inordinate amounts in severe sepsis and plays a pivotal role in the pathogenesis of a hypotensive septic shock-like state and organ dysfunction related to it (Jean-Baptiste 2007; Shimaoka and Park 2008). For example, TNF-α enhances vascular permeability, and promotes leukocyte recruitment to the endothelium (Legrand *et al* 2010). It acts on ECs and neutrophils provoking neutrophil-mediated tissue injury as well as enhancing expression of ICAM-1, VCAM-1 and chemokines in ECs. It further amplifies the inflammatory response in an autocrine and paracrine manner by activating monocytes/macrophages to secrete other pro-inflammatory cytokines mentioned in table 1.2 (Shimaoka and Park 2008; Schulte *et al* 2013).

1.1.2.1.2 IL-1β/IL-1α

Interleukin-1 (IL-1), released primarily from activated macrophages is functionally similar to TNF-α (Kellum and Decker 1996). The pro-inflammatory members of the IL-1 family include IL-1α and IL-1β which signal through two distinct receptors IL-1R1 and IL-1R2 respectively. Engagement of IL-1β with IL-1R2 belonging to the TLR/IL-1 receptor family triggers NF-κB driven pro-inflammatory pathways. Together with NLR containing multi-protein complexes primed by TLRs, pro-IL-1β activates caspase-1, which subsequently processes it to its active extracellular form IL-1β. IL-1α is more active as an intracellular membrane-associated precursor (Cinel and Opal 2009).

Both molecules TNF-α and IL-1β are known to act synergistically to trigger the expression of further factors such as IL-6, IL-8, IL-12 and IL-18 in the inflammatory cascade and induce a shock-like state marked by vascular permeability, severe pulmonary oedema, and haemorrhage (Peters *et al* 2003; Schulte *et al* 2013).

1.1.2.2 Lipid Mediators

Lipid mediators that are released after the initial inflammatory stimulus include eicosanoids like prostaglandins and leukotrienes and PAF which are derived from arachidonic acid in the cell membrane of neutrophils and macrophages (Bellingan 1999). The effects of these agents are summarised in table 1.3.

Lipid mediators	Effects
Prostaglandins (PG)- synthesised by microsomal enzyme cyclo-oxygenase (COX). Vasoactive metabolites are PGE_2, prostacyclin (PGI1) and thromboxane A_2 (TXA_2).	PGE_2, PGI1 cause hypotension; TXA_2 is a vasoconstrictor
Leukotrienes (LT)- synthesised by lipoxygenase. LTC4, LTD4 and LTE4 are the main metabolites.	Involved in vascular tone regulation and capillary permeability; LTB4 is chemotactic for PMNs, leukocytes, eosonophils and monocytes.
PAF	Promotes platelet activation mediating release of histamine, thrombosis and vascular injury by enhacing upregulation of adhesion molecules. Chemotactic for PMNs.

Table 1.3 Effects of lipid mediators during sepsis (Jean-Baptiste 2007)**.**

1.1.2.3 Nitric oxide

NO is arguably the most important local factor regulating vasomotor tone, blood haemodynamics and endothelial permeability. Production of NO is catalysed from L-arginine by three isoforms of NO synthases 1) eNOS 2) brain NOS 3) iNOS. The former two are constitutively expressed whereas iNOS is detectable only following stimulation by LPS, TNF-α, IL-1 (Sriskandan and Altmann 2008). The activation of constitutive NOS depends on the calcium-calmodulin system, lasts briefly and causes the production of small amounts of NO. Basal NO production by eNOS is necessary

for maintenance of endothelial barrier function (Cepinskas and Wilson 2008). This protective effect of NO is diminished during the inflammatory response due to the reduced production of NO by eNOS, possibly resulting from impaired PI3K/Akt pathway (Matsuda and Hattori 2007). The sepsis pro-inflammatory response triggers a sharp increase in systemic NO production via the upregulation of iNOS, which detrimentally increases vascular permeability (Hauser *et al* 2008). iNOS activation is triggered via NF-κB, lasts longer and causes the production of significantly larger amounts of NO in a calcium-independent manner (Kotsovolis and Kallaras 2010). The altered homeostatic balance of eNOS and iNOS thus contributes to widespread microvascular dysfunction.

1.1.2.4 Other mediators and mechanisms

The complement system is activated as part of the humoral innate immune system. The most potent complement protein C5a has been known to induce various cellular stress response mechanisms which are briefly summarised in table 1.2 (Hoesel *et al* 2006). After the initial surge of pro-inflammatory cytokines, the later stage of sepsis is characterised by production of anti-inflammatory mediators incuding IL-10, IL-13, TGF-β, soluble cytokine receptors (sTNFR, IL-1Ra), heat shock proteins, phosphatases and cortisol. Anti-inflammatory mediators mainly suppress the function of PMNs. In parallel, the adaptive immune response is induced upon interaction with the antigen presenting cells (APCs) that have encountered a pathogen. The cells of the adaptive immune system, such as naïve T cells, upon antigen recognition, proliferate to generate effector cells (Th1, Th2 and Th17) which in turn, release an array of distinct cytokines such as IL-2, IL-4, IL-5, IL-10 and IL-17 (Aziz *et al* 2013).

Cellular dysfunction characterised by excessive activation or reduced function is another hallmark of sepsis. Cellular apoptosis or necrosis is one of main cellular functions that has been widely researched. Apoptosis results in a dysfunctional adaptive system. Widespread lymphocyte and DC apoptosis also contributes to the state of immunosuppression. A large number of epithelial cells, macrophages/ monocytes and to some extent ECs also undergo apoptosis. Delayed apoptosis of neutrophils leads to prolonged neutrophil activity driving further organ injury (Remick 2007). ECs dysfunction after the initial hyperinflammatory response results in further damage to internal organs (elaborated in the next section). Damage to blood vessel endothelium results in dysregulated coagulation which manifests as Disseminated

Intravascular Coagulation (DIC) characterised by the widespread activation of the coagulation cascade and inhibition of fibrinolysis that results in the formation of micro-vascular thromboses throughout the body. The acute phase response characterised by secretion of acute phase proteins like C-reactive protein, serum amyloid A and coagulation proteins like fibrinogen and von Willebrand factor, induces the expression of major coagulation pathway triggers like the Tissue Factor. Tissue Factor is released from a variety of cell types like activated ECs, fibroblasts and circulating immune cells in response to TNF-α, IL-1, IL-6, LPS and promotes thrombus formation by activating thrombin and fibrin deposition, ultimately impairing tissue perfusion of vital organs (Remick 2007; Sriskandan and Altmann 2008). Activated thrombin stimulates pro-inflammatory cytokines and C5a, ending up in a vicious cycle that continually stimulates coagulation (Shimaoka and Park 2008). Thus, as DIC develops, there is a bidirectional interplay between coagulation and inflammation that worsens the ensuing damage.

1.1.3 Microvascular changes leading to organ dysfunction

The pathogenesis of sepsis-induced organ dysfunction is complex given the pleiotropic effects of the primary and secondary inflammatory mediators and non-cytokine mediators discussed above. Multiple cascades (coagulation, fibrinolysis and complement systems) that are activated, result in microvascular occlusion and vascular instability leading to impaired tissue perfusion and hypoxia and ultimately organ failure (Cohen 2002) (Figure 1.3). The endothelium activation and dysfunction play a central role in this process. Besides changes in their anti-coagulant properties, loss of barrier function, increased expression of adhesion molecules and production of inflammatory mediators, ECs also produce vasoactive agents such as vasodilating NO and prostacyclin and vasoconstricting endothelin that regulate the vascular tone, thus altering blood haemodynamics (Hack and Zeerleder 2001). EC dysfunction ultimately leads to increased permeability, altered vasomotor tone, and capillary flow shutdown in the microvasculature (Bateman *et al* 2003; Sriskandan and Altmann 2008). Mechanisms that alter endothelial permeability are described in the next section.
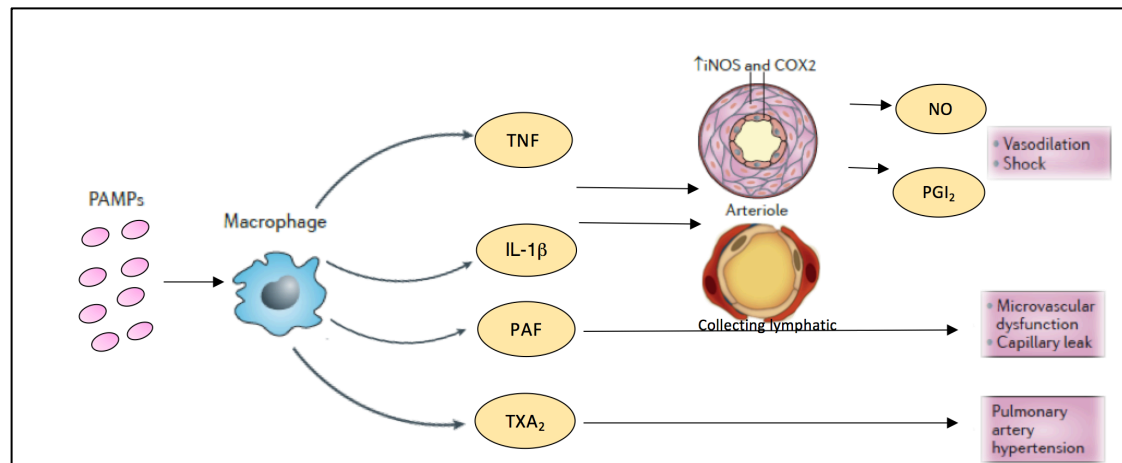
Figure 1.3 Simplified view of the pathogenesis of sepsis-induced organ dysfunction. Inflammatory cells such as macrophages recognise PAMPs, which trigger the release of cytokines. This process leads to the upregulation of iNOS and COX2 in vascular and lymphatic SMCs and ECs, which generate NO and PGI_2. Together these secondary mediators cause vasodilation and septic shock. Activated macrophages also release lipid mediators such as PAF, which causes microvascular dysfunction, capillary leak and TXA_2, which causes pulmonary hypertension. Adapted from (Fink and Warren 2014).

1.1.3.1 Mechanisms of barrier function disruption

Endothelial permeability is regulated by two pathways-transcellular and paracellular. The transcellular pathway allows the vesicle-mediated passage of macromolecules across the endothelial barrier. The paracellular pathway is mediated by opening and closure of endothelial cell-cell junction, which consist of two major junctional structures - Adherens junctions (AJs) and Tight junctions (TJs) (Bazzoni and Dejana 2004).

1.1.3.1.1 Adherens Junctions

AJs represent the majority of junctions in the endothelial barrier and are the key structures for maintenance of paracellular permeability to plasma fluid and proteins (Bazzoni and Dejana 2004). AJs have a ubiquitous distribution in the vasculature and are expressed in both blood and lymphatic vessels. They are comprised of transmembrane adhesion proteins of the cadherin family, which mediate homophilic adhesion and form multimeric complexes at the cell borders. ECs express a specific cadherin called vascular endothelial (VE)-cadherin. Under resting conditions, VE-cadherin, is linked through its cytoplasmic tail to the AJ proteins p120, β-catenin and plakoglobin. β-catenin and plakoglobin bind to α-catenin, which interacts with several actin-binding proteins linking VE-cadherin to the cytoskeleton (Figure 1.4). The complex clusters at junctions in a zipper-like fashion (Dejana et al 2008). In addition, VE-cadherin interacts with a receptor-protein called vascular endothelial phosphotyrosine phosphatase (VE-PTP) known to strengthen cell-to-cell adhesion (Bazzoni and Dejana 2004). Most conditions that increase permeability affect the organisation of the AJs, which can be accompanied by cell-retraction obvious by the widening of intercellular gaps. However, mechanisms such as internalisation of VE-cadherin or phosphorylation of AJ proteins weaken the junctions without any evidence of cell retraction (Bazzoni and Dejana 2004; Dejana *et al* 2008). Disorganization of VE-cadherin clustering has been implicated as the major underlying mechanism of vascular permeability in sepsis (Dejana et al 2008).
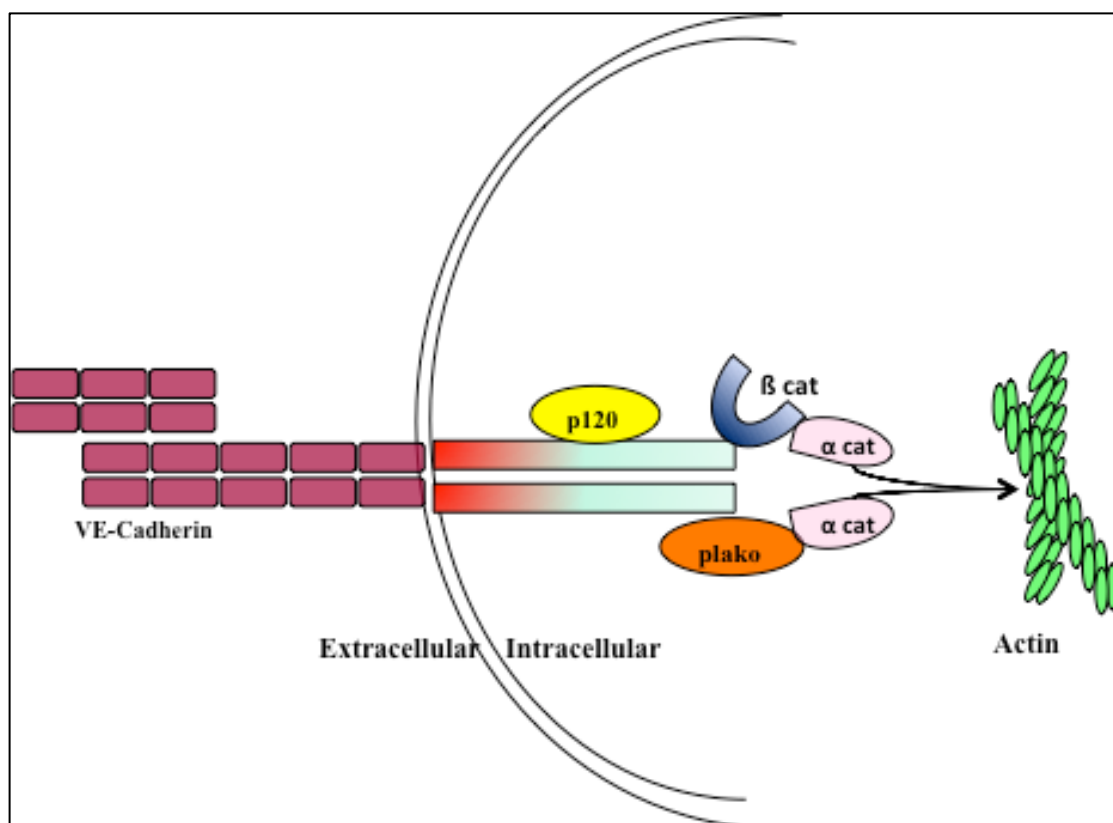
Figure 1.4 Molecular organisation of endothelial AJs. VE-cadherin, represented as a dimer, clusters at cell junctions to form multimolecular complexes that include the catenin proteins p120, β-catenin (βcat) and plakoglobin (plako). The cytoplasmic tail of VE-cadherin is linked to the cytoskeleton via α-catenin (αcat), which interacts with several actin-binding proteins. The AJ complex modulates the endothelial-barrier function via regulating VE-cadherin activity. Adapted from (Dejana *et al* 2008).

1.1.3.1.2 Tight Junctions

TJs constitute only one-fifth of the cell junctions in the endothelium, however they too are important in maintaining the integrity of the endothelial barrier (Mehta and Malik 2006). Occludin, claudins (claudin-5 being the only endothelial specific isoform), and Junctional Adhesion Molecule (JAM) comprise the main transmembrane proteins at TJs. Zona occludins (ZO) 1-3, are intracellular components of TJs that link the intracellular domains of the transmembrane proteins to the actin cytoskeleton (Vandenbroucke et al 2008). NF-κB is known to disrupt the organisation of TJ proteins to increase permeability, while maintaining the expression level of the proteins, however there is limited research into how permeability is regulated through tight junctions during inflammatory conditions (Vandenbroucke et al 2008).

1.1.3.2 Mechanisms affecting loss of VE-cadherin function

The pathophysiological importance of AJs in vascular inflammation during disease has been underscored in the literature and much emphasis has been laid on mechanisms that regulate VE-cadherin mediated adhesion as they play an important role in controlling vascular permeability (Kumar *et al* 2009). The main mechanisms affecting loss of VE-cadherin function are as follows: 1) Loss of junctional proteins destabilizes barrier function. TNF-α induced vascular permeability is associated with a reduction of VE-cadherin expression (Hofmann *et al* 2002). Increased iNOS expression in response to LPS is associated with decrease in VE-cadherin expression (Hama *et al* 2008). 2) Phosphorylation of β-catenin, plakoglobin and p120 and VE-cadherin itself dissociates them from the actin cytoskeleton and reduces the AJ strength. The VE-cadherin complex might become partially disorganized without any indication of cell retraction. Phosphorylation of VE-cadherin not only disrupts homophilic interactions of the complex, but can also result in endocytosis resulting in removal of VE-cadherin from the cell surface if phosphorylation occurs on the serine residues. This process is thought to mediate VE-cadherin internalization (Gavard and Gutkind 2006). Tyrosine phosphorylation of β-catenin reduces its affinity for the cadherin cytoplasmic tail, thus weakening its association with the cytoskeletal fibres (Dejana *et al* 2008). Permeability agonists induce tyrosine phosphorylation of VE-cadherin and its counterparts. It has been demonstrated that LPS can phosphorylate VE-cadherin on the tyrosine residues via SRC family kinase activation, which may reduce the junction strength as described (Gong *et al* 2008). 3) Mechanisms initiating cell retraction involve small GTPases, Ca^{2+} which are not of focus in this thesis (Aghajanian *et al* 2008; Vandenbroucke *et al* 2008).

Thus far, the described events clearly indicate that an end-result of endothelial activation and dysfunction and a key feature of early microvascular changes is increased permeability of the endothelium or loss of barrier function, which occurs in multiple organs during sepsis, leading to redistribution of body fluid and oedema. Fluid leakage from the intravascular space contributes to hypovolemia and hypotension (Schouten *et al* 2008). While investigations to date have mainly centered around blood endothelium impairment, contribution of the lymphatic system to oedema during sepsis has received little attention. The lymphatic microvasculature plays a unique role in the continuous removal of interstitial fluid and proteins and

impairments in the lymphatic system may have major implications in poor disease outcome. There is evidence that the prototypic inflammatory mediators released during sepsis impair lymphatic vessel contractility and endothelial barrier function (Aldrich and Sevick-Muraca 2013; Cromer *et al* 2014). Moreover, a recent study has elucidated a previously unidentified role of lymphatics in maintaining intestinal tissue integrity and conferring protection against gut-derived sepsis. Authors showed that acute ablation of lacteals (specialised intestinal lymphatics) compromised the integrity of the surrounding villi including blood vessels resulting in severe intestinal inflammation and sepsis (Jang *et al* 2013). Lymphatic dysfunction may be amenable to therapeutic strategies targeting mechanisms that cause these impairments and improve rates of survival. Moreover, early therapeutic intervention is increasingly being recognised as key in improving survival in sepsis. Data from clinical and experimental studies have suggested a strong link between microcirculatory impairments and MOF; however, there is lack of data to define microvascular changes in early sepsis (Ince 2005; Nencioni *et al* 2009; Spanos *et al* 2010; De Backer *et al* 2014). Hence, this study undertakes the investigation of changes in the lymphatic microvasculature during early sepsis.

The following section describes the structure, function and the dynamic nature of the lymphatic system as well as its role during sepsis. It also explores the current understanding of lymphatic vessel dysfunction during inflammatory insult, especially its contractile and barrier dysfunction.

1.2 The lymphatic vascular system

The lymphatic system plays an important role in maintenance of tissue fluid homeostasis, dietary lipid absorption and immune surveillance (Figure 1.5a). The lymphatic vessels primarily remove water, macromolecules, immune cells, lipids (in case of small intestinal lymphatics), and also clear antigenic or toxic macromolecules from the interstitium. The lymphatic vascular network comprises the initial lymphatic capillaries, pre-nodal and post-nodal collecting lymphatic vessels, lymph nodes, trunks and ducts (Figure 1.5b). The initial lymphatics are thin-walled, blind ended vessels lined by a single layer of non-fenestrated overlapping lymphatic endothelial cells (LECs). In contrast to blood capillaries, lymphatic capillaries have an incomplete basement membrane and lack pericytes. The adjacent LECs form overlapping intercellular junctions which mediate passage of fluid and particles into the vessel during increased interstitial fluid pressure. Baluk *et al* have shown discontinous button-like junctions occuring on the sides of the oak-leaf shaped LECs but lacking at the tips in the initial lymphatics. These junctions progress to another type of junctions arranged continuously in a zipper-like fashion at the level of collecting lymphatics (Baluk *et al* 2007). Both of these lymphatic structures contain VE-cadherin, occludin, claudin-5, ZO-1 protein, TJ-associated Ig-like transmembrane proteins endothelial cell-selective adhesion molecule (ESAM), JAM-A and PECAM-1/CD31 (Alexander *et al* 2010; Kesler *et al* 2013).

The overlapping junctions serve as primary valves or microendothelial valves that ensure unidirectional flow of lymph preventing convective reflow into the interstitum. This function is aided by fibrillin-containing filaments which pull open the valves during increased interstitial pressure at the same time keeping them anchored to the extra cellular matrix (ECM). The initial lymphatics drain into the precollecting lymphatic vessels that have both lymphatic capillary (oak leaf-shaped LECs) and collecting lymphatic vessel characteristics (valves). The precollecting vessels continue into the larger collecting lymphatics and contain three different layers in their wall: a monolayer of elongated ECs surrounded by a basement membrane; a media comprised of 2-3 layers of SMCs scattered with collagen and elastic fibres; and surrounded by an adventitia constituted by fibroblasts and connective tissue elements with nerves that innervate the vessel (von der Weid and Zawieja 2004). SMCs in the guinea-pig mesenteric lymphatics were observed to be mostly organised in the circular plane of

the vessel with frequently overlapping cells. These cells form a thread- or meshwork-like structure compared to larger vessels such as those in the bovine mesentery which form three distinct layers: an inner longitudinal, a middle circumferential and an external longitudinal layer in the media (Ohhashi *et al* 1977). They also contain numerous intraluminal valves (Figure 1.6) that prevent the retrograde flow of lymph (Jurisic and Detmar 2009). The collecting lymphatics are contractile unlike the initial lymphatics. Contractile segments of collecting lymphatics between valves were termed as lymphangions by H.Mislin in the 1960s. Lymphagions, 600-1000 μm long, act as pumps during active transport of lymph against a pressure gradient or as conduits during passive transport down a pressure gradient (Stucker *et al* 2008; (Zawieja *et al* 1993). The pre-nodal collecting lymphatic vessels pass through at least one or more lymph nodes, emerging as post-nodal lymphatics that drain into larger trunks and ducts. Ducts then return the lymph back into the blood circulation. Half of the total lymph formation in the body occurs in the intestines and liver out of the total lymph formed (1-2 l/day) (Swartz 2001; Zawieja 2005; Tammela and Alitalo 2010). Lymphatic vessels in most tissues pump fluid and proteins that comes from blood capillaries, however nearly all the lymph flowing through the mesenteric lymphatics is of intestinal origin (Fanous *et al* 2007). Hence, they can be more susceptible to damage during diseases such as sepsis in which the abdominal cavity is one of the primary sites of infection.
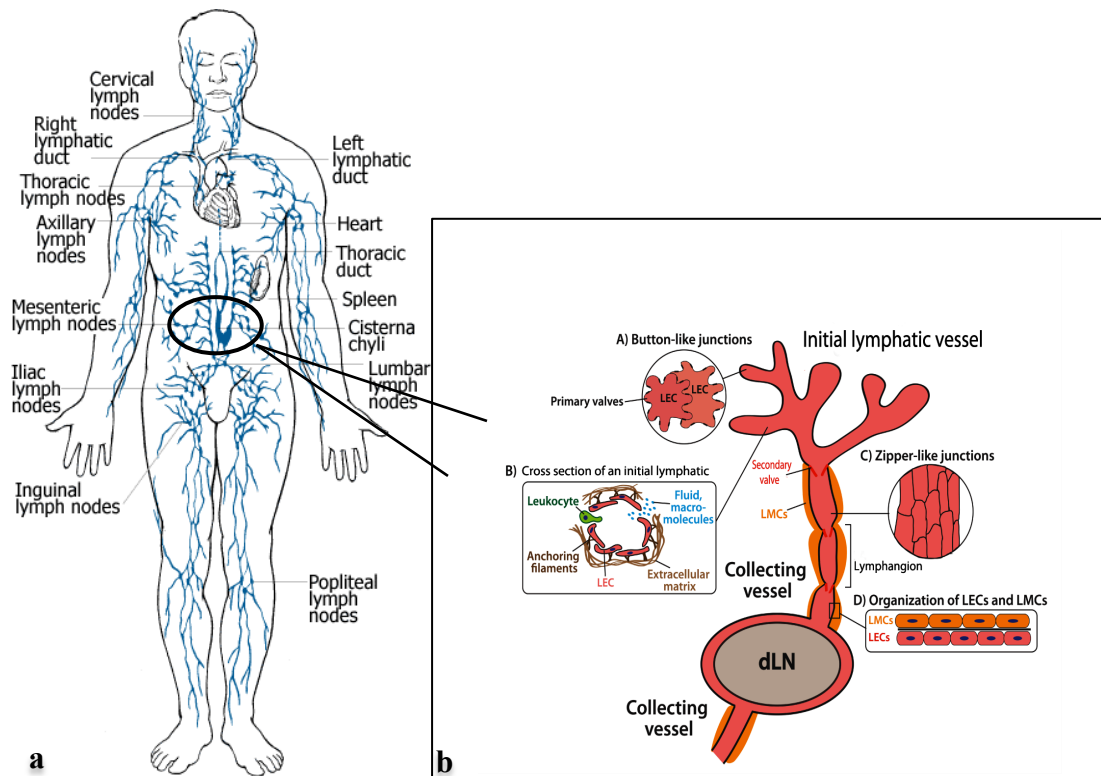
Figure 1.5 a) The lymphatic system b) The initial and collecting lymphatics. The lymphatic vasculature comprises of the small capillaries containing primary valves (A, B) that funnel into collecting vessels containing secondary valves and then into the thoracic duct or the right lymphatic trunk. LECs in collecting lymphatics are connected by continuous zipper-like junctions (C) and associate closely with lymphatic muscle cells (LMCs), which mediate contractility (D). The lymph travels to at least one draining lymph node (dLN) before ultimately emptying into the right or the left subclavian vein, where it is returned to the blood circulation. (Adapted from http://www.gorhams.dk/html/ the_ lymphatic_system.html; Vranova and Halin 2014).
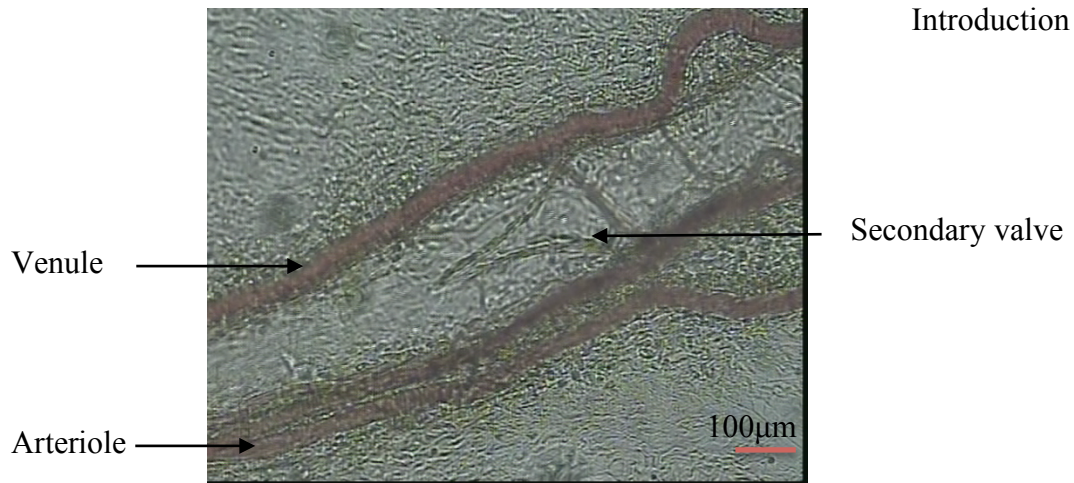
Figure 1.6 Intravital image of rat mesenteric collecting mesenteric vessel (110 µm) showing secondary valve. The large collecting lymphatic vessels course toward the root of the mesentery along with paired arteries and veins. In rat mesenteric lymphatics, these lymph vessels range from 40-200 µm and have prominent intraluminal valves that divide the vessels into segments called lymphangions (Zawieja *et al* 1993). The valves consist of bileaflets, which are lined on both sides by a specialized endothelium anchored to the ECM (Lauweryns and Boussauw 1973). High lymph pressure by incoming fluid upstream of a valve opens the leaflets enabling lymph flow, whereas retrograde flow closes the valve as the leaflets are pressed against each other. Therefore, valve opening and closure is controlled by periodic changes in fluid load within collecting vessels (Foldi 2006).

1.2.1 Physics of lymphatic transport-Pumps and Valves

The lymphatic system consists of two pumps- the extrinsic/passive and the intrinsic/active pumps to move lymph. The extrinsic pump relies on the cyclical compression and expansion of lymphatics by the external tissue forces e.g. lymph formation (which in turn depends on interstitial fluid pressure and strain of ECM), arterial and venous pulsations, respiration, skeletal muscle contractions, central venous pressure fluctuations and gastro-intestinal peristalsis. During expansion, the intralymphatic pressure which is lower than the interstitial fluid pressure, enables the entry of interstitial fluid into the lymphatics. Compression propels the lymph upstream towards the collecting lymphatics (Schmid-Schonbein 1990).

The intrinsic pump relies on the spontaneous phasic contractions of the lymphangions. To generate lymph flow along the length of the vessel, the lymphangions act as a series of small pumps separated by valves. Each lymphangion contracts out of phase with the adjoining one: one lymphangion contracts when the next one dilates. Thus,

the intraluminal pressure that the lymph propulsion needs, depends on the intrinsic pump and vector sum of the extrinsic forces (Swartz 2001). The phasic intrinsic contractions originate from an electrical pacemaker activity in the cells of the muscle layer (Ohhashi *et al* 1980; von der Weid *et al* 1996). Subsequent depolarization (called spontaneous transient depolarizations (STDs)) of the pacemaker cell produces an action potential and initiates a contraction (Zawieja 2005). The action potentials are mediated by synchronized Ca^{2+} release from intracellular stores through L-type or long-lasting Ca^{2+} channels (von der Weid 2001). Recent data from a study implicates the T-type 'transient' Ca^{2+} channels as possible pacemaker component. It is proposed that activation of these channels depolarizes membrane potential and regulates the frequency of lymphatic contractions via opening of L-type channels, which drive the strength of contractions (Lee *et al* 2014).

Efficient lymph propulsion requires the action potentials to rapidly propagate through the gap junctions connecting adjacent SMCs to allow a synchronised contraction (von der Weid 2001). Lymphatic vessels express contractile proteins characteristic of both vascular smooth muscle and cardiac muscle (striated). In addition to the rapid, phasic contractile activity exhibited by lymphatic muscle, it also exhibits slower, tonic form of contractions driven by a basal, myogenic tone (Davis *et al* 2009). These characteristics allow them to fundamentally function as both passive conduits and pumps (Muthuchamy *et al* 2003). For example, peripheral lymphatics such as mesenteric and femoral act mainly as pumping vessels while thoracic duct behaves more like an outflow conduit (Gashev *et al* 2004).

1.2.2 Modulation of lymphatic contractility

The intrinsic pump is coupled to the activity of the surrounding tissues and hence there are a number of mechanical, vasoactive and neuromodulatory factors that modulate the contractility of the intrinsic pump via inotropic (i.e., changes in the strength of contraction) and/or chronotropic (i.e., changes in the contraction frequency) effects (Zawieja 2009).

1.2.2.1 Physical factors
Physical factors that mainly modulate the intrinsic lymphatic pump are transmural lymph pressure/stretch and lymph flow/shear stress.

Transmural pressure (pressure gradient across lymphatic wall)/intraluminal pressure allows the lymphatic wall to distend and depends on the extralymphatic forces of lymph formation and pressure pulses generated by contractions of upstream lymphangions. Increasing interstitial pressures increase lymph formation which increases stretch on the lymphatic wall. Vessel distension due to intraluminal flow was also shown to be an important factor in determining lymph propulsion as it induced Ca^{2+} release from intracellular stores as well as influx of Ca^{2+} across the plasma membrane (Davis *et al* 1992). Several studies (Benoit *et al* 1989; Gashev and Zawieja 2001) have now proved that transmural pressure is not compulsory for pacemaking contrary to the initial paradigm suggesting that stretch/distension stimuli was required for initiation of contraction. However, transmural pressure is a modulating factor of contractility and causes positive inotropic and chronotropic changes in lymphatic contractility. For example, isolated bovine mesenteric lymphatic vessels show increased frequency of contractions when pressure is raised from 1 to 5 cm H_2O with maximum pumping activity at 5 cm H_2O (Gashev 2008; Zawieja 2009). von der Weid *et al* observed a marked depolarisation of resting membrane potential (Vm) with increase in stretch in wire-myograph mounted vessels, hence showing a close correlation between Vm and stretch-induced increases in contraction frequency (von der Weid *et al* 2014). Stretch initially also increases the phasic contraction strength, but eventually dampens it due failure to match contractile force with increasing load (Zawieja 2009). Hence, lymphatic pumping is quite sensitive to acute changes in transmural pressure and is physiologically important when oedemagenic stimuli like increased capillary pressure come into play. Increased lymphangion pumping serves as a negative feedback mechanism during periods of high pressure in lymphangions exerted by incoming fluid and prevents oedema by increasing lymphatic filling pressure and supporting the lymphangion outflow to match the increased lymphangion inflow. Besides an acute functional response to increases in transmural pressure, lymphatic vessels also exhibit an adaptive functional response to prolonged changes in pressure by behaving as stronger pumps at low pressure ranges and better conduits at high pressure ranges (Dongaonkar *et al* 2013). Again, such a response is necessitated by a physiological feedback mechanism to decrease interstitial pressure and regulate interstitial fluid volume (Dongaonkar *et al* 2009).

Lymph flow- Shear forces resulting due to lymph flow act on the lymphatic wall which alter vessel contractility. Gashev *et al* demonstrated how imposed flow mimicking high extrinsic flow conditions applied to rat mesenteric lymphangions has negative chronotropic and inotropic effects on the vessel. Experiments investigating effects of increased lymph flow demonstrated that an increase in axially induced-flow (at constant transmural pressure) caused inhibition of active pumping (loss of basal tonic contraction strength, reduced contraction frequency and amplitude of phasic contractions) in mesenteric lymphatics and thoracic duct and resulted in uninterrupted flow in the vessel. This effect was shown to be endothelium-dependent, predominantly due to the production of NO (Gashev *et al* 2002; Gashev *et al* 2004). Suppression of NOS with Nω-nitro-L-arginine methyl ester (L-NAME) or L-N^G-monomethyl arginine (L-NMMA) blocks the fall in contraction frequency and amplitude associated with imposed flow (Koller *et al* 1999; Gashev *et al* 2002; Tsunemoto *et al* 2003; Gasheva *et al* 2006). They proposed that imposed flow-dependent inhibition of the active lymph pump at high levels of lymph formation serves as an energy conserving mechanism, thereby decreasing lymph outflow resistance easing the removal of fluid and preventing oedema formation. In addition to the sustained forward flow through the lymphangion that can result in NO production from the lymphatic endothelium, evidence of phasic production of NO in association with the lymphatic contraction cycle has also emerged on further investigation.

Gasheva *et al* investigated the importance of intrinsic flow on the contractile function generated solely by the phasic lymphatic pump. Investigations in rat thoracic duct revealed an interesting self-regulatory NO-dependent mechanism in the vessels. The authors demonstrated an increase in contraction frequency and basal tone and decreased contraction amplitude after blockade of eNOS in rat thoracic duct segments under basal conditions (i.e. phasic flows associated with phasic contractions) not exposed to any imposed axial flow gradient (Gasheva *et al* 2006). Furthermore, it was reported that phasically contracting thoracic duct segments had a lower lymphatic tone than non-active segments. This difference is tone was attributed to an NO-dependent mechanism that altered tone via intrinsic flow-induced NO, as these effects were abolished after NO-synthase blockade using L-NAME (Gasheva *et al* 2006). These studies suggest that the vessel has a self-regulating mechanism where the active lymph pump is temporarily inhibited when filling occurs in a lymphangion. In contrast, in

segments with no flow, contractile activity was not inhibited. Thus, it is apparent that these vessels not only generate and propel flow through phasic contractions but also are capable of regulating flow via tonic contractions comparable to the tonic contractions in blood vessels that regulate blood pressure and flow. This gives a wider understanding of the role of NO in modulating contractile activity continuously in response to changes in local need. At low levels of inflow, low NO release will maintain a lymphatic pumping pattern whereas when flow dominates there is a switch to inhibition of contractions by increased release of NO. Authors describe the flow-mediated relaxation of lymphatics as a regulatory mechanism for an energy-saving efficient mode of lymphatic pumping (stronger, but fewer contractions per minute). This mechanism has also been reviewed thoroughly (Gashev 2008).

As shown in the schematic (Figure 1.7), Bohlen *et al* further validated the inherent role for NO in modulating intrinsic pumping activity of the collecting lymphatics during the contraction cycle. The initiation of lymphatic contraction triggers a transient rise in NO levels near the vessel wall within 1-3 s. With the concomitant rise in flow/shear stress, the valvular and tubular sections of the lymphatics increase their generation of NO, with the highest concentration of NO in the valve-bulb region and lower concentrations in the tubular portions of rat mesenteric lymphatics. Immunohistochemical analysis confirms a higher expression of eNOS in the bulb compared to tubular regions, possibly due to the increased density of ECs in the leaflets. It is therefore likely that the lymph flowing through the open valve leaflets exerts a high-shear force contributing to elevated levels of NO near the valve (Bohlen *et al* 2009; Bohlen *et al* 2011).

From the studies discussed above, it appears that there are two distinct mechanisms occurring during high steady-state imposed flow and phasic low-level shear patterns generated by intrinsic lymph pumping. Taken together, these studies reveal a high level of complexity in the shear-dependent regulatory mechanisms in lymphatic vessels.

After contraction, flow through the segment generates NO in the valvular region that results in dilation and improves the diastolic filling.

Valvular region

Tubular region

Contracting lymphangion; closed valve

Dilated lymphangion; open valve
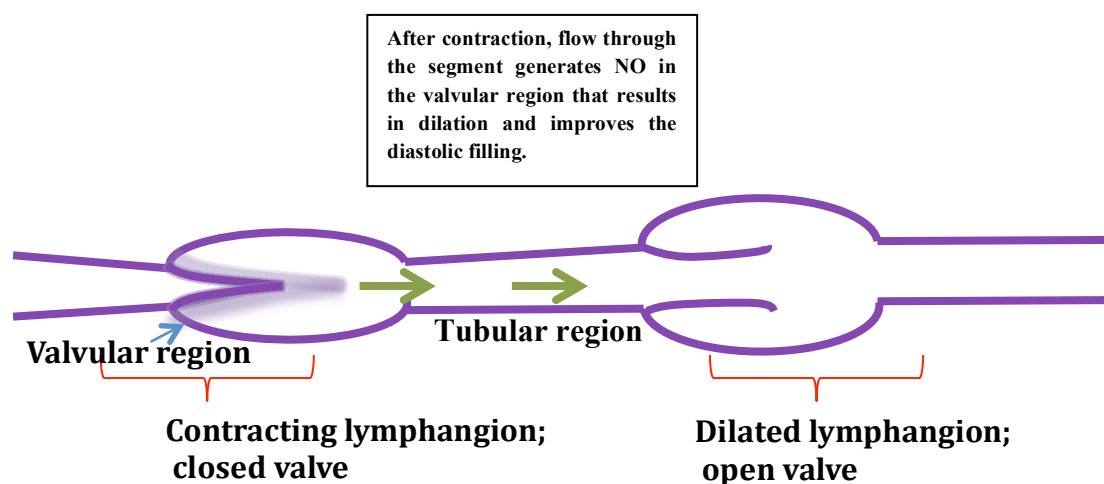
Figure 1.7 Simple schematic of systolic and diastolic phases of lymphatic contraction regulated by basal NO. It is hypothesised that contraction of the lymphangion results in increased flow and shear stress (depicted by shaded region), which stimulates NO production, allowing the diastolic filling to occur. Degradation of NO constricts the vessel, driving flow into the next lymphangion. Phasically generated spike-release of NO during low levels of lymph flow maintains pump function (Bohlen *et al* 2009).

1.2.2.2 Neural and humoral factors

Neural and humoral factors can also modulate intrinsic lymphatic pump activity and the tonic contraction/relaxation of the lymphatic muscle. Humoral factors such as prostanoids, leukotrienes, neuropeptides, catecholamines, natriuretic factors, reactive oxygen radicals and other traditional inflammatory mediators modulate lymphatic vessel contractility and lymph flow (Zawieja 2005). In addition, neuromediators important in immune and inflammatory responses, such as substance P, calcitonin gene related peptide (CGRP), neuropeptide Y or vasoactive intestinal polypeptide (VIP), have also been reported to strongly modulate lymphatic vessel contractility. It has been widely demonstrated that mediators such as NO and prostanoids such as prostacyclin and PGE_2 cause the lymphatic muscle to hyperpolarize inhibiting lymphatic contractility while on the other hand, PGH_2/TXA_2 increase it (Liao and von der Weid 2014). Among these, endogenous NO has emerged as a major player in modulating lymphatic function and lymph flow as discussed above.

1.2.2.2.1 Role of NO in modulation of lymphatic function

The collecting lymphatic vessel is influenced by multiple sources of NO under phyisological conditions. The main sources are : (1) eNOS in LECs produced due to shear-stress or pharmacological stimulation; (2) iNOS in immune cells or lymphatic muscle cells. Under inflammatory conditions, stromal cells can also produce NO via iNOS, independent of the endothelium (Chakraborty *et al* 2015; Munn 2015).

The following section will focus on the role of NO produced from eNOS in the lymphatic endothelium. As in the blood vasculature, eNOS-derived NO in the LEC layer in response to shear stress or flow activates the NO/cyclic guanosine 5'monophosphate (cGMP) pathway causing SMC relaxation through multiple cGMP-dependent protein kinases (PKG) (Ohhashi and Yokoyama 1994; von der Weid 2001). This intrinsic flow-induced/NO-dependent relaxation of lymphatic vessel was inhibited by a cGMP/PKG inhibitor and thus shown to be mediated via the cGMP/PKG regulatory pathway (Gasheva *et al* 2013).

Numerous *in vitro* and *in vivo* studies have demonstrated a role for NO in modulation of lymphatic pumping. Acetylcholine (Ach)-induced lymphatic smooth muscle relaxations are mainly mediated through the release of endothelial NO. ACh-induced NO and exogenous NO released by SNP (Sodium Nitroprusside, NO donor) reduced the frequency and amplitude of the rhythmic pump activity in isolated bovine mesenteric collecting lymph vessels (Yokoyama and Ohhashi 1993). von der Weid demonstrated that the lymphatic endothelium released NO endogenously to decrease the efficacy of STDs in guinea pig mesenteric lymph vessels. The reduction of STD frequency and amplitude was independent of the NO-mediated hyperpolarisation of the smooth muscle due to activation of K_{ATP} channels (von der Weid 1998). NO inhibited contractility primarily by production of cGMP via activation of both cGMP and cyclic-AMP-dependent protein kinases which in turn probably acted on the underlying $Ins(1,4,5)P_3$ receptor-mediated Ca^{2+} release from intracellular stores (von der Weid *et al* 2001; Ohhashi *et al* 2005). Thus, evidence from *in vitro* studies suggests that NO has an important role in modulating tone and vasomotion. Results from an *in vivo* study by Shirasawa *et al* suggested a potential role for eNOS in regulating lymph flow as 15-min superfusion of L-NAME in the mesenteric lymphatics caused a significant increase of frequency accompanied by a decrease in

diameter whereas a 15-min superfusion of aminoguanidine (iNOS inhibitor) caused no significant effect on frequency or diameter (Shirasawa *et al* 2000).

Furthermore, a study using eNOS$^{-/-}$ mice demonstrated enhanced constriction in the collecting lymphatics compared to wild type (WT) controls, which resulted in decreased total lymph flow (Hagendoorn *et al* 2004). Scallan and Davis studied isolated popliteal lymphatic vessels from eNOS$^{-/-}$ mice and WT mice during acute NO inhibition (exposure to L-NAME for 20 min), and found that NO ablation led to increased contraction amplitude and modest increases in frequency (Scallan and Davis 2013). However, Liao *et al* made conflicting observations in popliteal lymphatic vessels of both eNOS$^{-/-}$ mice and WT mice subjected to prolonged NOS inhibition (3 days of L-NMMA infusion), which exhibited elevated frequency, reduced amplitude and increased diameter (Liao *et al* 2011). It was hence proposed by Scallan and Davis that basal NO may possibly play a role in setting contractile amplitude at a level that can be increased or decreased to modulate lymph flow and that a small change in local concentration affects contraction strength in collecting lymphatic vessels. For example, in cutaneous hypersensitivity (CHS)-induced skin inflammation, NO has been shown to influence the contraction strength through changes in local concentration (Lachance *et al* 2013).

From the above studies, it appears that basal levels of eNOS are required for lymph propulsion and a decrease in these might lead to decreased lymph propulsion. The understanding of the role of NO to date as summarised in a current review is as follows. Relatively high concentrations of NO induced by agonists or high steady-state imposed flow inhibit both contraction frequency and amplitude whereas lower (basal) levels of NO are thought to decrease frequency but increase contraction strength/amplitude; however the latter opinion has been derived from experiments performed in rat thoracic duct under conditions where pressure was not variable. In collecting lymphatics, basal NO production depressed or strengthened contraction amplitude but not frequency in proportion to pressure changes (Chakraborty *et al* 2015). Thus, it is evident that basal NO production is needed for active lymph propulsion. In inflammatory conditions such as sepsis, both depleted levels of eNOS and increased levels of NO are generated by immune cells, such as macrophages, or by inflamed tissues, such as smooth muscle could certainly depress the pumping activity to an extent that halts the lymph propulsion.

As discussed in this section, multiple mechanisms regulate both the tonic and phasic components of lymphatic vessel pumping, thereby constantly adjusting vessel pumping ability to the combination mechanical forces and biochemical factors influencing the vessel environment (Gashev 2008; Munn 2015).

1.2.3 Lymphatic endothelial cell biology

LECs share many similiarities with blood vascular endothelial cells (BECs). They express most of the common EC markers for BECs including von Willebrand factor, CD31 and CD34. More exclusively they express lymphatic vessel endothelial hyaluronan receptor 1 (LYVE-1) (Oliver 2004), prospero-related homeobox 1 (Prox-1) (Wigle and Oliver 1999), podoplanin (Kriehuber *et al* 2001), and vascular endothelial growth factor receptor 3 (VEGFR-3) (Makinen *et al* 2001). Receptors of the tyrosine kinase family such as VEGFR-3 play an important role in the proliferation, migration and permeability of LECs (Swartz 2001; Pepper and Skobe 2003).

1.2.4 Lymphatics in disease

Dysfunction of the lymphatic system has been implicated in many diseases such as Milroy disease associated with primary lymphoedema and filariasis associated with secondary lymphoedema. When lymphatic channels are absent or blocked, plasma filtered out from the blood stream accumulates as protein-rich oedema. This state of static insufficiency or low output failure of lymph flow is generally termed as lymphoedema. Primary lymphoedema is a congenital disorder whereas secondary lymphoedema can arise from inflammation, obstruction following surgery or irradiation of tumours (Stucker *et al* 2008). In contrast, when microvascular filtration rises to an extent that it overloads the lymphatic machinery, a lymphoedematous state of dynamic insufficiency or high output failure of lymph flow arises (Johnston 1989). This occurs mainly in inflammatory diseases like inflammatory bowel disease, Crohn's disease and sepsis (Wu *et al* 2005; Wang and Oliver 2010).

1.2.4.1 Lymphatics and sepsis

One of the major pathologies resulting from sepsis is oedema. Development of oedema results from a simple hydrodynamic principle – the rate of lymph formation exceeds the rate of lymph return. These factors are in balance with each other under normal physiological conditions and in healthy individuals.

Oedema during sepsis may arise from:

1) Excess fluid in interstitum resulting in increased interstitial osmotic pressure due to increased permeability of post-capillary venules, inhibiting lymph uptake by the lymphatic capillaries

2) Intial lymphatics maintaining their drainage capacity but become overloaded resulting in a failure to decrease the intralymphatic pressure required for uptake from interstitium (The initial lymphatics work via an oscillatory pump mechanism where high interstitial pressure compared to intralymphatic pressure pulls them open). This overload may be due to impaired lymph propulsion by the collecting lymphatics.

3) Increased permeability of initial and collecting lymphatic vessels. Vessels are rendered leaky, overwhelming the interstitium with lymph (Brookes *et al* 2009; Aldrich and Sevick-Muraca 2013).

4) Damage to interstitial-lymphatic connections or changes in ECM composition (Swartz 2001).

The responses induced in the lymphatic system may occur due to inflammatory mediators or by direct effects of endotoxin. Endotoxin interactions with blood vessel endothelium has been shown to trigger devastating inflammatory cascades resulting in widespread microvascular permeability, vascular tone and altered blood haemodynamics (Dauphinee and Karsan 2006). However, there are only a few studies documenting the effects of endotoxin on the lymphatic vessels. Studies dating back to 1987 reported decreased lymphatic contractile activity (frequency and amplitude of contraction) following intravenous endotoxin administration in sheep intestinal lymphatics. Lymph flow rates increased for the first 40 min of endotoxin administration and then declined (Elias *et al* 1987). Additionally, Elias *et al* reported that endotoxin had no direct effect on the lymphatic vessels, the responses were suggested to be due to induced inflammatory mediators. However, a study done on endotoxin treated bovine mesenteric lymphatic vessels excluding flow (which contains humoral or cellular elements) decreased lymphatic pumping activity (Lobov and Kubyshkina 2004). Thus, direct effects of endotoxin may also impair lymphatic function resulting in oedema. In addition, LPS activated macrophages that enter the lymphatic vessels have been reported to release NO and prostaglandin, inhibiting

vessel contractions (Ohhashi *et al* 2005; Plaku and von der Weid 2006). More recent evidence of impaired pumping activity in lymphatics has emerged from a study, in which acute challenge with LPS in an endotoxemic guinea pig model showed increased pumping activity, resulting in rapidly increasing lymph flow during the first two hours of the challenge which remains elevated in later phase despite cessation of pumping activity (Nemoto *et al* 2011).

Mesenteric lymphatics play a central role in pathological responses to haemorrhagic shock, trauma and intestinal ischemia. Mesenteric lymph has also been implicated in transporting gut-derived inflammatory factors to other splanchnic organs during bacterial translocation after gut barrier failure and/or gut-derived sepsis in ICU patients, inducing a systemic inflammatory response that culminates into organ injury. *In vitro* studies show that post-shock mesenteric lymph from rats activates neutrophils, increases human umbilical vein and rat microvascular pulmonary artery endothelial cell permeability and causes EC injury. Injection of shocked lymph into healthy rats recreates a systemic septic state and causes MODS (Deitch *et al* 2006). Although the exact nature of these inflammatory factors remains to be determined, these factors maybe microbial (Deitch 2012) or non-microbial (Deitch *et al* 2006; Fanous *et al* 2007) and have been reported to initiate tissue injury through iNOS- and TLR4-dependent pathways (Deitch 2010).

However, the direct effects of these mediators on the lymphatic system are less well characterised with only a few research groups worldwide investigating the responses and mechanisms in this important system.

1.2.5 Lymphatics and inflammation

Inflammatory conditions usually alter the contractile behaviour in collecting lymphatic vessels instead of vessel density. Upon inflammatory stimulation, vessels undergo changes that are characterised first by loss of vessel tone and reduced contraction frequency, which affect the lymph transport capacity. These changes have been demonstrated in three different models of inflammation. Impaired lymphatic contractile activity and vessel dilation have been reported in a rat model of peritonitis (Umarova *et al* 2006), in a model of experimental ileitis in guinea pigs (Wu *et al* 2006) and lymphatic contractions were also suppressed in an oxazolone-induced acute skin inflammation in mice (Liao *et al* 2011). However, studies show that inflammation

induces both augmentation and reduction of lymphatic flow. For example, acute intestinal challenge with the inflammatory peptide N-formyl-methionyl-leucyl-phenylalanine (fMLP) (Benoit and Zawieja 1992), and oedemagenic stress (Benoit *et al* 1989), enhanced pumping activity in rat mesenteric lymphatics which has been suggested to lead to increase in lymph flow. These differences indicate that lymphatic pumping function is greatly impacted by the nature of the inflammatory stimulus (Aebischer *et al* 2014).

Molecules like NO and prostanoids that are strongly upregulated during the inflammatory process have powerful effects on lymphatic pumping during inflammation. Indeed, the inhibition of mesenteric lymphatic pumping during 2,4,6-trinitrobenzenesulfonic acid (TNBS)-induced ileitis in guinea pigs due to increased production of both NO and prostaglandins, has been demonstrated (Wu *et al* 2006). NO produced by immune cells surrounding collecting lymphatic vessels and in adjacent spaces of the interstitium has been shown to disrupt lymphatic function. For example, iNOS-expressing CD11b$^+$Gr-1$^+$ myeloid cells have been shown to attenuate lymphatic contraction by disrupting the NO gradients produced by eNOS under inflammatory conditions in mouse popliteal lymphatics *in situ*. Furthermore, NO produced via iNOS may cause chronic relaxation of peri-lymphatic SMCs, decreasing tone and inotropy, thus reducing the strength of contraction (Liao *et al* 2011).

Cytokines produced during inflammation have been shown to exert negative effects on LECs directly by altering barrier function *in vitro* (Chaitanya *et al* 2010). A recently published study using non-invasive near-infrared fluorescence (NIFR) imaging showed systemically decreased lymphatic propulsion as early as 4 h after separate intradermal administration of TNF-α, IL-1β and IL-6 in mice suggesting a pivotal role of cytokines in modulating lymphatic function (Aldrich and Sevick-Muraca 2013). Importantly, these effects were noted to be NO-dependent.

The lymphatic endothelium may have its own unique role in orchestrating the immune response to inflammatory mediators that are transported via the lymphatic vessel. LECs respond to inflammatory cytokines and bacterial antigens by up-regulating chemokines, adhesion molecules, and other cytokines. Lymphatic vessels drain lymphocytes, antigen presenting DCs, macrophages and soluble antigens from the site of infection transporting them to lymph nodes which is an immune-response mounting

zone (Pepper and Skobe 2003). The initial lymphatic endothelium is actively involved in driving lymphocyte and DC transmigration towards the lymphatics. The mechanism for this is via LEC release of chemokine CCL21, a ligand for chemokine receptor CCR7 expressed on DCs in response to inflammatory stimuli (Jurisic and Detmar 2009). Directed by chemokines CCL19 and CCL21 produced in the T cell zone, the activated DCs migrate to it and upon interaction with the T lymphocytes, mount an antigen specific T cell response (Liao and von der Weid 2014). Furthermore, LECs express a large repertoire of TLR molecules comprised of TLR1-6 and TLR9 (Pegu *et al* 2008) and increase the expression of TNF-α, IL-1β, IL-6, IL-8, VCAM-1, and ICAM-1 by TLR4 mediated recognition of LPS (Sawa *et al* 2008). iNOS induction has been shown in LECs and lymphatic SMCs in response to LPS (Robertson *et al* 2004). At the molecular level, the inflammatory response is under the transcriptional regulation of NF-κB, which is constitutively active in the lymphatic vasculature (von der Weid and Muthuchamy 2010). However, a dysregulated inflammatory response leads to impaired lymphatic function as evident from the studies mentioned earlier.

Collectively, this section highlights the role of the lymphatic endothelium in the development of immune and inflammatory responses and the effects of inflammation on collecting lymphatic vessels. This role has also been reviewed in detail recently (Liao and von der Weid 2014). Further investigations to better understand the mechanisms of lymphatic function regulation during inflammation are essentially required.

1.2.6 Lymphatic vessel permeability

Lymphatic endothelial barrier function has not been delineated so far, however it is very likely modulated during inflammation. A recent study demonstrated increased endothelial permeability to FITC-albumin in cultured LEC monolayer, following treatment with pro-inflammatory cytokines TNF-α, IL-6, IL-1β, IFN-γ and with LPS. The authors further showed that this effect was sensitive to NO blockade by L-NAME for all cytokines except IL-1β and LPS and accompanied by down-regulation of VE-cadherin protein levels in LECs (Cromer *et al* 2014). Whether lymphatic pumping is influenced by the increased permeability or the cytokines themselves was not investigated in this study. Indeed the current literature reports few studies to date that

have evaluated the direct effect of cytokines on lymphatic pumping (Hanley *et al* 1989).

According to their observations, Lynch *et al* suggested that the function of the initial lymphatic endothelial barrier or primary valves may be compromised during inflammation (Lynch *et al* 2007). Since the initial lymphatics and the collecting lymphatics exist in continuum, a speculative assumption can be made that the endothelial barrier may be compromised in the collecting lymphatic vessel during inflammation contributing to increased leakage of fluid. Collecting lymphatics have predominantly closed junctions facilitating effective propulsion of lymph. Experiments performed during the 1960s concluded that the lymphatic system retains all solutes with molecular mass larger than MW 2300–6000 (Mayerson, 1963). Consistently, Ono *et al* suggested that small molecular hydrophilic substances (MW 4,400) are permeable from the intraluminal to extraluminal compartment of isolated pre-nodal lymph vessels and that the LECs may play a barrier role in the permeability of large molecular hydrophilic substances (MW 4,400 to 12,000) through the wall of these vessels (Ono *et al* 2005). More recently, studies showed that permeability to albumin does not differ between venules and collecting lymphatic vessels, with a role for the collecting vessels in solute exchange speculated (Scallan and Huxley 2010). Furthermore, a study examining size-dependent regulation of permeability of the lymphatic endothelium to hydrophilic substances revealed that LEC layers allowed the passage of 4 kDa dextran, but not 12 or 66 kDa dextran. TNF-α or IL-1β significantly increased the permeability of human LECs (obtained from afferent lymph vessels nearest to the sentinel lymph node) to 4 and 12 kDa dextran via Rho kinase activation and the ERK 1/2 mediated F-actin redistribution in the LEC (Kawai *et al* 2014). These findings reflect a key role for the LEC layer in the transport of hydrophilic substances through the collecting lymphatic vessel wall.

The lymphatic endothelium is actively involved in the regulation of fluid and cell transport. One study explored the function of the endothelium in this respect particularly in inflammation and tissue injury and showed that the lymphatic endothelium is highly responsive to heightened transmural flow. Particularly of relevance to our interest, were the results demonstrating increased lymphatic permeability measured by the functional uptake of dextran in mice tail and an *in vitro* permeability assay, consistent with reorganization and downregulation of PECAM-1

and VE-cadherin. These findings suggest that transmural flow might serve as an early inflammatory cue for lymphatics, (Miteva *et al* 2010) and changes in lymphatic permeability may also be associated with large changes in fluid preload (input pressure) that have been shown to significantly affect contractile function.

It is possible that in an inflammatory state, permeability increases whereupon lymph leaks into the tissue space, thereby compromising lymphatic function. ECs of collecting lymphatic vessels are joined by continuous zippers, similar to those in adjacent blood vessels. Inactivation of VE-cadherin at AJs, by administration of a function-blocking antibody, resulted in dispersion of VE-cadherin at zippers in lymphatics, similar to previous studies of junctions in blood vessels (Baluk *et al* 2007). More recently, dermal LECs treated with TNF-α showed a redistribution of both AJs and TJs exhibiting a dominant discontinuous morphology (Kakei *et al* 2014). Another study showed a strong downregulation in the expression of TJ molecules claudin-5 and ZO-1 in the inflamed lymphatic vessels of UVB-exposed WT mice and a marked increase in permeability of LECs after claudin-5 knockdown (Kajiya *et al* 2012). Thus, permeability mechanisms similar to those in blood vessels may be operating in the lymphatic vessels and this needs further investigation.

The studies reviewed in this section provide overwhelming evidence that inflammatory mediators released or gaining entry into the lymphatic vessel during inflammatory conditions affect vessel function. Hence, the mechanisms modulating this is a crucial area of investigation in order to interpret the pathophysiological events occurring in lymphatics in inflammatory conditions. Besides investigating the pathophysiology of lymphatics in inflammatory conditions, this project will also investigate the effects of angiopoietins on lymphatics. The angiopoietin (Ang) signaling system has been defined as a major endogenous cell signaling system that helps maintain vascular stability through anti-inflammatory and anti-hyperpermeability mechanisms (Fukuhara *et al* 2010). The following section explores the potential of angiopoietins as a therapeutic target for improving lymphatic function during sepsis.

1.3 Angiopoietins

The discovery of angiopoietin ligands and their corresponding Tie receptor more than a decade ago introduced a vascular specific receptor tyrosine kinase signaling system with important roles in angiogenic remodelling and stabilisation of blood and lymphatic vessels (Augustin and Fieldler 2008).

1.3.1 The Tie Receptors

Two Tie receptors, Tie-1 and Tie-2 have been identified which are receptor tyrosine kinases consisting of an N-terminal angiopoietin binding domain and a C-terminal tyrosine kinase domain (Figure 1.8). They are predominantly expressed by ECs of the blood and lymphatic vessels and hematopoietic stem cells. Tie-2 is constitutively expressed whereas Tie-1 expression is upregulated by shear stress (Augustin and Fiedler 2008).
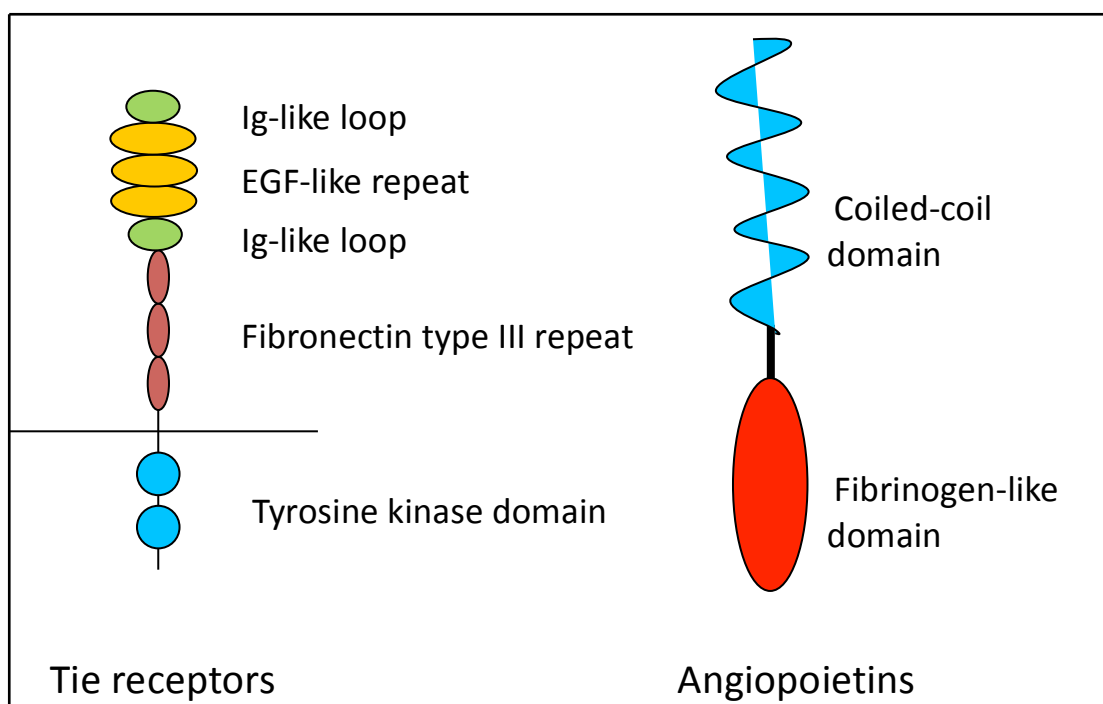
Figure 1.8 Structure of Tie receptors and angiopoietins (Adapted from Augustin and Feidler, 2008).

1.3.2 The Angiopoietins

The angiopoietin family includes four ligands Ang-1, Ang-2 and Ang-3/4 and two corresponding tyrosine kinase receptors, Tie-1 and Tie-2. Ang-1 and Ang-2 are well known ligands of Tie-2 which act as an agonist and antagonist respectively in the blood vasculature but as agonists in the lymphatic vasculature. Two other ligands, Ang-3 and Ang-4 have also been identified; Ang-3 is the mouse orthologue of Ang-4 and acts as a species specific Tie-2 antagonist whereas Ang-4 is an agonist. No ligand has been identified for Tie-1 to date. The angiopoietins are secreted glycoproteins consisting of an N-terminal coiled-coil oligomerizing domain and a C-terminal fibrinogen-like Tie-2 binding domain (Figure 1.8). Ang-1 has a multimeric conformation and is expressed by many cell-types including pericytes, SMCs and fibroblasts. Studies with recombinant forms of Ang-1 have shown that tetrameric forms are necessary for the activation of Tie-2 in ECs. Owing to its constitutive expression, Tie-2 is found to be constitutively activated by Ang-1. In contrast, Ang-2 has a strictly regulated expression exclusively in ECs where it is stored in Weibel-Palade bodies at low levels (Augustin and Fieldler 2008; (Kobayashi and Lin 2005).

1.3.3 Role of Angiopoietin/Tie system in the embryogenic and adult vasculature

The Ang-Tie system is not required for vasculogenesis or for the initial embryonic formation of the lymphatic vasculature. However, both the Tie receptors are critical during later phases of embryonic and postnatal development for subsequent remodeling and maturation of the blood and lymphatic vasculatures (Thurston 2003). Tie-1 and Tie-2 deficient mice die during embryogenesis due to reduced vascular integrity which results in impaired cardiac function, hemorrhage and microvessel rupture. Throughout the embryo, blood vessels do not remodel or form heirarchical networks. Tie-2 expression was shown by immunohistochemical staining to be present in developing lymphatics throughout embryonic and neonatal life and in LYVE-1 positive lymphatic vessels of adult mouse ear skin and small intestine (Wu and Liu 2010). The specific role of Tie-2 in development and maintenance of the lymphatic vasculature remains unclear as Tie-2 was undetectable in lymphatic vessels in Tie-2 GFP transgenic mice (Dellinger *et al* 2008). Tie-1 is known to regulate the binding of ligands to Tie-2 and modulate its signaling by preventing Tie-2 activation (Hansen *et al* 2010). Recent work also suggests that Ang-1 can induce Tie-1 phosphorylation in

cultured LECs, and BECs in a Tie-2-dependent manner and recruit both Tie-1 and Tie-2 to cell-cell contacts (Wu and Liu 2010).

Ang-1 deficient mice show a phenotype similar to Tie-2 deficient mice indicating that Ang-1 is an indispensable ligand for Tie-2 (Saharinen *et al* 2008). Transgenic Ang-1 overexpressing neonatal mice show enlarged vessels covered by pericytes. A striking observation in these transgenic mice was the formation of leakage resistant blood vessels in both neonatal and adult mice (Thurston *et al* 2005). Thus, Ang-1 plays a key role in promoting blood vessel integrity in the adult vasculature, in addition to other critical primary functions such as vessel remodelling and stabilisation during vascular development. Ang-1 is the primary regulator of vascular quiescence in the adult vasculature as suggested by its ability to initiate cell survival signals and prevent activation of endothelium in some studies. Ang-1 is also involved in physiological and pathological angiogenesis and lymphangiogenesis which have been observed in models of over expression (Morisada *et al* 2005; Tammela *et al* 2005). However, the pro-angiogenic role of Ang-1 is rather controversial and appears to depend on a milieu of other angiogenic signals (Eklund and Olsen 2006).

In contrast, Ang-2 null mice appear to have defects only in the lymphatic vasculature with the lymphatic vessels in the intestine being disorganized and less branched. The lymphatic was rescued by Ang-1 knocked into the Ang-2 locus suggesting redundant roles for Ang-1 and Ang-2 as Tie-2 agonists in the lymphatic vasculature (Gale *et al* 2002). However, strong systemic expression of Ang-2 results in embryonic lethality and phenotypic characteristics similar to that of Ang-1 and Tie-2 knockout mice, confirming its antagonist functions during development in the vasculature (Augustin and Fieldler 2008; (Saharinen *et al* 2008).

1.3.4 Protective effects of Angiopoietin-1

Due to the involvement of angiopoietins in regulating vessel permeability and the increased vascular permeability during sepsis, several preclinical studies have shown that Ang-1 has many potential clinical benefits in the treatment of vascular inflammation, leakage and tissue oedema. Initially, it was shown that Ang-1 overexpression in mice resulted in the formation of leakage-resistant blood vessels covered by pericytes (Thurston *et al* 1999). This group further reported a vessel sealing effect mediated by Ang-1 delivered via adenovirus (Ad.Ang-1) in mice against various inflammatory agents (Thurston *et al* 2000). Ang-1 also inhibited VEGF-induced pro-inflammatory adhesion molecule expression including ICAM-1, VCAM-1 and E-Selectin in human umbilical vein endothelial cells (HUVECs), thus reducing leukocyte adhesion (Kim *et al* 2001). In the adult vasculature, Ang-1 restricted the number and size of gaps at the inter-endothelial junctions of inflamed venules, thereby reducing inflammation-induced EC permeability (Baffert *et al* 2006). More recently, it was found that Ang-1-Tie2 binding could block LPS-induced activation of NF-κB in macrophages (Gu *et al* 2010). Thus, the anti-permeability and anti-inflammatory effects are evident from these studies and demonstrate potential to exploit as a therapeutic agent in clinical studies.

1.3.5 Protective effects of Angiopoeitin-1 in endotoxemia

Ang-1 cell-based and gene-based therapies have improved survival in various models of endotoxemia (Novotny *et al* 2009). Investigators have shown that LPS attenuates Ang-1 and Tie-2 expression in liver, diaphragm and lung contributing to enhanced leakage during endotoxemia (Mofarrahi *et al* 2008). Witzenbichler *et al* demonstrated that mice over expressing Ad.Ang-1 were more resistant to endotoxic shock and were protected from systemic leakage as indicated by reduced oedema in the lungs. Expression of the leukocyte adhesion molecules E-selectin, ICAM-1, and VCAM-1 was also suppressed (Witzenbichler *et al* 2005). Similar observations were reported in an acute-lung injury model (Huang *et al* 2008). More stable and equally potent variants of Ang-1 have also attenuated vascular leakage in models of endotoxic shock. Hwang *et al* have shown restoration of PECAM-1 levels by COMP.Ang-1 (see below), subsequently reducing leukocyte extravasation (Hwang *et al* 2009). Recent data from our lab has also shown that matrillin Ang-1 (MAT.Ang-1) (see below), another variant

of Ang-1 reduces microvascular leakage and improves blood flow in septic mice (Alfieri *et al* 2012). These findings provide strong evidence for a crucial anti-inflammatory and anti-permeability effect of Ang-1 during sepsis.

1.3.6 Ang-1 variants

Due to the concerns over biosafety of adenoviral vectors, Cho *et al* developed Ang-1 variants containing a minimal coiled-coil domain, which retained the property of oligomerization and was short enough to avoid problems of aggregation and insolubility (Cho *et al* 2004). Septic shock is a condition with widespread inflammation and gene therapy using adenoviral vectors may pose the danger of adverse inflammatory reactions that may occur from incomplete inactivation of the viral replication machinery (Ye *et al* 2007). Morevoer, large-scale production of recombinant Ang-1 is limited by the aggregation and insolubility of the protein and the protein activity often varies after purification. Cartilage oligomeric matrix protein Ang-1 (COMP.Ang-1) and MAT.Ang-1 are highly soluble, stable and potent forms of human Ang-1 that form mainly pentamers and tetramers respectively. In MAT.Ang-1, the N-terminal domain has been exchanged for the shorter domain of Chicken Matrillin-1. Similarly, in COMP.Ang-1, N-terminal portion is replaced with short coiled-coil domain of cartilage oligomeric matrix protein (Cho *et al* 2004).

1.3.7 Angiopoietin/Tie induced vascular signaling

Each of the five autophosphorylated tyrosine residues of the Tie-2 receptor activates a different signaling pathway by interacting with specific signaling molecules (Augustin and Fieldler 2008). Figure 1.9 depicts the signaling pathways activated by Ang-1 in ECs. The PI3K and ERK1/2 pathway form the major signaling cascades that together mediate the endothelial cell survival, proliferation, cell-migration, motility, anti-permeability and anti-inflammatory effects of Ang-1 (Eklund and Olsen 2006). P85, the regulatory subunit of PI3 kinase interacts with phosphorylated Tie-2 activating cell survival kinase Akt. Ang-1 cell survival effects are mediated by phosphorylation and inhibition of the forkhead transcription factor Foxo1 (known to up-regulate expression of genes associated with vascular destabilization and endothelial cell apoptosis) following Akt activation which contributes to endothelial cell survival and blood vessel stability. A role for A20 binding inhibitor of NF-κB activation 2 (ABIN-2) in Ang-1-induced anti-inflammatory effects has been shown. ABIN-2 is recruited to Tie-

2 by Ang-1 and protects EC inflammatory gene expression by inhibiting NF-κB activation (Fukuhara *et al* 2010).
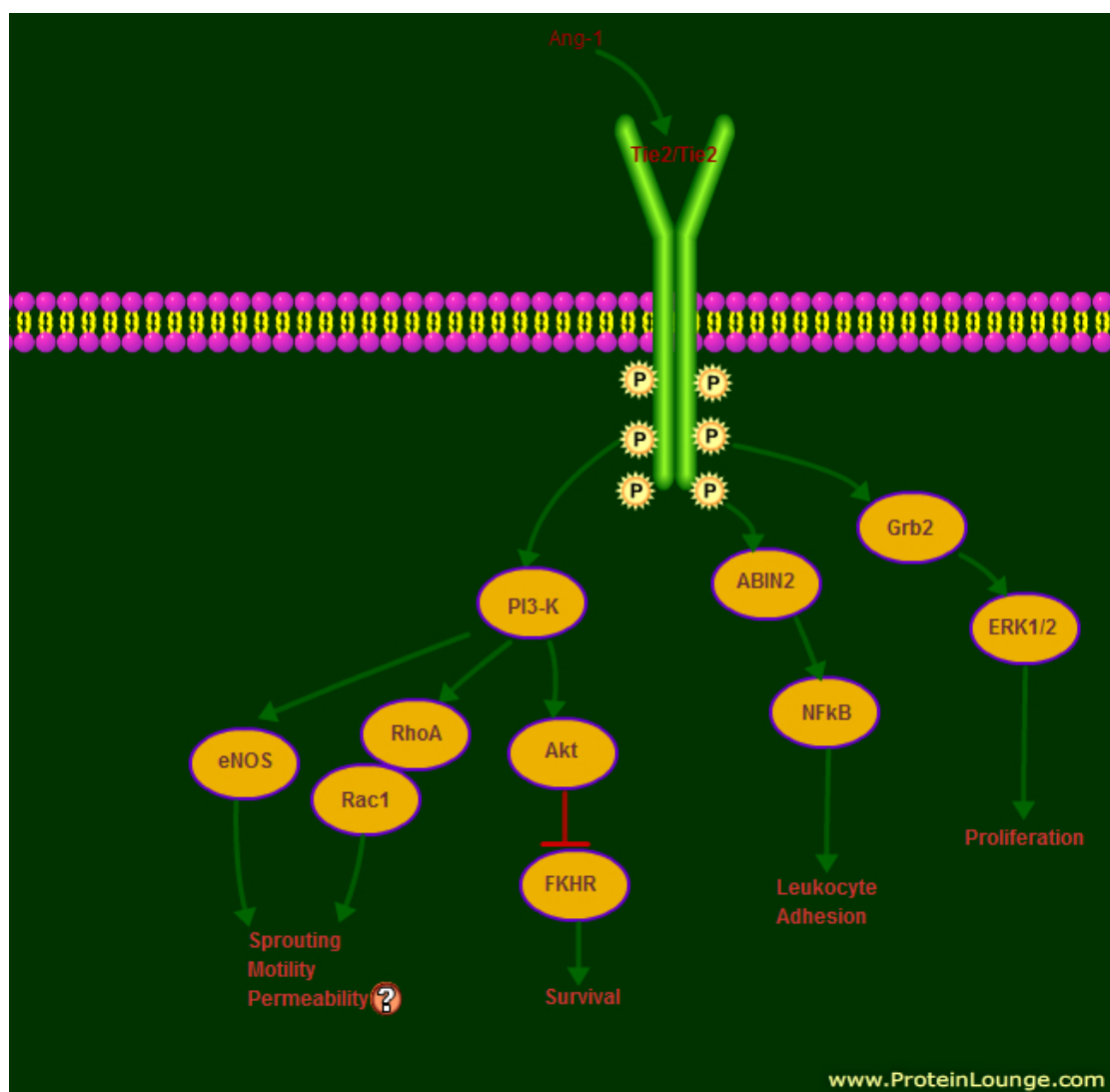
Figure 1.9 Schematic representation of signaling pathways activated by Ang-1 in ECs. Various cellular functions regulated by Ang-1 are indicated in red. Ang-1 activated PI3K (i) promotes cell survival via stimulation of Akt that results in inhibition of FKHR (also known as Foxo1) (ii) increases endothelial motility by activating GTPases RhoA and Rac1 (iii) phosphorylates eNOS which potentially plays a role in reducing endothelial permeability. ERK1/2 stimulation induces EC proliferation via its ability to recruit Grb2 and ABIN-2 inhibits leukocyte adhesion via NF-κB. FKHR- Forkhead transcription factor; Grb2- Growth factor receptor-bound protein 2. Adapted from (Brindle et al 2006).

Two groups have unravelled the mechanisms involved in anti-permeability/vessel stabilizing effects of Ang-1. They showed that in ECs with intact cell-cell adhesion, Tie-2 is recruited in response to Ang-1 at the cell-cell contact forming a distinct signaling complex. In contrast, cells with absent cell-cell adhesions have Tie-2 complex anchored to the cell-ECM interface by Ang-1 (Fukuhara *et al* 2008; Saharinen *et al* 2008). Tie-2 expressed in adjacent cells trans-associate via a bridge formed by the multimeric Ang-1 molecule resulting in a homophilic bonding. The Akt pathway is preferentially activated by the Tie-2 engaged in this complex (Fukuhara *et al* 2008). One of the downstream effector molecules phosphorylated by Akt is eNOS (Eklund and Olsen 2006). Consistently, Saharinen *et al* have reported the phosphorylation of eNOS by Akt and its co-localization at cell-cell junctions (Saharinen *et al* 2008). Hence, it is apparent that the Akt-eNOS pathway has a distinct role in vessel stabilization and permeability, but the specific role of eNOS is not clear yet. Ang-1 has been demonstrated to maintain pulmonary eNOS expression and bioactivity after LPS challenge (Witzenbichler *et al* 2005) and MAT.Ang-1 sustained the increase in abdominal muscle tissue eNOS expression during endotoxemia in studies published from our lab (Alfieri *et al* 2012), thus providing direct evidence that the beneficial effect of Ang-1 is likely to be mediated by eNOS-derived NO. Ang-1 also maintained vascular reactivity in hypoxia-treated superior mesenteric arteries with intact endothelium from haemorrhagic-shock rats through the Tie-2-Akt-eNOS pathway (Xu *et al* 2012).

The co-localization of VE-PTP with Tie-2 at cell-cell contacts has also been reported as another mechanism through which AJs maintain vascular stability (Saharinen *et al* 2008). VE-PTP (essential for maintenance and remodelling of the blood vascular system) has been shown to form a complex with Tie-2 and promote dephosphorylation acting as a critical modulator of Tie-2 signaling (Augustin and Fieldler 2008). Thus, during conditions of increased permeability, recruitment of VE-PTP by this activated complex may introduce more VE-PTP to VE-cadherin, reduce the tyrosine phosphorylation of VE-cadherin, which strengthens the AJs in addition to the Tie-2 bridge (Nawroth *et al* 2002; Nottebaum *et al* 2008). Ang-1 has been shown to regulate permeability in EC monoloayers via PECAM-1 and VE-cadherin by reducing VE-cadherin phosphorylation and suppressing dissociation of VE-cadherin from β-catenin (Gamble *et al* 2000). Such mechanisms may be involved in the suppression of inter-endothelial leakage in reponse to inflammatory agents like LPS which have been

shown to phosphorylate VE-cadherin (London *et al* 2009). More recent data has shown that Ang-1 promotes lymphatic integrity by modulating TJ molecule expression in lymphatic capillaries and collecting vessels during inflammation. Down-regulation of both claudin-5 and ZO-1 was blocked in UVB-exposed K14-Ang-1 mice and *in vitro* studies revealed that Ang-1 enhanced the stability of LECs via up-regulation of claudin-5, as well as ZO-1 (Kajiya *et al* 2012). A crucial role has thus emerged for Ang-1 in maintaining the integrity of cell-junctions in conjunction with cell-cell adhesion molecules.

There are other possible mechanisms by which Ang-1 reinforces the cell-cell contact during inflammatory conditions, such as those induced by LPS. Ang-1 appears to exert its protective effects on hyperpermeability, in part through inhibition of the intrinsic apoptotic signaling pathway as has been shown in haemorrhagic shock induced rats. Caspase-3 dependent cleavage of β-catenin occurs during apoptosis, a mechanism inhibited by Ang-1 (Childs *et al* 2008). Mechanisms involving inhibition of Rho have also been reported, two members of the Rho family of small GTPases, Rac and Rho increase and decrease barrier function respectively, Rac-mediated inhibition of Rho via p190RhoGAP being critical for the anti-permeability effect of Ang-1 against endotoxin-induced vascular leakage (Mammoto *et al* 2007).

From the mechanisms described above, it is evident that eNOS and VE-cadherin are important components of the complex signaling cascade initiated by Ang-1-Tie2 interaction in ECs. The ability of Ang-1 to inhibit NF-κB driven cytokine production and downregulate iNOS in conjunction with increasing expression of protective eNOS strengthens its potential to maintain lymphatic vessel function during sepsis. Furthermore, its ability to promote junctional integrity by regulating the assembly of adhesion proteins such as VE-cadherin and claudin-5 at EC-EC junctions make it an even more attractive candidate for therapeutic intervention in sepsis.

1.4 Hypothesis

Although a significant body of literature exists on lymphatic vessel dysfunction during sepsis, the effects of potent inflammatory mediators on lymphatic vessel function such as pumping and permeability during early phase of sepsis have not been clearly established previously. This study aimed to elucidate more clearly the effects of inflammatory mediators on collecting lymphatic vessels within the intestinal mesentery by analysing the changes in macromolecular leak and variables such as contraction frequency and amplitude under conditions mimicking sepsis. Further, it aimed to investigate the mechanisms through which inflammatory mediators may modify these variables, mainly the role of NO, a key modulator of lymphatic vessel function. The study also investigated the effects on Ang-1 on lymphatic vessel function. Though the role of Ang-1 in the lymphatic endothelium is largely unexplored, Ang/Tie signaling is an important component of the lymphatic network (Morisada *et al* 2005). It is known that Ang-1 acts as an agonist in the lymphatic vasculature, however its direct effects on the integrity of lymphatics and pump function in inflammatory conditions have not been investigated yet. Ang-1 appears to be a versatile molecule with a wide range of biological functions. It has the theoretical advantage of influencing multiple facets of the septic cascade. This potential therapeutic role of Ang-1 can be harnessed by the much compromised lymphatic system during sepsis. Thus, this thesis will examine the hypothesis that:

Inflammatory mediators released during sepsis compromise lymphatic pump function and increase lymphatic vessel permeability which is improved by Ang-1.

The aims of this project are to investigate whether

1) collecting lymphatic vessels become leaky during sepsis.
2) the pumping mechanism of collecting lymphatic vessels becomes impaired during sepsis and is improved by Ang-1.
3) alterations in lymphatic vessel pumping are mediated via NO regulation.
4) the expression of VE-cadherin in the collecting lymphatic endothelium is altered during sepsis.

These aims will be evaluated using a combination of *in vivo* and *ex vivo* techniques described in the next section.

Chapter Two

Materials and methods

2.1 Preparation of reagents

2.1.1 Conjugation of Fluorescein Isothiocyanate-Bovine Serum Albumin (FITC-BSA)

FITC was conjugated to BSA by a method previously published by our lab (Brookes and Kaufman 2005). FITC isomer I (90%, Sigma-Aldrich) 0.0378g, 2g BSA (98%, Sigma-Aldrich) and 20 ml bicarbonate solution (0.12g Na_2CO_3 (anhydrous), 0.74g $NaHCO_3$) were combined in a large stoppered test tube. The conjugation components were then mixed gently, left overnight and centrifuged at 5000 rcf for 10 min. The supernatant was transferred into an a 15 cm long dialysis tubing (12, 400 MW cut off) and dialysed for 12 h in 2 L of Nairn's solution (17g NaCl, 0.692g $NaH_2PO_4.H_2O$, 2.14g $NaHPO_4$) in a large conical flask. This was replaced with 4 L of fresh Nairn's and stirred for a further 12 h. The dialysis tubing was then removed and FITC-BSA conjugate (~66 kDa) was stored at -20°C in 1ml aliquots in the dark. All steps were performed at < 5°C to avoid denaturing the BSA.

2.1.2 Other Reagents

LPS (*E.coli* serotype 055:B5; 0127:B8): A stock solution of LPS was prepared by dissolving in 0.9 % saline (*in vivo* experiments) or Dulbecco's Phosphate Buffered Saline (DPBS) (*in vitro* experiments) to give a concentration of 5 mg.ml^{-1}, then sonicated for 30 min in an ultrasonic bath. The solution was stored in a glass container at 4°C. On the day of the experiment, the stock solution was diluted in saline to give the appropriate concentration (w/v) for each rat (*in vivo*) or an appropriate volume was added to bath to give a final concentration of 50 µg/ml (*in vitro*).

Sodium thiopental (MW=264.3)**:** A 50 mg.ml^{-1} stock solution of thiopental was prepared by dissolving in 0.9 % saline. On the day of the experiment, thiopental was prepared by diluting the stock solution to give a final concentration of either 10 or 20 mg.ml^{-1}.

N$^\omega$-nitro-L-arginine methyl ester (L-NAME) (FW = 269.69): On the day of the experiment, 10^{-1}M L-NAME was prepared by dissolving 0.2697g L-NAME in 10 ml APSS (Appendix II) and appropriate volumes were used to give a final concentration of 1mM or 10mM in the bath. Alternatively, 0.1mM L-NAME was prepared from 10^{-2} M L-NAME achieved by dissolving 0.02697g L-NAME in 10 ml APSS.

N$^{\omega}$-nitro-D-arginine methyl ester hydrochloride (D-NAME) (FW = 269.69): On the day of the experiment, 10^{-1}M D-NAME was prepared by dissolving 0.2697g D-NAME in 10 ml in APSS and appropriate volumes were used to give a final concentration of 1mM or 10mM in the bath.

Sodium Nitroprusside (SNP) (FW = 297.95)**:** On the day of the experiment, 10^{-1}M SNP was prepared by dissolving 0.297g in 10 ml APSS and appropriate volumes were used to give a final concentration of 1mM in the bath.

MAT.Ang-1 (FW: 43kDa)**:** MAT Ang-1 was a gift from Dr Richard Kammerer, University of Manchester and it was prepared according to the original published protocol (Cho *et al* 2004). On the day of the experiment the stock was diluted in APSS to give a final concentration of 250 ng/ml in the bath.

Human recombinant angiopoietin-1 (HR.Ang-1): 1ml stock Ang-1 (25μg/ml) solution was made by dissolving 25μg Ang-1 (FW: 70kDA; R&D Systems, UK) in 1 ml PBS containing 0.001g BSA. All aliquots (30 μl) were stored at -20°C. Single aliquots were thawed for use on the day of the experiment and were added to the bath to give a final concentration of 250 ng/ml.

TNF-α: 10 μg/ml stock solution was made by dissolving 10 μg TNF-α in 1 ml DPBS and stored in 5 μl aliquots at -20°C. Aliquots were thawed prior to the experiment and appropriate volumes were added to the bath to achieve final concentrations of 10, 30, 100 or 500 ng/ml.

IL-1β: 5 μg/ml stock solution was made by dissolving 5 μg IL-1β in 1 ml DPBS and stored in 5 μl aliquots at -20°C. Aliquots were thawed prior to the experiment and appropriate volumes were added to the bath to achieve final concentrations of 10 or 100 ng/ml.

Indomethacin: On the day of the experiment, 1mM indomethacin was prepared by dissolving .0035g in 10 ml APSS and appropriate volume (30 μl) was used to give a final concentration of 10μM in the bath.

Primers: Primers for iNOS were synthesized by Sigma-Aldrich (UK) and arrived in lyophilized powder form that was reconstituted to 100 μM by addition of sterile distilled H_2O according to instructions given in the technical datasheet.

2.2 Animals and Anaesthesia

2.2.1 Animals- *in vivo* studies

Male Wistar rats weighing between 150-300g (n=19) were obtained from Charles River Laboratories and housed in University of Sheffield Biological Services for 1 week before experimentation. Animals were maintained under standard conditions of temperature (19-22 °C), relative humidity (45-75%) and 12/12 h light/dark cycle, generally in groups of 3-5 in cages containing sawdust. Food in the form of a standard pelleted commercial diet and tap water were available *ad libitum*. All procedures were performed under the Home Office Animal Scientific Procedures Act (1986), project license number PPL 40/2809 and personal license number PIL 40/9251.

2.2.2 Anaesthesia

Gaseous anaesthetic agents

Animals were anaesthetised by diffusing a combination of isoflurane and oxygen (95% O_2/5% Isoflurane) in an inhalant box for induction and then maintained on the same concentration outside the box via a tube (95% O_2/3% Isoflurane). The depth of anaesthesia, determined by pedal reflex was maintained by adjusting the ratio of isoflurane to oxygen.

Intravenous anaesthetic agents

A commercially available preparation of thiopental sodium (Archimedes Pharma Ltd) was used. The central tail vein was cannulated using a 25G paediatric butterfly needle and held in position with surgical tape. Animals were given an induction bolus dose of 30 mg/kg thiopental after which isoflurane inhalation was stopped. A maintenance dose at the rate of 10 mg/kg/hr thiopental was continuously infused via an anaesthetic infusion machine. This regimen provided up to five hours of a light plane anaesthesia and adequate analgesia (Brookes *et al* 2000). Adequate anaesthesia was determined by the pedal reflex regularly during surgery and the level of thiopental infusion was adjusted to maintain an appropriate anaesthetic depth.

2.3 Surgical procedures- Non-recovery

2.3.1 Cannulations

Animals were placed in a supine position on a heat mat. An electric trimmer was used to shave a small area of fur on the neck and a midline incision was made using a stainless steel surgical blade to perform tracheostomy. A portex cannula (size 0.58mm x 0.96mm) bevelled at one end was inserted approximately 1 cm into the trachea and secured with a silk suture. The purpose of this cannulation was to maintain respiration and allow removal of any secretions from the bronchial tree throughout the experiment. For jugular vein cannulation, about 1 cm of the vessel to the right of the trachea was exposed using two pairs of curved forceps via blunt dissection and the fat was cleaned using a pair of angled forceps. A suture was passed under the vein and the distal end was ligated to occlude blood flow. A small incision was placed at the proximal end of the vein, as close to the heart as possible. A tiny incision was made close to the occlusion using a fine spring bow scissors. The clamp was then removed after which a bevelled polypropylene cannula (size 0.76mm x 1.65mm) was inserted approximately 1 cm into the vein and secured in place with a suture. A small volume of blood was withdrawn to ensure that the cannula was placed in the correct position. This was then flushed back through the cannula with 50 units.ml^{-1} heparinised saline (approximately 0.1 ml) to ensure that the blood within the cannula remained uncoagulated. The left carotid artery was also cannulated to allow continuous measurement of blood pressure using the BIOPAC MP system. Two pairs of curved forceps were used to expose the carotid artery to the left of the trachea. The carotid artery and vagus nerve were isolated and gently separated from each other by blunt dissection. Two silk ligatures were passed under the artery. The first was tied tightly at the distal (head) end and the second was left loose while the proximal (heart) end of the artery was clamped using a small artery clamp. A small incision was made just under the head end of the artery and a bevelled silicone cannula (size 0.020" x 0.037") attached to a 23G blunted needle and 1ml syringe containing heparinised saline, was inserted into the artery till it reached the clamped end. The second suture was then tied around the artery and cannula to secure it in position. The clamp was then released and 50 units/ml of heparinised saline (approximately 0.1 ml) flushed through the carotid cannula to prevent clotting.

2.3.2 Mesentery Preparation

The rat mesentery was prepared for observation of the microcirculation by intravital microscopy (Figure 2.1). The method was originally described by (Zweifach 1948) and modified by (Kalia *et al* 1997). The area of the abdomen, below the rib cage and above the urethra was shaved using an electric trimmer. A scalpel blade (size 15) was then used to make a midline incision through the skin followed by an incision along the linea alba which was cauterised to prevent any micro-bleeding. The area of the abdomen surrounding the incision was draped with gauze (5cm x 5cm) and moistened with sterile saline warmed to 37°C. The proximal end of the ileum attached to the large bowel and the adjoining mesentery were exteriorised assisted by cotton buds soaked in saline. The area of interest was selected by counting ten mesenteric windows in a retrograde direction commencing at the large intestine, along the length of the small intestine to ensure that the region selected in each animal was similar. Care was taken to exteriorise the mesentery gently thus preventing any damage to the mesenteric vessels. The area of interest was carefully examined to find a mesenteric window that contained a lymphatic vessel, visible to the naked eye as a milky white vessel surrounded by fat. These vessels were located close to the sub-mucosal mesenteric border usually running parallel to a venule. A 'window' was defined as an area of mesentery, framed by a branching mesenteric artery and vein which contained smaller blood, lymphatic vessels and nerves. The intestine and mesentery was moistened throughout the procedure with regular application of warm saline. The rest of the mesentery was repositioned gently into the abdominal cavity using saline soaked cotton buds.

Five 5-0 silk sutures were placed through the superficial layer of the ileum to enable mounting on the coverslip. The rat was then transferred on to the heating mat on the Perspex board. The mesentery was carefully spread on a coverslip and the sutures were attached to the Perspex peg using Blu-tack to hold the mesentery in a firm position. Gauze moistened with saline was placed along the anti-mesenteric border and the preparation was covered by saran wrap to prevent it from dehydration. Saline was applied every 15 min and after each recording. A preparation was considered viable for experimental analysis if it showed:

1) No obstruction of the lymphatic vessels by fat.
2) Good blood flow (venular and arteriolar) and lymphatic flow without any signs

of stasis or sluggish flow.

3) No macromolecular leak during the stabilisation period.

Figure 2.1 A rat mesentery prepared for *in vivo* microscopy. *Windows of mesentery framed by branching blood vessels are visible. Lymphatic vessels covered by fat run parallel to the blood vessels. The ruler is in mm scale.*

2.4 *In vivo* microscopy

The animal laid on the perspex board was transferred to the microscope stage of a fluorescent microscope (Leica DMLM), which was equipped with a tungsten lamp for transmitted light and a 100 W mercury arc lamp for epi-illumination with blue light. Following administration of FITC-BSA (0.5 ml) via jugular vein, images were recorded using transmitted light for 2 min and fluorescent light for a maximum of 15 sec every 30 min for the experimental duration of 4 h. Images were not exposed to blue light for more than 15 sec to prevent photobleaching. Intravascular administration of FITC-BSA and epi-illumination with blue light (493 nm) resulted in green fluorescence (518 nm). The power output of the blue light was 7-15 mW, measured using an optical power meter prior to the start of the experiment and it was ensured that the spot size of light was constant between experiments. The area of interest (AOI) was observed through a 10x objective, images were captured by a CCD camera (JVC), displayed on a high resolution monitor (Triniton, Sony) and recorded by a professional DVD recorder (MP-6000 Datavideo) for off-line analysis using Image proplus.

2.5 Data Collection and Analysis

2.5.1 Measurement of Cardiovascular Variables and Temperature

Temperature (every 30 min) and cardiovascular variables: rate (beats per min) and mean arterial pressure (mmHg) were recorded throughout the experiment during the experimental protocol. Parameters were measured via the carotid cannula which was connected to a pressure transducer and a BIOPAC MP system (Biopac systems, Inc.). This system consisted of a data acquisition unit (MP100) connected via a USB to a desktop computer installed with the Acq*Knowledge* application. The application digitalised the analogue signal and enabled waveforms of cardiovascular variables to be recorded directly and continuously on disk while a real time display on the computer provides continuous monitoring. The software was calibrated prior to the experiment using an adapted mercury manometer. Body temperature (°C) was monitored via the oesophagus by inserting a thermistor probe connected to a digital thermometer.

2.5.2 Microcirculatory Variables

The data collected and recorded on DVD was analysed off-line using image analysis software Image Proplus (Media Cybernetics, Inc.) to determine changes in lymphatic and venular vessel macromolecular leak and lymphatic diameter. Image Proplus allows acquisition of files from DVDs to characterise objects using automatic measurement tools.

Vessel diameter

The system was calibrated for the 10x objective of the Leica microscope using a stage micrometer, enabling vessel diameter to be quantified in microns. An image of the stage micrometer was taken and the Spatial Calibration dialog box was brought up on Image proplus. The units (μm) were selected, and a line was placed onto the image using the image button. The line was then stretched over the known distance. A reference calibration was thus generated. Diameter was measured from trans-illuminated images of the vessel and was quantified by placing a line across the width of each vessel. At each time point measurements were taken from the inner edge of the vessel wall. Three separate measurements were taken and the mean value was used for analysis. Images used for measurement were captured when there was no flow or contractile activity in the vessel. Since diameter of the vessel was not uniform along

the length of the vessel, it was ensured that a similar site was chosen for measurement in each image. Images were placed side by side and a ruler was used to identify similar sites for measurement.

Macromolecular leak

The fluorescence intensity within the lymphatic vessel, venule and interstitium was quantified from images captured during exposure to fluorescent light. The fluorescence intensity is proportional to the FITC-BSA in each area. The software assigned an integer value to the brightness of the fluorescence (arbitrary 8 bit grey scale), with values ranging from 0 which represented black, to 255 which represented white. The gain and offset (brightness and contrast) were 32 and 34 for analysing fluorescent images and remained constant throughout all experiments. A mean of three grey scale values was obtained by placing three small boxes ($441 \ \mu m^2$) in each vessel. Intensity in the interstitium was measured by choosing 3 random sites immediately adjacent to the venule.

2.5.3 Statistical analysis

Statistical differences between different groups were determined through two-way ANOVA with Sidak's post-hoc analysis by the GraphPad Prism statistical software package version 6.0e for Mac OS X. Within group variation was assessed using a one-way ANOVA followed by Dunnett's multiple comparisons test. Data were expressed as mean ± SEM, and values $p < 0.05$ were considered significant.

2.6 Pressure myography

2.6.1 Animals-*ex vivo* studies

Male Sprague Dawley rats weighing between 170-250g were obtained from Harlan or Charles River Laboratories and maintained as described in section 2.2.1. Experiments were performed on vessels (n=91) obtained from 91 animals.

2.6.2 Schedule 1 procedure

Rats were placed in an anaesthetic box and anaesthetized with 95% O2/5% Isoflourane. Once loss of consciousness was observed and confirmed by loss of pedal reflex, the animal was removed from the box and immediately culled via cervical dislocation in accordance with the UK Home Office Animal Scientific Procedures Act (1986).

2.6.3 Mesentery removal

An incision of approximately 3 cm was made from below the rib cage extending to the urethra. Curved forceps and dissection scissors were used to cut the skin (with attached fur) and the abdominal muscle. Using saline soaked cotton buds, loops of ileal mesentery were exteriorised and excised from the wall using spring scissors. The mesentery was the immediately immersed in 4°C HEPES solution and washed 2-3 times with the same, to clear any loose connective tissue and blood.

2.6.4 Set-up

The pressure myography setup is illustrated in figures 2.2 and 2.3.

Chamber preparation

The organ bath of the pressure myograph (Living Systems Instrumentation) was filled with 3 ml Dulbecco's Modified Eagle Medium F12 (DMEM-F12) or Albumin-physiological salt solution (APSS). A 10 ml syringe was used to withdraw APSS from the organ bath, through the cannula and the tubing into the syringe. This process was repeated with the opposite cannula and tubing to ensure that all vessel chamber connections were perfused with the media. The myograph components flushed twice. During the second time this process was done, withdrawal of the media was done slowly to ensure no air bubbles were present in the myograph tubing and cannulae.
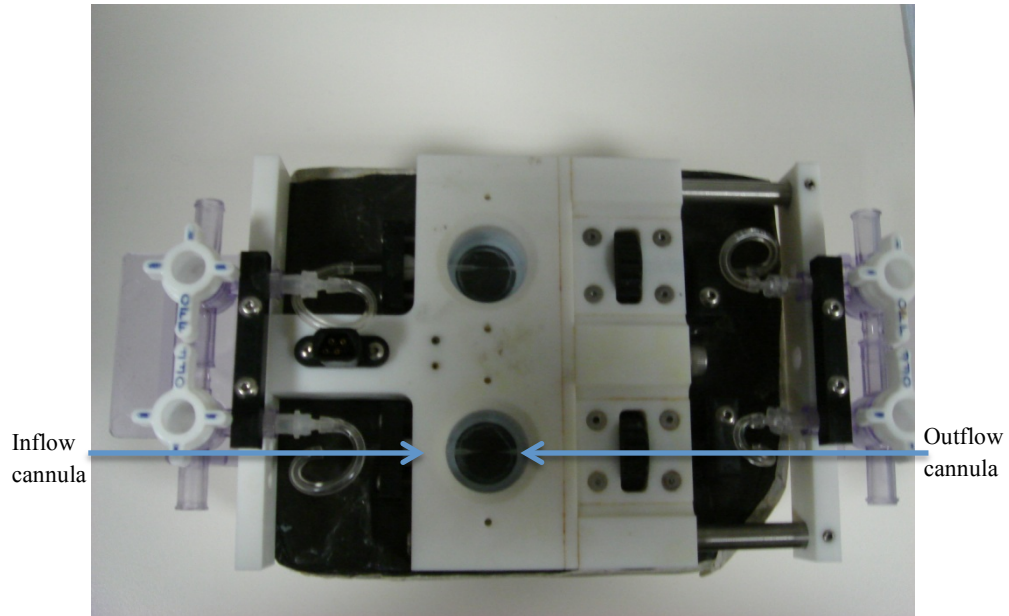
Figure 2.2 Pressure myograph. *The chamber consists of an organ bath with two hollow glass cannulae extending into the bath from opposite sides. Cannula tips have a distinct bevelled edge, which facilitates vessel cannulation. Upon filling the cannulae and organ bath with media, an isolated vessel, dissected from surrounding adipose tissue, can be mounted across the cannulae and tied in place, creating a sealed tube from one cannula tip to the other. The media-filled vessel can then be inflated to physiological pressure, subjected to flow and doses of desired substance can be applied extraluminally via the organ bath. Continuous observations can be made through the transparent cover slip at base of the myograph which can be positioned on the objective of an inverted microscope (TS100; Nikon, Japan).*

Ties

To make ties, single fibres were removed from a 0.5 cm long multifilament braided nylon thread (Living Systems Instrumentation, USA). Fibres were looped to form a single knot using fine forceps and stored in a small petri dish. Prior to the washing of the chamber with media, the ties were positioned onto the cannulae.

Pressure tower
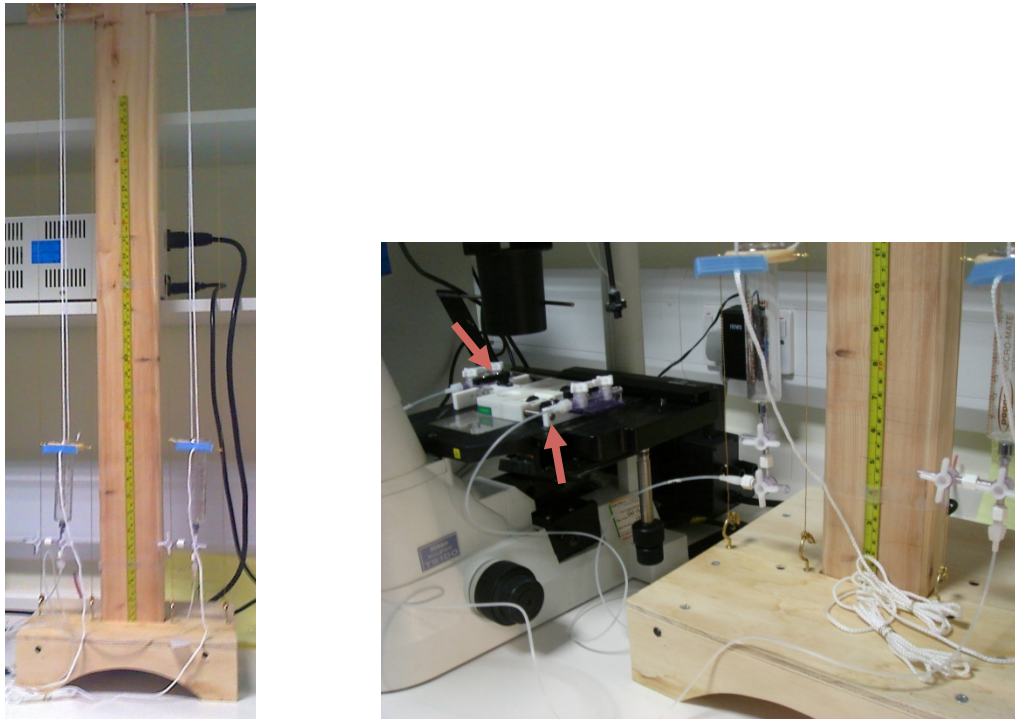
Figure 2.3 Custom-built pressure tower. *Both the inflow and the outflow ends (indicated by arrows) of the myograph are attached to the media-filled syringes via tubes. Intraluminal pressure or a pressure gradient (user defined to induce flow) in the vessel can be controlled precisely by raising the height of each reservoir.*

Dissection dish preparation

The dissection dish (Living Systems Instrumentation) was filled with cold HEPES and stored at 4°C before use. The mesentery was pinned out in the dissection dish using 0.45 x 12 mm needles such that it was immersed in the HEPES and could be easily viewed under the dissecting microscope (S6E; Leica) (Figure 2.4).
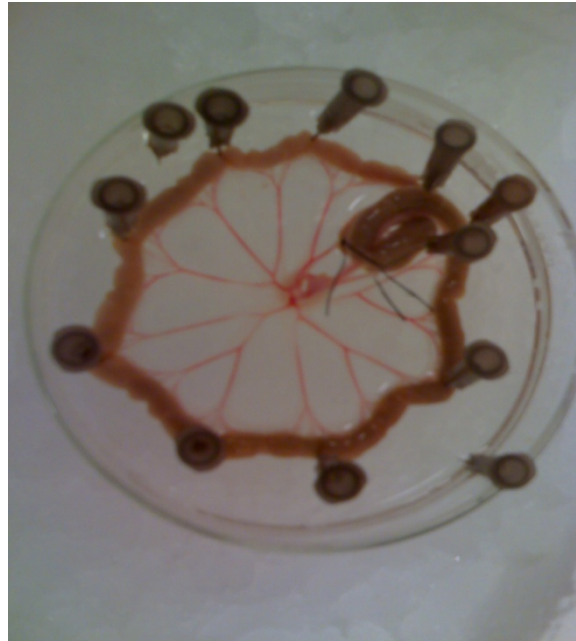
Figure 2.4 Dissection dish. *The dish is lined with several millimeters of Sylgard® material which enables pinning of delicate tissue for dissection under the microscope.*

Vessel dissection

A dissecting microscope and attached light unit was used to locate lymphatic vessels in the tissue pinned out on the dissecting dish. A first, second or third order venule was selected and lymphatics adjacent to it were located by removing the adipose tissue visible on the surface with fine forceps. Further dissection of the lymphatic was performed if i) the size of the lymphatic was approximately more than 80 μm ii) no branches were encountered till a minimum 1 cm length of the vessel was dissected iii) the length of the lymphangion was more than 1 cm. Dissection of another vessel was undertaken if any of these criteria were not satisfied. Extreme care was taken not to damage the lymphatic wall while removing the fat globules, fibres or tiny arterioles entwined around it.

Vessel transfer

The isolated dissected lymphatic vessel was resected at both ends from the tissue. The inflow end of the vessel was held with fine forceps and the vessel was immediately and carefully transferred into the organ bath of the prepared pressure myograph for cannulation.

Mounting of the lymphatic vessel onto inflow cannula

Two forceps were used to grip the edges of the inflow end of the lymphatic. This enabled the vessel to be manipulated and positioned onto the inflow cannula tip, following which the tie (previously looped onto the cannula) was moved over the inflow end of vessel to secure it tightly onto the cannula tip.

Clearance of vessel

The outflow end was opened with help of fine forceps to prevent excess pressure build up while flushing the vessel. To flush the vessel, a media-filled tube was attached to the inflow end of the myograph. The valve was opened and the tube raised manually to a maximum height 5 cm from the level of the vessel to allow flow into the vessel at a pressure of not more than 5 cm H_2O, allowing the lymph to be released into the organ bath. Care was taken to ensure pressure in the vessel did not rise above 5 cm H_2O as this would damage the endothelial layer of the vessel. Once all lymph was cleared, the tube was cleared and the valve was closed.

Mounting onto outflow cannula

The retractable cannula was then moved forward towards the outflow end of the lymphatic. Two forceps were used to grip the outflow end of the vessel and to position onto the outflow cannula tip. The thumbwheel was then readjusted to the appropriate distance for the vessel to be tied onto the cannula as described for inflow end of the vessel. The bath was replenished with fresh media to ensure no lymph or other metabolites were present in the organ bath during experimentation.

Confirmation of vessel integrity

The vessel was aligned in a straight position by adjusting the thumbwheel. The vessel was pressurized by opening both the outflow and inflow tap. Damage was assumed if the vessel appeared constricted in any region or lost pressure. If this occurred, a new vessel was used. The vessel was deemed suitable for experimentation after confirmation of these features of integrity.

Temperature

A temperature controller (TC-02; Living Systems Instrumentation) enabled direct thermoregulation in the bath via an electronic feedback system. The controller was connected to the myograph, and set to 37°C with lower and upper alarm boundaries of

36-39°C, respectively. A thermistor sensor that remained submerged in the bath without touching the walls of the bath monitored the bath temperature.

Vessel measurements

The diameter of the vessel was measured manually using the video dimension analyser (VDA) (V94; Living Systems Instrumentation). The vessel was magnified x10 and observed via a microscope-mounted camera (XCST30CE; Sony) and displayed on a black and white video monitor (CMM1200N; Costar). A solid white scan line with measurement intervals was superimposed by the VDA on the video monitor. These intervals were aligned with the boundaries of both left and right walls of the vessel, giving diameters of left and right vessel walls, as well as luminal diameter. The VDA tracks diameters of vessels ranging from 50 to 350 μm using an analogue video signal. The instrument senses optical density changes of the vessel image at a chosen scan line seen on the TV monitor which were displayed as measurements continuously on digital panel meters. The diameter measurement was calibrated to indicate dimensions directly in microns according to the calibration procedure described in the VDA instruction manual. Images were recorded on a professional DVD player for off-line analysis.

2.6.5 Pre-experimental procedures

Stabilisation- flow and pressure

The stopcocks at both ends of the myograph were opened, and the inflow syringe was raised higher than the outflow syringe to ensure that the lumen was filled with media. Following this the inflow syringe was lowered to 3 cm and the vessel allowed to equilibrate for 15-30 min until a stable contraction pattern was observed. The vessel was considered viable for experiment if the following criteria were satisfied during the equilibration period

    i)   The development of spontaneous tone at pressures $\leq$ 3 cm H_2O.

    ii)   The development of spontaneous contractions with an amplitude of > 30% of maximal passive diameter.

    iii)   Contractions are reasonably uniform over entire length of the vessel.

Vessels that did not meet these criteria were discarded. Datasets from vessels that developed irregular contraction patterns during an experiment were not used for subsequent analysis. Where a step-pressure protocol was used, pressure was set to 1, 3

or 5 cm H_2O for 5 min until a new contraction pattern stabilised at each time point recorded. Figure 2.5 shows an isolated RMLV in diastolic and systolic phase.
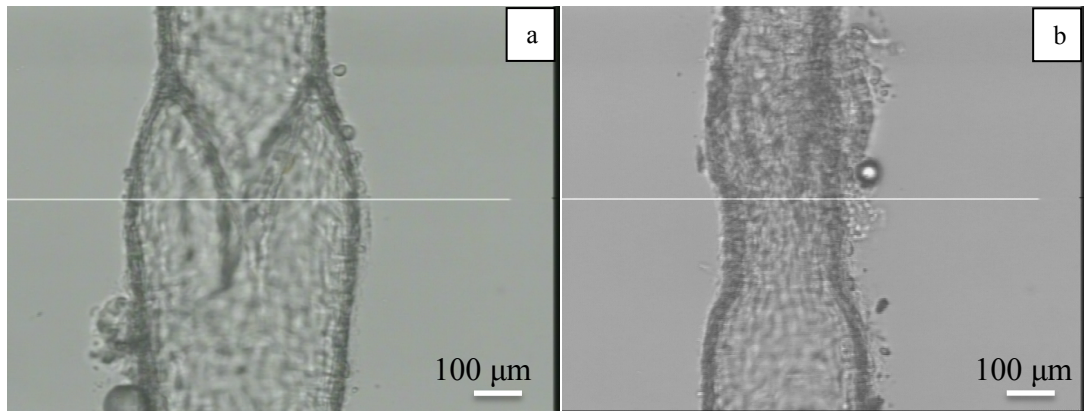
Figure 2.5 Isolated RMLV pressurised at 3 cm H_2O in a myograph chamber.

a) Lymphatic diastole (EDD-120 μm) b) Lymphatic systole (ESD-74 μm).

2.6.6 Data Analysis

After completion of each experiment, the video recording was analysed offline using ImageProplus. The system was calibrated using a micrometer, enabling vessel diameter to be quantified in microns as described previously. Measurements were taken from the inner edge of the vessel wall during lymphatic systole and diastole.

Frequency was computed on a contraction-by-contraction basis in each minute.

Amplitude was calculated as follows:

AMP= EDD-ESD, where EDD is the end-diastolic diameter and ESD is the end-systolic diameter at any given pressure.

Percentage dilation was calculated as follows:

% dilation= $\dfrac{EDD-EDD_0}{EDD_0} * 100$ where EDD_0 is the diameter at baseline

Maximum tone at a particular pressure was calculated as follows

$\dfrac{D_{Ca-free}- D_{pressure}}{D_{pressure}} * 100$ where $D_{Ca-free}$ is the diameter in Ca-free APSS and $D_{pressure}$ is the diameter at any given pressure.

2.6.7 Statistical Analysis

Statistical differences between different groups were determined through two-way ANOVA with Tukey's post-hoc analysis by the GraphPad Prism statistical software package. Variation within groups was determined using one-way ANOVA followed by Tukey's multiple comparisons test. Data were expressed as mean ± SEM, and values p < 0.05 were considered significant.

2.7 Fluorescent Immunohistochemistry

2.7.1 LYVE-1 imaging

Rat mesenteric lymphatic vessel (RMLV) were isolated and cannulated in the myography chamber and rinsed with DPBS extra- and intraluminally. Vessels were incubated with 1 μg/ml anti-mouse LYVE-1 Alexa-fluor 488 monoclonal antibody (20 μl in 1 ml DPBS) for 30 min at RT. Vessels were then rinsed with DPBS after incubation and observed under a confocal multiphoton microscope (Upright Zeiss LSM 510) with 10x/0.3 water dipping objective for LYVE-1 staining. The microscope fitted with an Ar laser detected LYVE-1 conjugated with Alexa-fluor at 488 nm. Z stack images for 3-D reconstruction were acquired using the Zeiss Image Browser software.

2.7.2 Tie-2/VE-Cadherin Imaging

Confocal microscopy was performed in Prof Zawieja's lab during a lab visit to the Cardiovascular Research Institute, Texas A & M University.

RMLV were isolated from rats fasted for 24 h. The vessels were cannulated in the myography chamber, rinsed with DPBS and fixed in freshly prepared 2% Paraformaldehyde-DPBS for 1 h at RT. Intraluminal rinse was performed by cannulating the vessel at one end and flushing any lymph fluid which may result in non-specific binding. After fixing, vessels were rinsed in DPBS for 5 min. This step was repeated 3 times with both extra- and intraluminal rinse the third time (Step 2). Vessels were then permeabilized with methanol cooled at -20°C for 5 min. Step 2 was repeated again and vessels were transferred to a petridish for incubation in blocking solution. Vessels were incubated in the blocking solution (50 mg BSA (1%) and 250 μl normal donkey serum (5%) in 5 ml DPBS) for 60 min at RT. The vessels were cut and removed into the following solutions for IHC staining: V1 (vehicle-treated) + 20 μl anti-mouse Tie-2 polyclonal goat IgG antibody (primary) at 1:50 in 1 ml blocking

solution or 20 μl anti-mouse VE-cadherin polyclonal goat IgG antibody (primary) at 1:100 in 1ml blocking solution; V2 (vehicle-treated) + normal goat IgG (same concentration as the primary antibody for V1) in blocking solution. This was followed by incubation overnight at 4°C and step 2 was repeated again. The vessels were incubated in Alexa-fluor 647 conjugated donkey anti-goat IgG antibody (secondary) at 1:200 for 1 h at RT followed by step 2. Stained vessels were observed under confocal microscope (Leica TCS SP2) for Tie-2/VE-cadherin expression. Average 2-D projections of the stacks of confocal images were taken at 0.5 μm intervals in the z-axis.

2.8 RNA Isolation

RNA isolation was performed to measure eNOS and iNOS gene expression in non-stimulated and stimulated RMLV.

2.8.1 Tissue harvesting and stabilisation of RNA

Mesentery: The mesenteric tissue was rapidly dissected from the anesthetized animal and quickly rinsed in DPBS. It was then transferred to a dissection dish filled with *RNAlater* RNA stabilization reagent sufficient to completely cover the tissue in the dissection dish and equilibrated for at least 30 min at RT. Up to 15 vessels were isolated from the tissue. Vessels were cleaned of all extravascular tissue to ensure that RNA isolated was specific to the cells of the lymphatic wall. The cleaned vessels were transferred to a 0.5 ml microcentrifuge tube containing 200-400 μl of fresh RNA*later*, which preserves the gene expression profile by protecting cellular RNA *in situ*. Samples were stored at 4°C for a day or immediately used for RNA isolation (Bridenbaugh 2012).

Lung: Two samples of lungs were resected from 2 freshly sacrificed male Wistar rats. One sample was stored in RNA*later* and the other was flash frozen in liquid nitrogen and stored in -70 °C. Lungs were chosen as a positive control for the experiment as differential expression of all three types of NOS isoenzymes has been reported in normal rat lung tissue under baseline conditions (Ermert *et al* 2002).

2.8.2 Disruption and homogenization of starting tissue

Mesentery: To release all the RNA contained in the sample, complete disruption of cell walls and plasma membranes of cells and organelles is required. The lysates produced by disruption are then homogenized to reduce viscosity. A rotor-stator

homogenizer was used for simultaneous disruption and homogenization of RMLV. The RNA*later* stabilised tissue was suspended in the lysis buffer provided with the kit being used and immediately disrupted and homogenized using a conventional rotor-stator homogenizer with a 7 mm probe, performed in a microcentrifuge tube until uniform homogenization was obtained. The probe was applied to the sample in bursts of 10 s over 40-60 s or until no visible pieces remained.

Lung: To obtain optimal RNA yield and purity, the amount of starting material as specified for animal tissues in the manufacturer's protocol (< 30 mg) was not exceeded. The lung tissue was disrupted using a mortar and pestle and homogenized using syringe and needle. Tissue was ground to a fine powder under liquid nitrogen and the suspension was transferred into a liquid nitrogen-cooled 2 ml microcentrifuge tube, allowing the nitrogen to evaporate without allowing sample to thaw. The lysis buffer was then added, and rapidly homogenized using the syringe and needle. The lysate was passed through a 0.9 mm needle attached to a sterile plastic syringe 5-10 times.

2.8.3 RNA extraction

Total RNA extraction from RMLV was attempted with three different RNA isolation kits in accordance with the manufacturer's protocol: Sigma's GenElute Mammalian TotalRNA Miniprep kit, *mir*Vana PARIS Kit, and RNeasy Mini Kit. RNA extraction was also attempted using organic phase extraction method. Different methods were attempted due to the low RNA yield, which was insufficient for RT-PCR analysis. Total RNA extraction from lungs was performed using Sigma's GenElute Mammalian TotalRNA Miniprep kit.

2.8.3.1 RNA purification using Sigma's GenElute Mammalian TotalRNA Miniprep kit

The kit employs the silica-based solid-phase purification method. The tissue was transferred to an appropriate tube for homogenization, 500 μl of the Lysis solution/2-ME mixture was added to the RNA*later* stabilized tissue. After homogenization (as described in 2.5.2), the tissue was pipetted into a GenElute Filtration Column and centrifuged at 12000g for 2 min. The filtration column was discarded. 500 μl of 70% ethanol solution was added to the filtered lysate and it was vortexed thoroughly. Up to 700 μl of the lysate/ethanol mixture was then pipetted into a GenElute Binding Column. The column was centrifuged at maximum speed for 15 s at the end of which

the flow-through liquid was discarded and the collection tube retained. The binding column was then returned to the collection tube and any remaining lysate/ethanol mixture was applied to the column. The centrifugation was repeated. Column washes were then performed. First column wash: 500 µl of Wash Solution 1 was pipetted into the column and centrifuged at maximum speed for 15 s. The binding column was then transferred into a fresh 2.0 ml collection tube. Second column wash: The flow-through liquid and the original collection tube were discarded. 500 µl of ethanol containing Wash Solution 2 was pipetted into the column and centrifuged at maximum speed for 15 s. The collection tube was retained in this step. Third column wash: A second 500 µl volume of Wash Solution 2 was pipetted into the column and centrifuged at maximum speed for 2 min to dry the binding column. RNA was eluted after the column washes. RNA elution: The binding column was transferred to a fresh 2 ml collection tube. 30 µl of the Elution Solution was added into the binding column and centrifuged at maximum speed for 1 min. The purified RNA was obtained in the flow-through eluate.

2.8.3.2 RNA purification using mirVana PARIS Kit

This kit combines the advantages of organic extraction and solid-phase extraction methods. 625 µl of ice-cold cell disruption buffer was added to the RNA*later* stabilized tissue. Once the lysate was homogenized, it was mixed thoroughly with an equal volume of 2X Denaturing Solution at RT. The mixture was incubated on ice for 5 min. Acid-Phenol:Chloroform equal to the total volume of the mixture was added to the tube and vortexed thoroughly for 30-60 s. The tube was centrifuged for 5 min at 10,000g at RT to separate the mixture into aqueous and organic phases. The upper aqueous phase was carefully removed without disturbing the lower phase or the interphase and transferred to a fresh tube. 1.25 volumes of RT 100% ethanol was added to the aqueous phase and mixed thoroughly. The lysate/ethanol mixture was pipetted onto a filter cartridge and centrifuged for 30 s until the mixture had passed through the filter. 700 µl miRNA Wash Solution 1 was applied to the filter cartridge and centrifuged for 15 s. The flow-through was discarded from the collection tube and the filter cartridge replaced into the same collection tube. 500 µl of Wash Solution 2/3 was applied and drawn through the filter cartridge by centrifugation. The cartridge was washed again with a second 500 µl of Wash Solution 2/3. The flow-through was discarded, the filter cartridge was replaced in the same collection tube and the

assembly was spun for 1 min to remove residual fluid from the filter. The cartridge was then transferred to a fresh collection tube. RNA was eluted in the Elution solution provided with the kit. 100 µl of preheated Elution Solution was applied to the center of the filter and centrifuged for 30 s to recover RNA. The eluate was collected and stored at -20°C.

2.8.3.3 RNA purification using Bridenbaugh's organic phase extraction method

An optimized protocol for the isolation and preparation of RNA from rat microvessels developed by Bridenbaugh (2012) was used in the next attempt due to the resulting low yield and purity of RNA from RMLV. The protocol is based on the standard organic phase extraction method for RNA purification. In this method, the isolated cleaned vessels were transferred from RNA*later* to a 2.0 ml microcentrifuge tube containing 500 µl of chilled TRIzol Reagent (TRI Reagent$^{®}$, Sigma-Aldrich) and immediately homogenized at 30,000 rpm for 20-30 s using a rotor-stator homogenizer with a 7 mm stainless steel generator. The sample was then placed on ice immediately until the next step. To ensure the complete dissociation of nucleoprotein complexes, the samples were vortexed and allowed to stand for 10 min at RT. 100 µl of chloroform was added to the sample and mixed for 1 min by repeated inversion. The sample was incubated for 5 min at RT and then centrifuged at 12000g at 4°C. This step separates the mixture into 3 phases: a red organic phase (containing protein), an interphase (containing DNA) and a colorless upper aqueous phase (containing RNA). The aqueous phase was carefully transferred to a new 1.5 ml centrifuge tube. 400 µl of isopropanol was added and mixed. The sample was allowed to stand for 5-10 min at RT and centrifuged at 12000g for 10 min at 4°C. The supernatant was removed and the RNA precipitate in the form of a pellet was washed with 500 µl of cold 75% EtOH, vortexed gently for 10 s and then centrifuged at 7500g for 5 min at 4°C. The pellet was air dried for 10 min at RT and any supernatant removed. 15 µl of 75°C RNase-free water was added to the RNA pellet and it was gently vortexed several times to resuspend the pellet.

2.8.3.4 RNA Purification using RNeasy Mini Kit

RNAeasy Mini Kit designed for purification of up to 100 µg of total RNA from small amounts of animal cells and tissues was used in the fourth attempt. The technology employs silica-based membrane to selectively bind RNA. The RNA*later* stabilized tissue was suspended in 600 µl lysis buffer RLT. QIAzol agent was also used in place

of lysis buffer RLT in one experiment to achieve more optimal tissue lysis. The lysate was centrifuged for 3 min at full speed, supernatant removed by pipetting and then transferred to a new microcentrifuge tube. 1 volume of 70% ethanol was added to the cleared lysate and mixed immediately by pipetting. Up to 700 μl of the sample including the precipitate was added to an RNeasy spin column placed in a 2 ml collection tube and centrifuged for 15 s at 10,000 rpm. The flow-through was discarded. 700 μl RW1 was added to the RNeasy spin column and centrifuged for 15 s at 10,000 rpm to wash the spin-column membrane. The flow-through was discarded. 500 μl buffer RPE was then added to the RNeasy spin column and centrifuged for 15 s at 10,000 rpm to wash the spin membrane. The flow-through was discarded again and the step was repeated. The column was centrifuged for 2 min in this step to ensure the complete drying of ethanol from the column. The column was placed in a new 1.5 ml collection tube. 30 μl RNase-free water was added directly to the spin column membrane and centrifuged for 1 min at 10,000 rpm to elute the RNA.

2.8.4 Eliminating genomic DNA contamination

TURBO DNA-*free* Kit was used to eliminate any contaminating DNA from purified RNA preparations. 0.1 volume of 10X TURBO DNase Buffer and 1 μl TURBO DNase was added to the RNA and mixed gently. The tube was incubated at $37^{\circ}C$ for 30 min. Resuspended DNase Inactivation Reagent (0.1 volume) was added and mixed well. The tube was incubated at RT for 5 min and flicked 2-3 times to mix the contents. It was then centrifuged at 10,000g for 1.5 min to pellet the DNase Inactivation Reagent. The supernatant was carefully transferred into a fresh tube and stored at $-20^{\circ}C$ for further analysis.

2.8.5 Quantification of RNA

UV spectroscopy is the most widely used method to quantitate RNA. The concentration and quality of the total RNA purified was determined by measuring the absorbance at 260 nm and 280 nm in a spectrophotometer (Nanodrop ND-1000). An A_{260} reading of 1.0 is equivalent to ~40 μg/mL single-stranded RNA. An A_{260}/A_{280} ratio of 1.8–2.1 indicates highly purified RNA (http://www.ambion.com/techlib/tn/94/949.html). The integrity of RNA was assessed by Agarose Gel analysis.

2.9 cDNA synthesis

High capacity RNA-to-cDNA Kit (Applied Biosystems) was used to quantitatively synthesise single-strand cDNA from the total RNA. 2 μg of total RNA was used per 20 μl reaction. The kit components were allowed to thaw on ice, and the RT reaction mix was prepared with the volume of components tabulated below. The mix was prepared on ice.

Component	Volume/Reaction (μl)	
	+RT	-RT
2X RT Buffer	10.0	10.0
20X RT Enzyme Mix	1.0	-
Nuclease-free H_2O	6	6
RNA sample	3	3
Total per reaction	20.0	20.0

Table 2.1 RT reaction mix with volume of components

cDNA RT reactions were performed. 20 μl of RT reaction mix was aliquoted into each tube, which were then sealed and centrifuged to spin down the contents and eliminate any air bubbles. The thermocycler was programmed under the following conditions:

	Step 1	Step 2	Step 3
Temperature (^{o}C)	37	95	4
Time	60 min	5 min	∞

The reaction volume was set to 20 μl, the reactions were loaded into the cycler and RT run was started. The tubes were stored at 4°C until agarose gel analysis of the cDNA.

2.10 PCR

PCR was used for second strand synthesis and amplification of the synthesised cDNA. The reactions components (tabulated below) were assembled on ice and quickly transferred to a thermocycler with the block preheated to the denaturation temperature (95°C).

Component	Reaction (µl)
PCR Mastermix, 2X	10
Forward primer, 10 µM	3
Reverse primer, 10 µM	3
cDNA template	1
Nuclease-free water	3
Total	20

Table 2.2 PCR reaction mix

The thermocycling conditions were set as follows. Amplified DNA was analysed using agarose gel electrophoresis.

Step	Temp (^{o}C)	Time (min)
Initial Denaturation	94	8
3 cycles	62	1
30 cycles	60	1
Final extension	72	10 min
Hold	4	∞

Table 2.3 Thermocycling conditions for PCR

2.11 Agarose Gel Electrophoresis

A standard 2% agarose gel was prepared as follows. 2 g of agarose gel was added into a microwavable flask along with 100 mL of 1x TBE. The flask was microwaved for 1-3min until the agarose started to boil and completely dissolved. The agarose solution was allowed to cool down. 20 µl EtBr (0.2 µg/ml) was then added to the solution and it was slowly poured into a gel tray with the well comb in place. The gel was left to solidify at RT for 15-20 min. Once the gel had solidified it was placed into the electrophoresis unit. The unit was filled with 1x TAE running buffer to completely immerse the gel. A molecular weight ladder was loaded into the first lane. Loading buffer was added to the samples and they were loaded into the adjacent wells. The gel

was run at 150V until the dye indicated that the samples had reached 75-80% of the way down the gel. It was removed carefully and placed under a UV transilluminator to visualise the DNA bands.

Chapter Three

Effect of LPS on rat mesenteric lymphatic vessels in vivo

3.1 Introduction

Lymphatic dysfunction has long been associated with oedema and inflammation; however, integrity of the lymphatic endothelial barrier during inflammation has only recently been an area of focus for lymphatic biologists (Cromer *et al* 2014; Kawai *et al* 2014). A study published from our lab (Brookes *et al* 2009) reported macromolecular leak of FITC-BSA (66 KDa) from extrasplenic lymphatics in endotoxemic rats, thus allowing leakage of protein-rich fluid into interstitial spaces, contributing to hypovolemia and hypotension. In this study, we wanted to evaluate the integrity of the lymphatic barrier, particularly mesenteric collecting lymphatic vessels in response to inflammatory stimuli such as LPS, which is associated with increased blood endothelial permeability during sepsis. Mesenteric lymph has been implicated in transporting gut-derived inflammatory factors to other splanchnic organs during gut-origin of sepsis following conditions like hemorrhagic shock, trauma and intestinal ischemia (Fanous *et al* 2007). Thus, they play a pivotal role in the pathological response to sepsis and are likely to dysfunction in this inflammatory mileau. Several studies have demonstrated that endotoxemia disturbs the lymphatic pump mechanism and affects lymph flow rates (Elias *et al* 1987; Elias and Johnston 1990; Nemoto *et al* 2011), but the timeline of alterations in lymphatic pumping and how it correlates with lymph flow is not well defined. An understanding of how lymphatic barrier and vessel contractile function is affected during endotoxemia could lay the groundwork for investigating the initial mechanisms that disrupt lymphatic function and lead to the development of interventions to improve the resolution of inflammation. The aim of this study therefore, was to investigate the effects of LPS on macromolecular leak, tone, contractions and lymph flow in the mesenteric collecting lymphatic vessel. We hypothesised that changes in lymphatic physiology begin to occur during early stages of sepsis (0-4 h) including macromolecular leak from mesenteric lymphatics, reduced contractions and flow. The time period 0-4 h has been associated with alterations in blood endothelial barrier function during sepsis (Andrew and Kaufman 2001) and it stands to reason that this was chosen for our study. These changes were investigated using an *in vivo* model of sepsis induced using continuous low dose infusion of LPS. Fluorescent intravital microscopy with 66 KDa FITC-BSA was used during the 4 h exposure to LPS.

3.2 Experimental Design

The protocol followed is outlined in figure 3.1. Details of animal anaesthesia and surgery can be found in section 2.2.

3.2.1 Experimental groups

To examine differences in macromolecular leak, tone, contractions and lymph flow in the collecting lymphatic vessel, rats were allocated randomly into two experimental groups LPS or saline. LPS with doses ranging from 150 µg/kg/hr-1 mg/kg/hr was used. Number of experiments (n) performed with each LPS concentration was limited to three, as the expected endotoxemic response was not observed. A higher concentration was used to achieve an endotoxemic response at each dose and experiments were terminated at n=3, once this was not observed.

1) Control (n=6)
2) LPS 150 µg/kg/hr (n=3)
3) LPS 300 µg/kg/hr (n=3)
4) LPS 600 µg/kg/hr (n=3)
5) LPS 1 mg/kg/hr (n=3)

3.2.2 Stabilisation period (t= -45 to -30 min)

Animals were allowed an equilibration period of 15 min following surgery, prior to the administration of FITC-BSA. During this time the carotid cannula was connected to the blood pressure transducer. At t=-30, FITC-BSA (100 mg.kg^{-1}) was administered via the jugular cannula.

3.2.3. Recordings

Pre-baseline recordings (t= -15 min)

Microcirculatory and cardiovascular variables were recorded prior to the start of the experimental period. If macromolecular leak was occurring from venules or blood flow was poor at this point (i.e. prior to LPS administration), the preparation was deemed not viable for experimentation and the animal euthanised by thiopental overdose.

Baseline recording (0 min)

A baseline recording was made at this time-point, immediately before LPS administration. Macromolecular leak measurements at all experimental time points were compared to this baseline value.

Experimental Period (t=0-4 h)

Temperature and arterial blood pressure were recorded online throughout the experimental period. The AOI was recorded onto DVD using transmitted light for 2 min and fluorescent light for 15 s with 10x objective.

- 120 min	Surgery
- 45 min	Stabilisation period
- 30 min	Administration of FITC-BSA (100 mg.kg^{-1}) i.v.
0 min	Continuous infusion of 150 μg.kg^{-1}.hr^{-1} LPS or equivalent volume of saline (1 ml.kg^{-1}) i.v.
	Record IVM images of lymphatics and body temperature every 30 min, arterial blood pressure, heart rate throughout.
240 min	Animal euthanised by thiopental overdose.
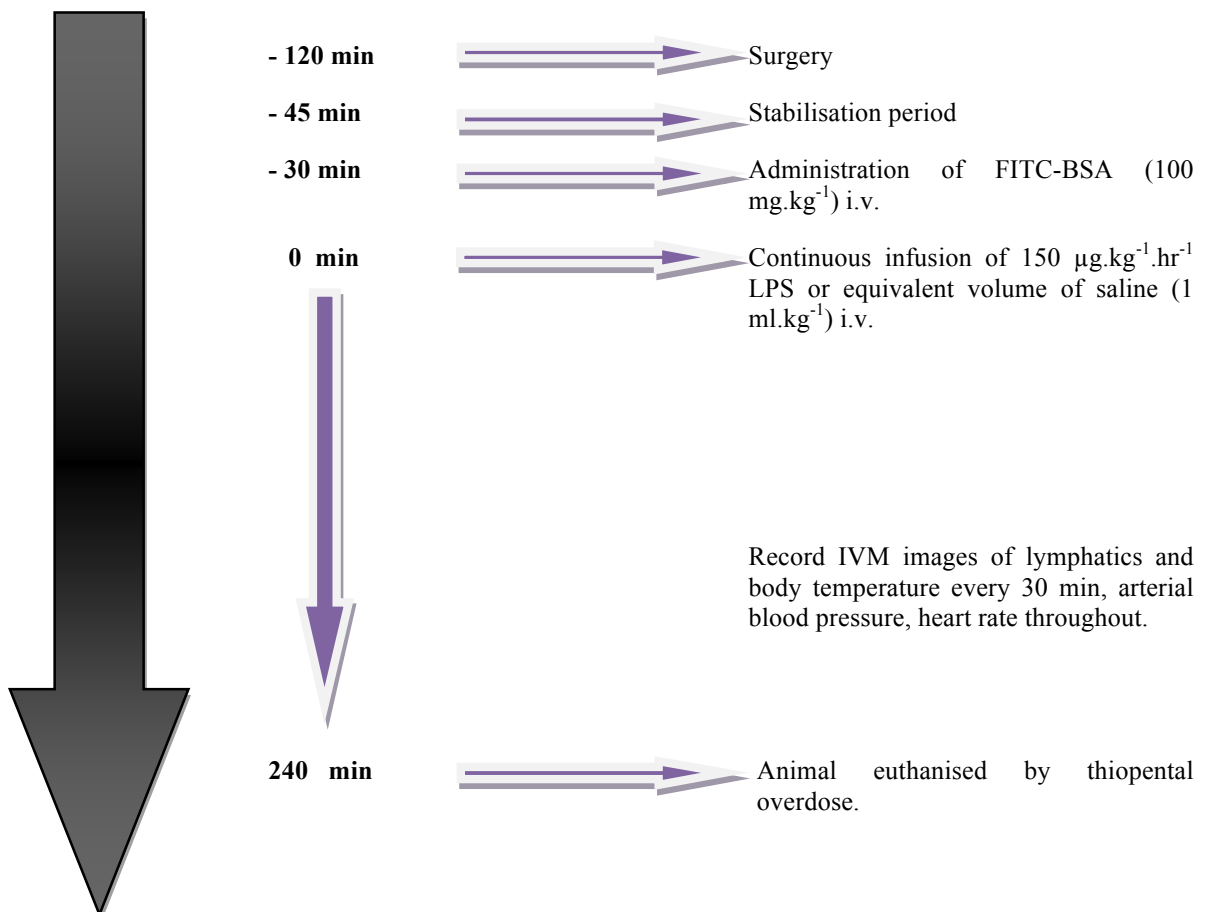
Figure 3.1 Timeline demonstrating the experimental protocol of control and LPS experiments.

3.3 Results

3.3.1 Cardiovascular Variables

LPS (055:B5; Endotoxin units - 600,000 EU, 1.2 x 10^6 EU and 3 x 10^6 EU) was administered in doses ranging from 150 µg/kg/hr – 1 mg/kg/hr. Doses were increased as the expected hypotensive response shown in previous studies published from our lab was not observed at lower doses. A different serotype of LPS (0127:B8) was also administered at the rate of 150 µg/kg/hr in a separate experiment; however, it failed to elicit the expected hypotensive response (Figure 6.1, Appendix III). Experiments using the same batches of LPS to induce endotoxemia in rats performed in parallel in our lab for another study also failed produce a hypotensive response in animals (Personal communication received from Julia Beglov).

LPS at 600 µg/kg/hr reduced MAP significantly ($p < 0.05$) compared to baseline (45-135 min) but the effect was not significant compared to controls (Figure 3.2). Changes in MAP over four hours at all other doses of LPS were not significant compared to baseline (no LPS) or controls. A short-lived hypotensive phase was noticeable in all LPS treated groups; however this effect did not reach statistical significance. LPS at higher doses (600 µg/kg/hr and 1 mg/kg/hr) induced a significant increase ($p < 0.05$) in heart rate compared to controls; however the time points over which this was observed were variable at different doses (Figure 3.3). This suggests the onset of tachychardia two hours post infusion, which was the only noticeable trend in the cardiovascular variables that correlated with increasing doses of LPS. 150 µg/kg/hr LPS (0127:B8) also induced a significant increase ($p < 0.05$) in heart rate at 4 h compared to controls (Figure 6.2, Appendix III). No changes were observed in the control group (Figures 3.2, 3.3). There were no differences between groups at baseline (Table 3.1).

Group	MAP (mmHg)	Heart Rate (bpm)
Saline	121.9 ± 6.7	329.2 ± 23.1
LPS (150 µg/kg/hr)	122.2 ± 6.7	346.8 ± 9
LPS (300 µg/kg/hr)	114.5 ± 4.8	330.1 ± 28.4
LPS (600 µg/kg/hr)	140.3 ± 4.4	356.2 ± 3.4
LPS (1 mg/kg/hr)	124.9 ± 6.9	335.1 ± 29.3

Table 3.1 Mean (± SEM) baseline MAP and heart rate for all experimental groups.
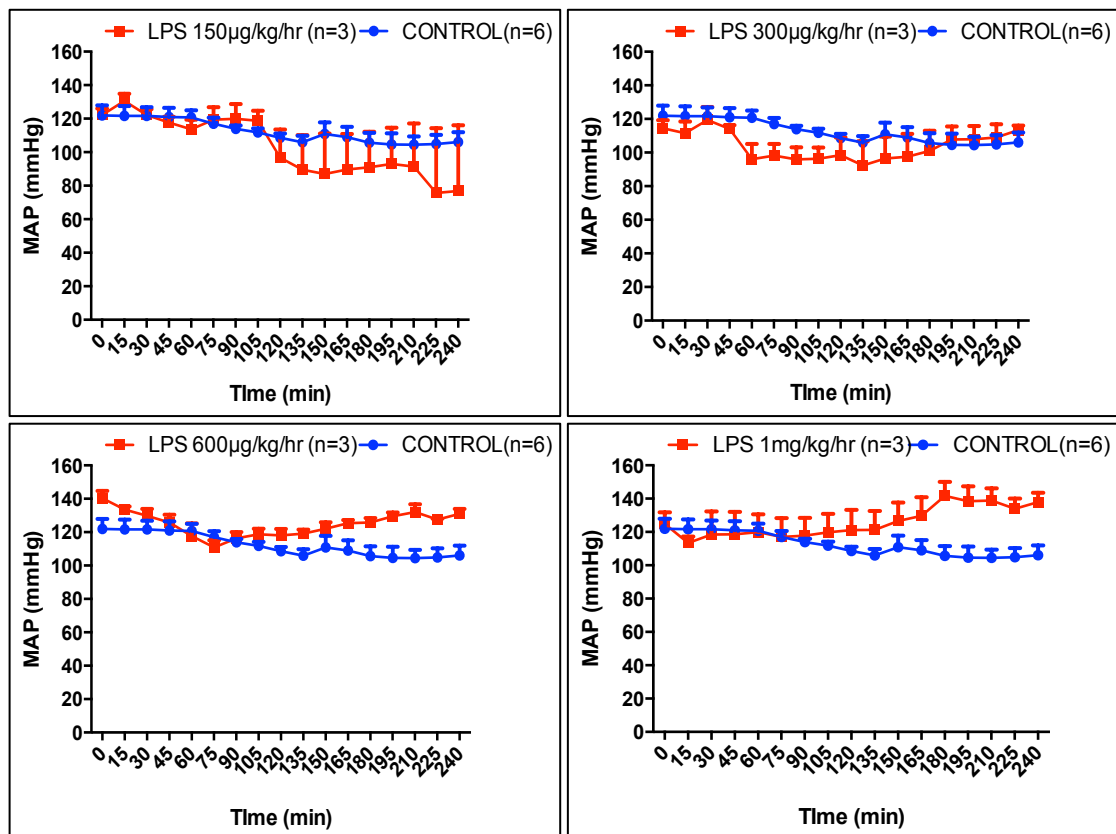
Figure 3.2 Mean arterial pressure (MAP) (mean ± SEM) in LPS and control groups. No significant differences were observed between experimental and control groups.
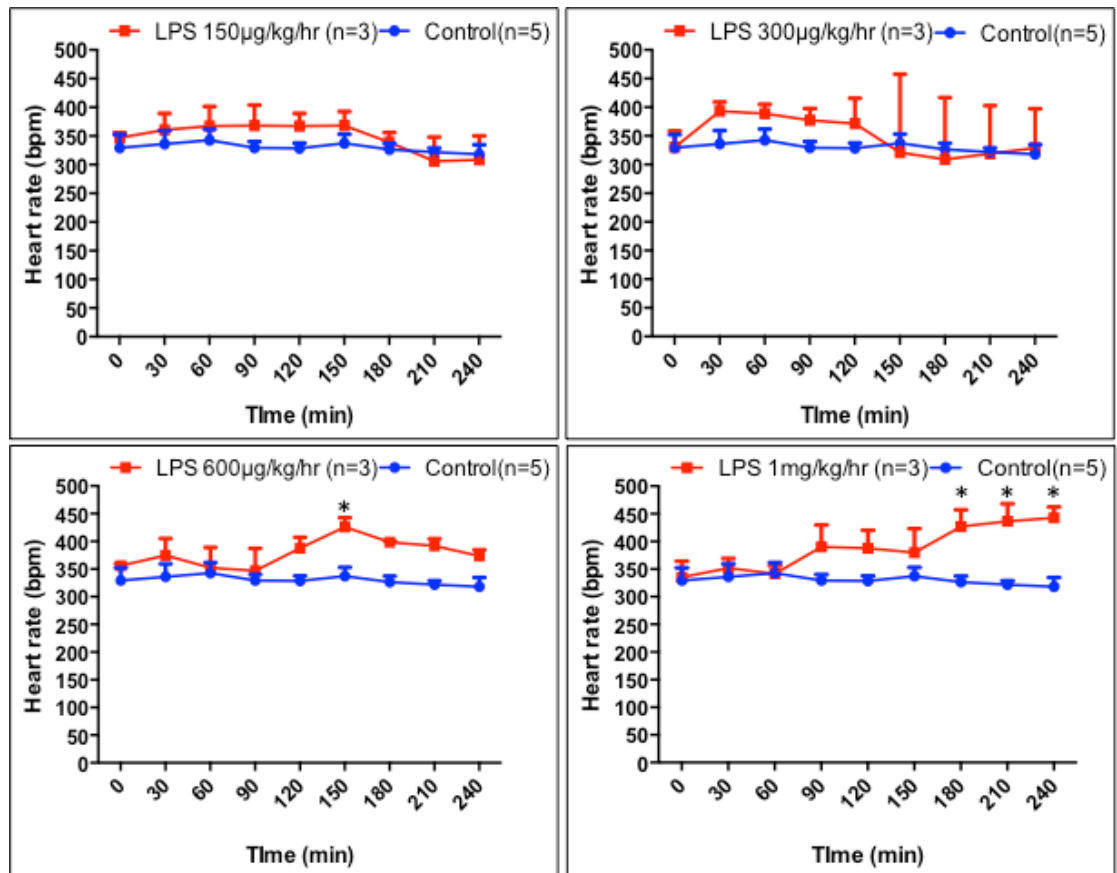
Figure 3.3 Heart rate (bpm; beats per minute) (mean ± SEM) in LPS and control groups. LPS induced an increase in heart rate at 600 μg/kg/hr and 1 mg/kg/hr. *p < 0.05 significantly different to saline.

3.3.2 Lymphatic vessel Diameter

There were fluctuations in diameters of lymphatic vessels in both LPS and control groups throughout the experiment but these were not significant compared to baseline (Figure 3.4). LPS compared to controls induced minimal changes in diameter. Lymphatic vessel diameters were not significantly different between groups at baseline (Table 3.2).

Group	Lymphatic vessel diameters (µm)
Saline	80.2 ± 11.2
LPS (150 µg/kg/hr)	75 ± 13.1
LPS (300 µg/kg/hr)	99.8 ± 13.2
LPS (600 µg/kg/hr)	68.8 ± 5.4
LPS (1 mg/kg/hr)	78.7 ± 6.5

Table 3.2 Mean (± SEM) baseline lymphatic vessel diameters for all experimental groups.
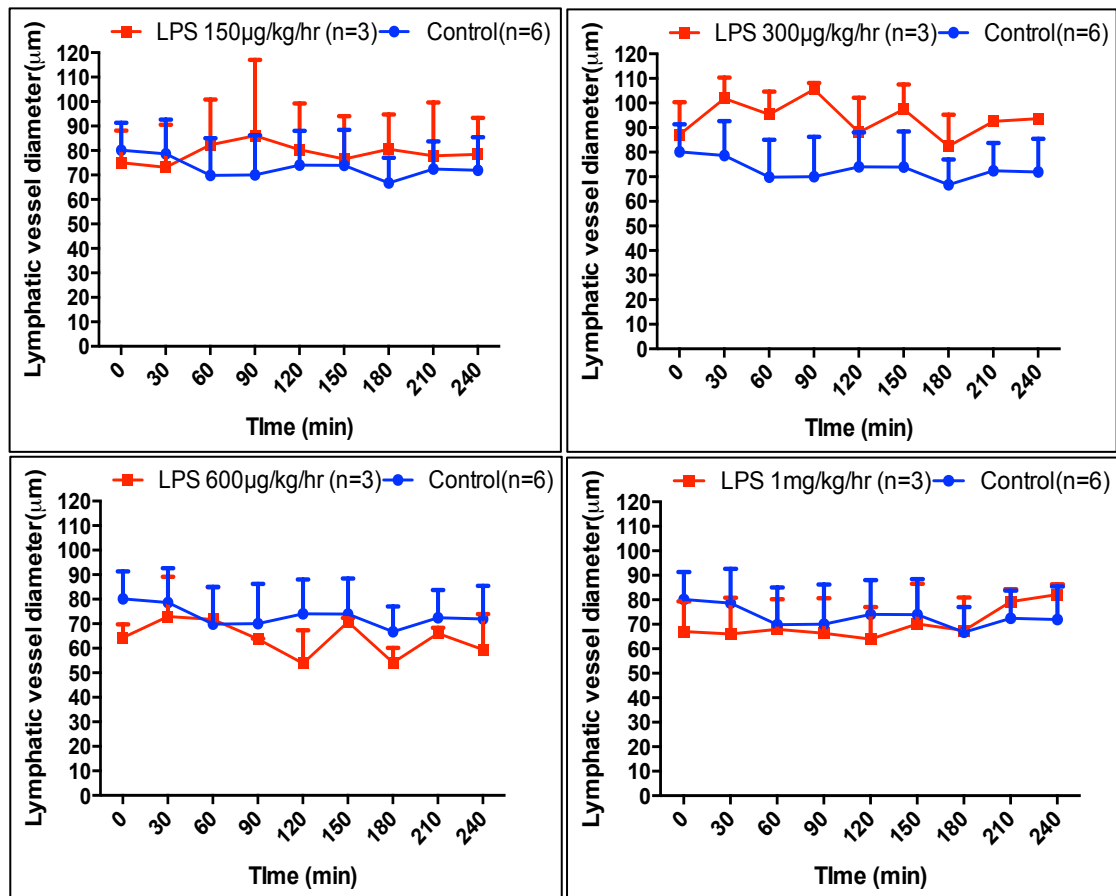
Figure 3.4 Lymphatic diameters (mean ± SEM) in LPS and control groups. Diameters were not altered significantly by different doses of LPS compared to controls.

3.3.3 Macromolecular Leak

Control and LPS treated animals did not demonstrate significant changes in macromolecular leak compared to baseline. There was a significant increase ($p < 0.05$) in leak at 150 µg/kg/hr LPS at 2 h but any differences in macromolecular leak at other doses did not reach significance compared to controls (Figure 3.5). 150 µg/kg/hr LPS (0127:B8) did not induce leak (Figure 6.3, Appendix III).
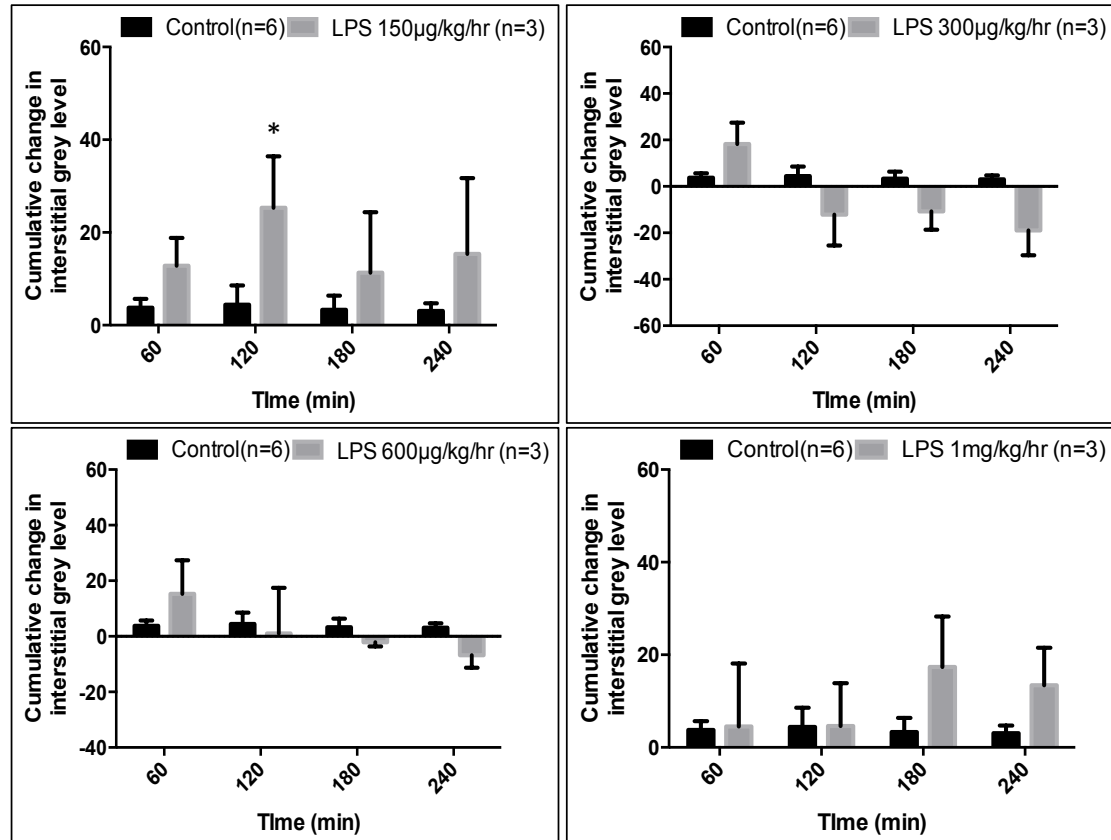
Figure 3.5 Effect of LPS on macromolecular leak. Macromolecular leak is expressed as mean cumulative change in grey level (arbitrary units) (±SEM). Significant difference in leak was observed at 150µg/kg/hr LPS dose (t=2 h) compared to the control group. Levels were not significantly altered at other doses. *$p < 0.05$ significantly different to control.

3.3.4 Levels of FITC-BSA in lymphatics

Levels of FITC-BSA in lymphatic vessels in the control and experimental groups following administration of FITC-BSA are indicated in table 3.3. Levels of FITC-BSA in lymphatic vessels decreased significantly ($p < 0.05$) at later time points in groups administered with LPS at 300 µg/kg/hr and 1 mg/kg/hr compared to controls. A similar trend was observed at 600 µg/kg/hr but the decrease was not statistically significant compared to control (Figure 3.6). 150 µg/kg/hr LPS (0127:B8) significantly decreased ($p < 0.01$) FITC-BSA in the vessels at 4 h (Figure 6.4, Appendix III). FITC-BSA fluorescence is maintained within the lymphatic vessels and post capillary venules in control conditions (Figure 3.7). Figure 3.8 shows macromolecular leak in the interstitium after intravenous administration of 300 µg/kg/hr LPS.

Group	Grey levels in lymphatic vessels
Saline	39.8 ± 6.6
LPS (150 µg/kg/hr)	48.5 ± 9.5
LPS (300 µg/kg/hr)	53.2 ± 12.2
LPS (600 µg/kg/hr)	46.5 ± 9.9
LPS (1 mg/kg/hr)	65 ± 19.1

Table 3.3 Mean (± sem) baseline grey levels in lymphatic vessels for all experimental groups.
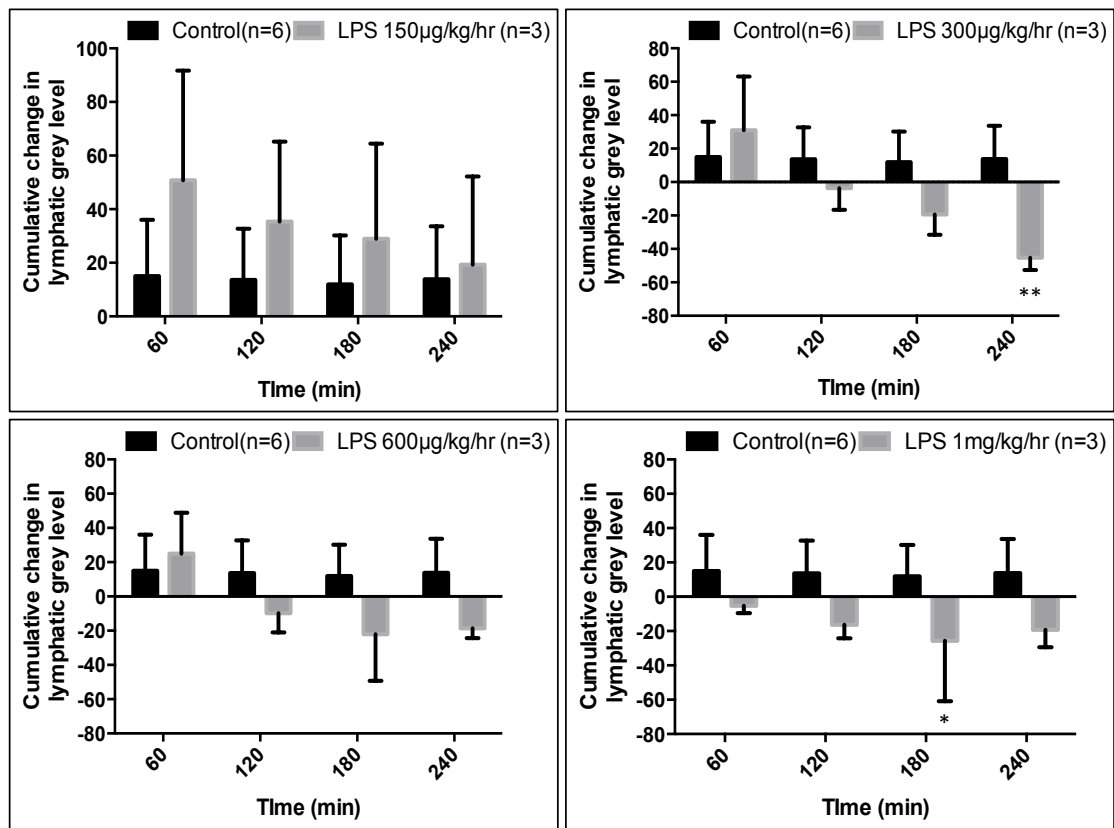
Figure 3.6 Effect of LPS on level of FITC-BSA in lymphatic vessel. Change in protein concentration within the lymphatic vessel is expressed as mean cumulative change in grey level (arbitrary units) (± SEM). A gradual decrease in grey levels is observed at subsequent time points at all doses of LPS compared to control group which is significant at 3 and 4 h at doses 1 mg/kg/hr and 300 µg/kg/hr respectively. *p < 0.05, **p < 0.01 significantly different to control.
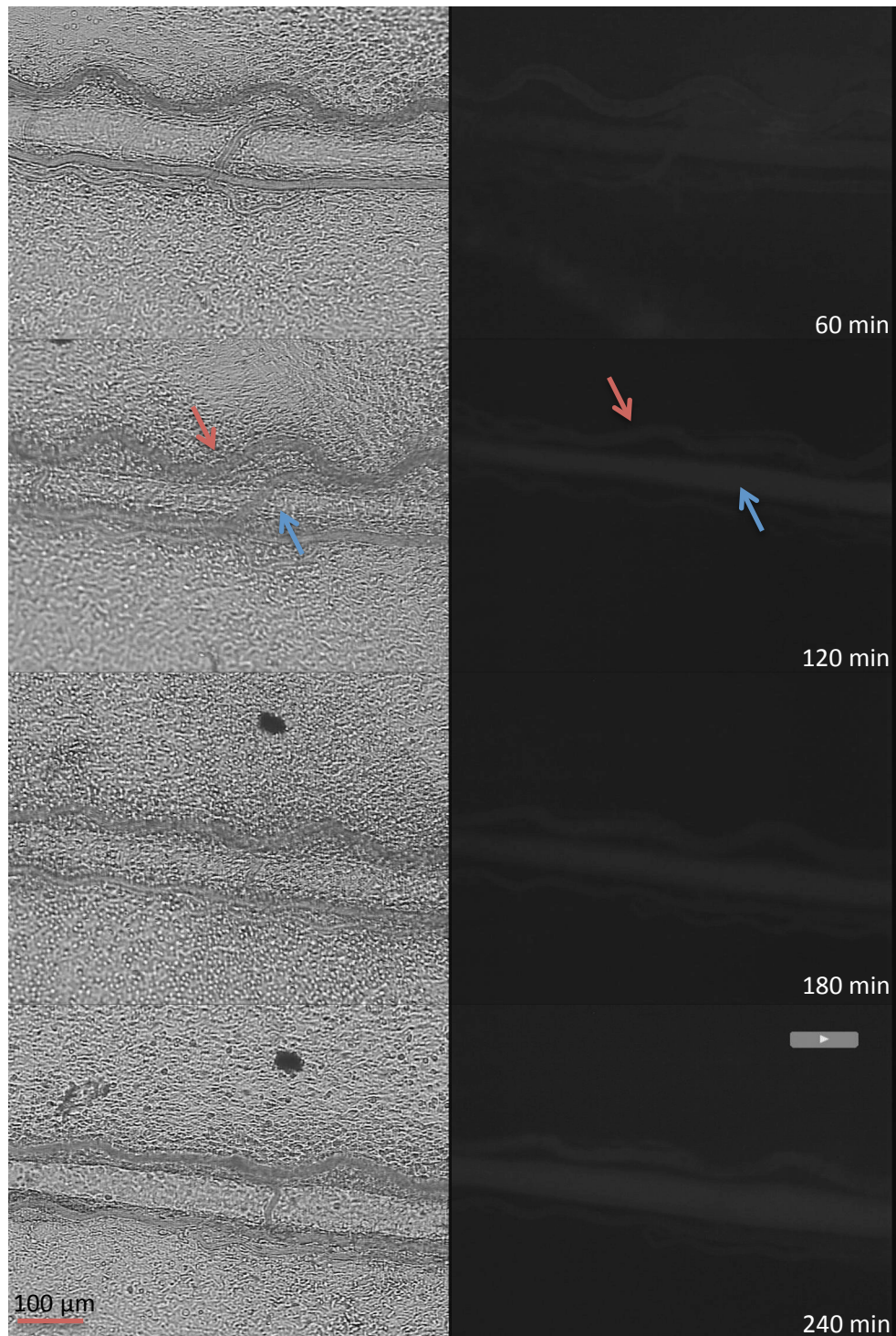
Figure 3.7 IVM images of rat mesenteric lymphatic vessels (40-60 μm) demonstrating FITC-BSA levels in the vasculature at 60, 120, 180 and 240 min after intravenous administration of saline (control). FITC-BSA was activated by blue light (495 nm), to induce fluorescence. It can be observed that intact lymphatic vessel (indicated by blue arrow) and post-capillary venules (indicated by red arrow) maintain FITC-BSA within the vasculature.
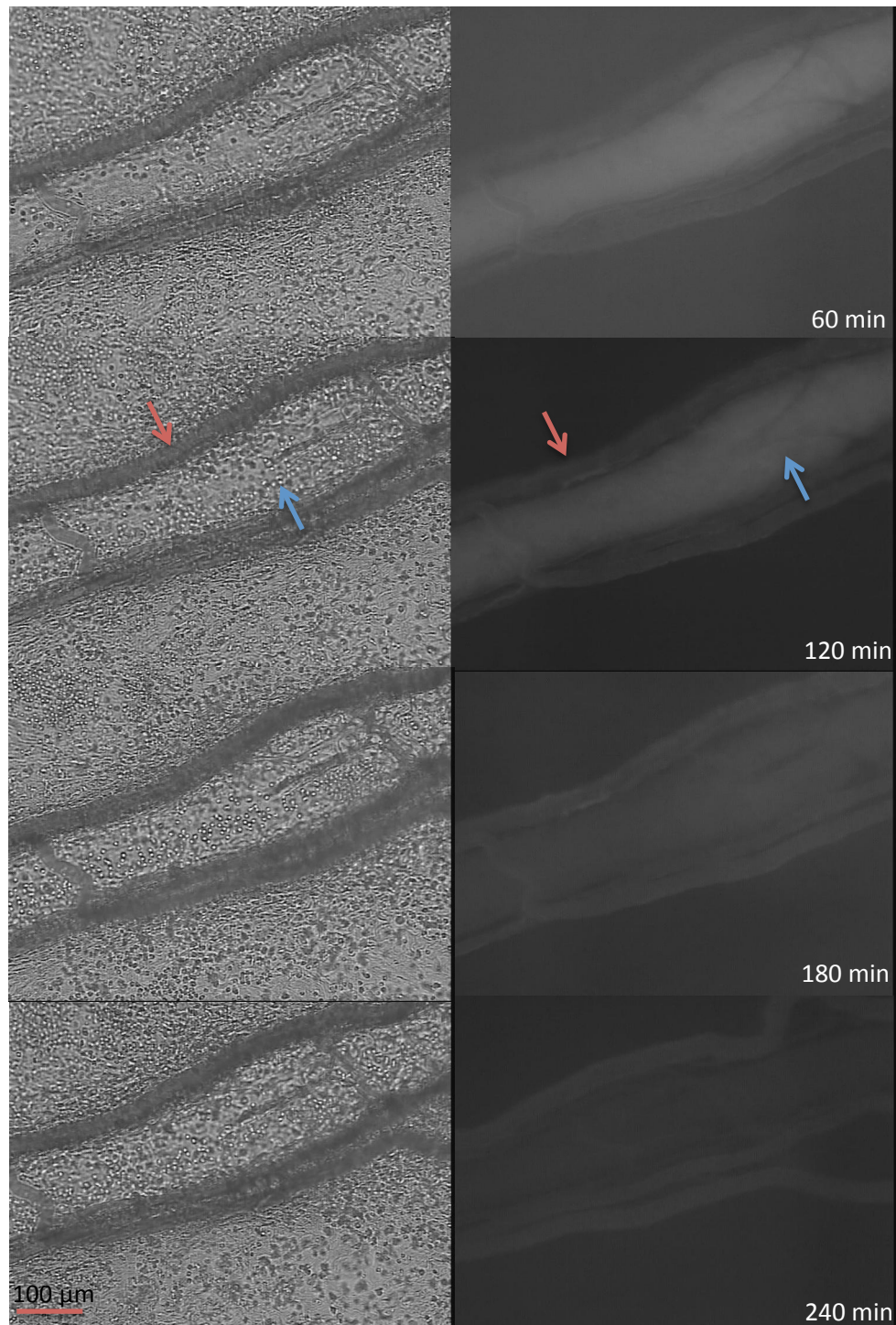
Figure 3.8 IVM images of rat mesenteric lymphatic vessels (90-110 µm) demonstrating FITC-BSA levels in the vasculature and interstitium at 60, 120, 180 and 240 min after intravenous administration of LPS (300 µg/kg/hr). FITC-BSA was activated by blue light (495 nm), causing it to fluoresce. White flare in the interstitium indicates leakage of FITC-BSA from vasculature when integrity of the endothelium is compromised. Macromolecular leak may occur from lymphatic vessel (indicated by blue arrow) and post-capillary venules (indicated by red arrow).

3.4 Summary of results

The dose range of LPS (150 μg/kg/hr-1 mg/kg/hr) used did not induce marked hypotension but induced tachychardia at higher doses (600 μg/kg/hr and 1 mg/kg/hr).
LPS did not elicit obvious changes in lymphatic diameter at any dose.
Increasing doses of LPS did not alter macromolecular leak.
Higher doses of LPS (300 μg/kg/hr and 1 mg/kg/hr) decreased levels of FITC-BSA from the lymphatic vessels evident from the lower than baseline values at later time points (4 and 3 h respectively).

3.5 Discussion

The aim of these experiments was to assess the effect of LPS on various lymphatic parameters. Although the haemodynamic response favours the conclusion that endotoxemia was triggered in the animals at higher doses of LPS, the levels of interstitial leak did not represent an endotoxemic pathophysiology i.e. minimal leak from the vessels. Moreover, it was not possible to evaluate effects on contractility and flow for reasons discussed below. These observations have called into question the suitability of the model to investigate our hypothesis.

3.5.1 Low dose infusion model of endotoxemia

The model of continuous low dose LPS infusion in anaesthetised rats was used to mimic the more subtle pathophysiological septic response, which may be more clinically relevant in patient groups showing pathophysiological responses such as haematological alterations and elevated cytokine levels (Rittirsch *et al* 2007). This model is non-lethal but haemodynamic changes such as prolonged hypotension and tachychardia, which represent the classical features of sepsis, have been reported to occur (Andrew and Kaufman 2001; McGown *et al* 2010). However, the data is conflicting since prolonged hypotension using this regime of endotoxin administration was not demonstrated in other studies (Huang *et al* 1994; Bennett *et al* 2004; Gardiner *et al* 2005). A normotensive response throughout the duration of LPS infusion, even at high doses has also been reported widely (Schmidt *et al* 1996; Schmidt *et al* 1998). In agreement with the latter studies, we observed a largely normotensive response, accompanied by a transient phase of early hypotension with all doses of LPS administered. The short-lived hypotension has been attributed to LPS-induced secretion of endothelial kinins that trigger NO and prostacyclin (Fleming *et al* 1992). Elevated NO may not always result in prolonged hypotension as these effects may be dependent on the time lapsed between surgery and LPS administration, at least during early endotoxemia (Mailman *et al* 1999). Authors reported that LPS reduced blood pressure for only 15 min when injected in rats 2 h post-surgery, whereas caused hypotension for 2 h when injected 15 min post-surgery. It is possible that rats developed a desensitisation to the hypotensive effects of LPS in our study, as was suggested by authors from their observations, since LPS was administered ~2 h after surgery was initiated.

In the current study, tachychardia was observed in experimental groups treated with higher doses of LPS, indicating increased cardiac output to match the increased oxygen demand similar to previously published studies from both our laboratory and others (Bateman *et al* 2003; McGown *et al* 2010). Thus, the haemodynamic response indicates that the low dose infusion of LPS at the higher concentration resulted in endotoxemic rats.

3.5.2 Flow

Lymph flow is an important modulator of lymphatic function as it affects lymphatic contractility and tone by means of wall-shear stress (Gashev *et al* 2002; Gashev *et al* 2004; Dixon *et al* 2006). The pattern and magnitude of flow can either activate or inhibit the intrinsic lymph pump, thus influencing the force of lymph propulsion. Oedemagenic stress increases lymph flow due to increased rates of lymph formation resulting from raised interstitial pressure (Benoit *et al* 1989). Increased lymphatic outflow has also been reported during hypovolaemic shock (Magnotti *et al* 1998) and after endotoxin exposure (Lattuada and Hedenstierna 2006; Nemoto *et al* 2011). However, as the inflammatory insult increases, cessation of lymphatic flow occurs (Elias *et al* 1987). Hence, an estimation of the flow profiles within the lymphatic vessels under normal and pathophysiological conditions is vital to understanding lymphatic dysfunction. For example, it has been proposed that temporal changes in shear stress determine the production of endothelium-derived factors that modulate pumping (Munn 2015). In our studies, visual observations did not identify any obvious differences in lymphatic flow in the presence or absence of LPS. However, observations made in this manner are subjective and non-quantitative and the possibility remains that subtle changes may be occurring in lymphatic flow during the early stages of endotoxemia. The standard video microscopy available in our laboratory has limitations in measuring flow as the camera has an imaging rate of 25 frames/sec, which is not sufficiently sensitive. Flow in mesenteric lymphatics has been measured with a high-speed imaging system at the rate of 500 frames/sec (Dixon *et al* 2005). This technique has the advantage of allowing measurement of cell velocity throughout the cycle of the lymphatic phasic contraction. Propulsive function has also been measured using the NIRF imaging system where responses to acute inflammatory insult locally and systemically were successfully investigated (Aldrich and Sevick-Muraca 2013). Hence, future studies are required using systems to accurately compare

lymph flow velocities under different treatments and in dilated and quiescent lymphatics, as it occurs in sepsis (Liao and von der Weid 2014).

3.5.3 Contractility

In rat mesenteric lymphatics, regular spontaneous contractions form the basis of an active lymph pump. These contractions are well co-ordinated and propagated throughout the vessel (Zawieja *et al* 1993). However, in the current study we found that in most preparations, segments of vessels that were visible (mostly branches of collecting lymphatics) did not show consistent contractile activity and hence could not be used to accurately measure pump frequency. There may be various reasons for lack of a consistent contraction pattern. According to one of the earliest observations by (Hargens and Zweifach 1977), lymphatic contractions in mesenteric collecting lymphatics are irregular and varied with intraluminal pressure. Indeed, studies performed later have shown the profound mutual interdependency of contraction frequency and intraluminal pressure exerted by changes in lymph flow (Gashev *et al* 2002; Gashev *et al* 2004). This is especially relevant to the mesenteric lymphatics because of their role in gastrointestinal function. The rate of lymph formation, a principal passive force influencing lymph flow, in these lymphatics, are highly variable as they are directly dependent on intestinal digestion and absorption (Gashev *et al* 2004). Also, the possibility of a depressant effect on contractions by thiopental cannot be ignored, as previously reported in a study investigating the effects of barbiturates (10^{-4} M or greater dose) on lymphatic contractility (McHale and Thornbury 1989). FITC photoactivation has also been shown to reduce lymphatic contraction frequency (Zhang *et al* 1997). Another reason that the vessels observed had weak contractions maybe the constant application of exogenous saline potentially causing oncoctic changes in the tissue and impair lymphatic contractility similar to observations by (Galanzha *et al* 2005). Hence, due to these confounding factors it would be preferable to use an *in vitro* method that excludes the influence of extrinsic forces, to assess the effects of LPS and other pharmacological agents on contractility.

3.5.4 Diameter

The lymphatic muscle tone largely determines the lymphatic vessel resistance, which in turn regulates the lymph flow and output (von der Weid and Zawieja 2004). *In vitro* studies have shown that a certain degree of basal tone exists in lymphatic vessels

similar to arterioles (Gashev *et al* 2004); however, in contrast to arterioles, lymphatics exhibit myogenic constrictions and dilations to intraluminal pressure changes (Davis *et al* 2009). Authors suggested that the myogenic response may be an important modulator of vessel tone during acute inflammatory/oedematous conditions preventing overdistension of the vessel. In our studies, there were no discernible changes in the diameter of vessels during early endotoxemia compared to controls. Results suggest that vessel tone remains robust in the first 4 h of LPS-induced endotoxemia. However, it is possible that the effects of changes in preload that are known to increase vessel diameter are being compensated by a myogenic constriction response, thus maintaining a robust vessel tone during the period of our observation. Hence, an *in vitro* model that excludes the effects of incoming fluid pressure would be more suitable to assess changes in lymphatic vessel tone.

3.5.5 Macromolecular Leak

Significant differences in interstitial grey levels are an indicator of the loss of endothelial integrity in the surrounding microvasculature. Although, this method is not a direct permeability measurement in post-capillary venules as described by (Michel 2004), it is used as an indication of changes in vessel integrity (Walther *et al* 2003; McGown *et al* 2010; Reeves *et al* 2012). Changes in interstitial grey levels were not significant between control and experimental groups although there were increases in some LPS groups. However, it is difficult to determine whether the leak in the interstitium is venular or lymphatic because of the close proximity of the two vessels, which is a major limitation of the study. Moreover, declining grey levels in the lymphatics and the interstitium suggest the possibility of increased lymphatic clearance rather than 'leaky' lymphatics. The slightly increased fluorescent intensity in lymphatic vessels of endotoxemic rats, during the first hour of administration indicates a higher uptake of FITC-BSA from the interstitium compared to control rats. This may be the result of increased lymphatic contractility as shown previously (Elias *et al* 1987; Elias and Johnston 1990) and possibly increased flow, which supports the possibility of increased lymphatic clearance at later time points. Another ambiguity in interpreting the dynamics of macromolecular efflux and uptake is presented by the lower than baseline values at LPS doses of 300 and 600 μg/kg/hr which suggest that the FITC-BSA is being cleared from the interstitium rapidly. In contrast, in groups receiving 150 μg/kg/hr and 1 mg/kg/hr LPS, interstitial grey levels were increased over the 4 h

period indicate two possibilities: (i) that the effects of LPS at 150 μg/kg/hr and 1 mg/kg/hr are less potent on lymphatic contractility resulting in less clearance and (ii) the effects of LPS are more potent such that the interstitial overload of FITC-BSA from leaky venules is not compensated for even by increased pumping, thereby resulting in more leak but less clearance. One factor that favours the latter possibility is the EU of LPS used for different doses. Whereas n=2 experiments each at doses of 300 and 600 μg/kg/hr were performed with LPS containing EU 6×10^5 and 1.2×10^6, experiments at doses of 150 μg/kg/hr and 1 mg/kg/hr LPS were performed with a higher EU (3×10^6). Experiments with LPS containing higher EU correlate to increased interstitial grey levels indicating a more potent effect thus favouring the latter possibility. The inability to measure the contractile characteristics in this model makes it difficult to ascertain the reason for this discordant data. The results derived from this model did not yield any conclusive evidence for our hypothesis that macromolecular leak may occur from collecting lymphatics during inflammatory conditions as induced by LPS.

3.5.6 Summary and future directions

This is the first study to investigate the effects of LPS on macromolecular leak from mesenteric lymphatics. Further studies were not performed, as this model was deemed unviable for accurate measurement of functional lymphatic parameters *in vivo*. Nevertheless, our speculation that LPS increases lymphatic permeability is supported by studies showing that extra-splenic lymphatics allow the efflux of large protein molecules into interstitial spaces during endotoxemia *in vivo* (Brookes *et al* 2009) and more recently by a study demonstrating leaky lymphatic vessels in inflamed skin of mice (Kajiya *et al* 2012). These findings further substantiate our hypothesis and warrant a further investigation into LEC barrier dysfunction during inflammation. We suggest that macromolecular leak from lymphatics could be investigated using a technique that allows observation of leak into the interstitium exclusively from lymphatics. Trzewik *et al* employed such a technique that involved micropipette manipulation to investigate transport of fluorescent microspheres (.31 μm) across the endothelium into the lumen of initial lymphatics in the rat cremaster muscle (Trzewik *et al* 2001). This technique could be used to design experiments to measure changes in permeability in mesenteric lymphatics. However, this model may still pose a problem in accurate measurement of contractility. An *ex vivo* model as described by Ono *et al*

would be most viable for assessment of both lymphatic endothelial barrier function and contractility during early endotoxemia (Ono *et al* 2005).

Chapter Four

Effect of inflammatory mediators on

rat mesenteric lymphatic vessels

ex vivo

4.1 Introduction

The importance of the role of lymphatics in the direct induction and resolution of inflammation has surfaced from studies spanning the last decade (Hong 2013; Lachance *et al* 2013; Liao and von der Weid 2014). However, this role can be severely compromised in diseases such as sepsis, hence making it an imperative to study the effects of external and internal inflammatory mediators on the lymphatic system in disease, and identify agents to restore their functionality. The model we used in the *in vivo* study was not suitable for characterising lymphatic vessel responses in the early endotoxemic phase as discussed. Hence, the purpose of our *ex vivo* study was to address this issue by investigating the direct effects of LPS and cytokines released in early sepsis on RMLV.

Further, we were interested in the mechanisms mediating these effects. Numerous studies have demonstrated the role of NO in modulating lymphatic contractility and tone. This role has been elaborated in section 1.2.3.3. Under physiological conditions, NO is mostly derived from constitutively expressed NOS. The expression of the inducible form is usually triggered during inflammatory conditions and it is well known that eNOS is destabilised concomitantly (Steyers and Miller 2014). Recent literature suggests that eNOS plays an important role in the regulation of lymphatic pumping and tone. Two important studies confirm that eNOS in LECs is essential for maintaining robust lymphatic contractions under physiological conditions, hence depleted levels of eNOS in the inflammatory state result in impaired contractile activity (Liao *et al* 2011; Scallan and Davis 2013). Since LPS is known to disrupt the delicate physiological balance between eNOS and iNOS in the blood vasculature (McGown and Brookes 2007), we speculated the possibility of similar mechanisms operating in the lymphatic vasculature on exposure to inflammatory mediators, thus effecting the production of NO and consequentially altering contractility. Hence, we investigated whether effects of mediators were NO mediated and levels of eNOS/iNOS were altered.

We were also interested in the potential role of Ang-1 in counteracting the effects of inflammatory mediators on lymphatic vessels due to the burgeoning evidence of its anti-inflammatory effects in blood vessels, particularly restoration of permeability via eNOS upregulation (Alfieri *et al* 2014). NO derived from eNOS is attributed to play a

protective role against the toxic effects of LPS-released mediators and hence we wondered if Ang-1 could protect lymphatic pump function by providing beneficial NO.

These questions led us to hypothesise that LPS and cytokines such as TNF-α and IL-1β impair lymphatic contractility via NO regulation and Ang-1 has a protective effect on pump function in inflamed vessels.

This study aimed to utilise lymphatic pressure myography to investigate this hypothesis. This system allows the *ex vivo* study of isolated lymphatic vessels under controlled pressure and flow, excludes any external neural, physical or hormonal factors and removes the sources/sinks for NO production/action (Chakraborty *et al* 2015). Hence, any effects observed could be attributed to the direct actions of inflammatory mediators than to a secondary consequence of inflammatory outcomes such as oedema (Chakraborty *et al* 2011). Moreover, rat mesenteric lymphatics exhibit much stronger contractile characteristics as isolated vessels (Gashev *et al* 2002; Gashev *et al* 2004).

4.2 Control Optimisation

The technique was initially learnt at Dr Zawieja's lab in Texas A&M University using a set-up where the myography chamber was designed to allow continuous suffusion of the media (DMEM-F12 or APSS) into the bath. Only one experiment with each medium was performed due to time constraints, however vessels exhibited a stable frequency throughout the duration of the experiment (Figure 6.5, Appendix IV). The experimental design had to be altered when experiments were initiated in the University of Sheffield as continuous suffusion was not possible using the chamber model available in the laboratory. To mimic early endotoxemia and observe the effects of LPS, it was important to achieve a stable frequency of contraction for ~3 h. Different protocols (Table 4.1) were attempted to determine the volume of media and intervals at which it should be replaced to maintain a robust vessel for the length of the experiment. Vessels were maintained in DMEM-F12 and APSS with or without changes in pressure and a number of studies (each study denoting a group) were undertaken to obtain optimal bath conditions. Ordinary one-way ANOVA followed by Tukey's multiple comparisons test was used to analyse differences within groups to determine change in frequency over 3 h.

Protocol for media replacement in the bath	Effects on frequency of contraction
DMEM-F12 replaced every 30 min with changes in pressure	High variability at 1.5 h and 3 h
DMEM-F12 replaced every 1 h with changes in pressure	High variability at 1.5 h and 3 h
DMEM-F12 replaced every 1 h without changes in pressure	Reduced contractions at 3 h
APSS replaced every 45 min with changes in pressure	High variability at 1.5 h
APSS replaced every 45 min without changes in pressure	Stable frequency up to 3 h
APSS not replaced	Stable frequency up to 2 h; rapid decline after 2 h
1mM Ca^{2+} dissolved in ultrapure water added to APSS every 30 min after equilibration	Stable frequency up to 2.30 h

Table 4.1 Different media replacement methods that were attempted to obtain a stable frequency for the duration of the experiments (~3 h).

The first set of experiments was performed using DMEM-F12. Media was replaced every 30 min or 1 h in two groups of experiments. Since our aim was to perform frequency measurements at a range of pressures, vessels were subjected to 1, 3 and 5 cm H_2O at three different time-points. A range of pressures was used to mimic intraluminal pressure variation in physiological conditions (Gashev *et al* 2004). There were differences between the frequency of contractions at 1.5 h and 3 h at 3 cm H_2O in both groups from baseline. Change in frequency at 1.5 h (3 ± 6) and 3 h (2 ± 2) in the group where media was replaced every 30 min was considerably different from baseline (11 ± 4). Similarly, differences in frequency change from baseline (12 ± 2) were also notable at 1.5 h (8 ± 4) and 3 h (5 ± 4) in the group where media was replaced every 1 h. Though these differences were not significant, groups exhibited high variability indicated by the error bars (Figure 4.1). A third group of experiments

was then performed without changes in pressure to minimise variation in frequency, but reduced contractions were observed at 3 h.

The next set of experiments was performed with APSS (Figure 4.2). Considerable differences in frequency from baseline were observed at different time points in vessels subjected to pressure changes (group 1). Change in frequency at 1.5 h (5 ± 4) and 3 h (1 ± 3) was considerably different from baseline (7 ± 1). Differences were minimal in vessels maintained at 3 cm H_2O (group 2). The protocol was modified further (group 3) as it could not be used in further experiments involving addition of other agents to the bath. For example, when the protocol was used with experiments that involved the addition of LPS to the bath, stable frequency was disrupted. Addition of 1mM Ca^{2+} maintained a fairly stable frequency throughout the experiment. Vessels also exhibited consistent amplitude therefore ensuring stable vessel characteristics. Figures 4.3 and 4.4 depict the frequency and amplitude changes in the vessel every 5 min up to 2.5 h, respectively.   Experiments were also performed without replacing the media. Stable frequency was observed in this group (group 4) for at least up to 1.5 h after which there was a rapid decline in frequency. Hence, the protocol used for group 3 was used in further experiments to ensure optimal conditions that minimised variation in vessel frequency and 2.5 h was chosen as the standard duration of experiments, as there was a considerable reduction in frequency after this time-point in group 3. Baseline frequency is indicated as (mean $\pm$ SEM) contractions/min and amplitude as (mean $\pm$ SEM) micrometers.
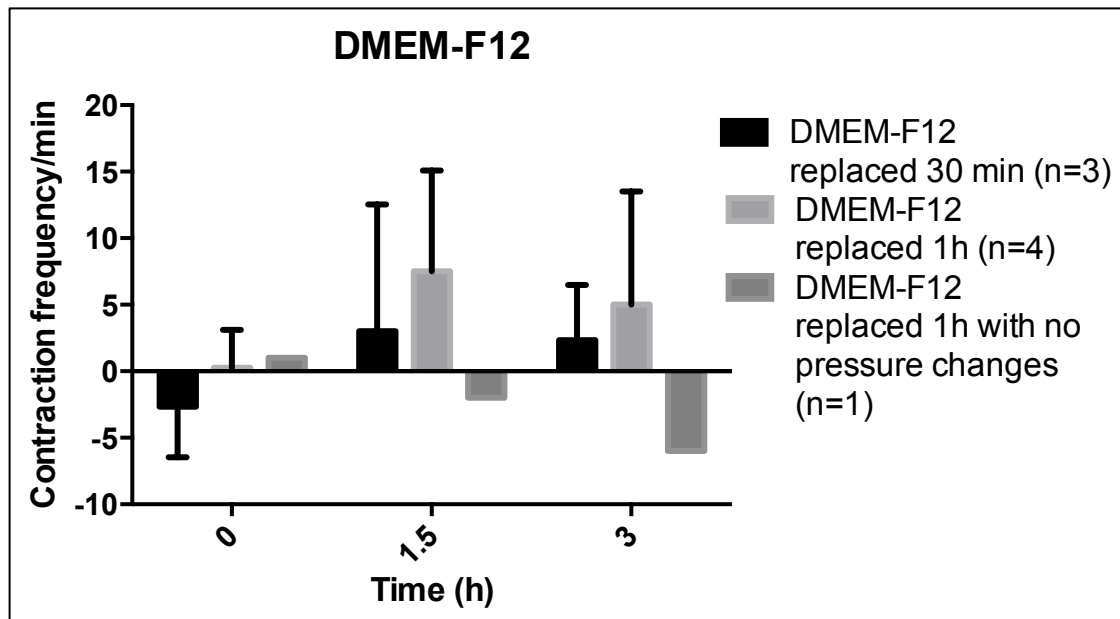
Figure 4.1 Change in frequency of contractions (mean ± SEM) at 3 cm H$_2$O in vessels maintained in DMEM-F12 which was replaced with fresh media every 30 min and 1 h with or without pressure changes. No significant differences in frequency were observed at different time points in groups. Baseline frequency for DMEM-F12 replaced every 30 min= 11 ± 4, DMEM-F12 replaced every 1 h= 12 ± 2, DMEM-F12 replaced every 1 h with no pressure changes= 8.
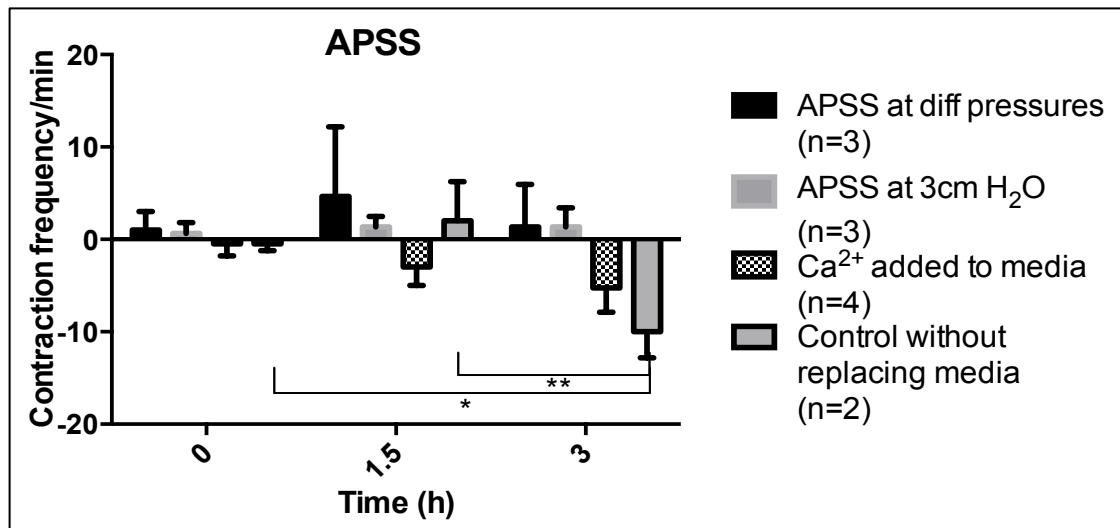
Figure 4.2 Change in frequency of contractions (mean ± SEM) at 0, 1.5 and 3 h in vessels maintained in APSS 1) replaced every 45 min at different pressures and at 3 cm H$_2$O 2) with Ca^{2+} added to media and 3) without replacing media. Change in frequency in control without replacing media was significantly different at 3 h from baseline and 1.5 h. No significant differences were observed between time-points in other groups. *p < 0.05 vs baseline, **p < 0.01 vs 1.5 h. Baseline frequency for APSS at different pressures (3 cm H$_2$O shown in graph) = 7 ± 1, APSS at 3 cm H$_2$O= 7, and for control without replacing media=10 ± 2.
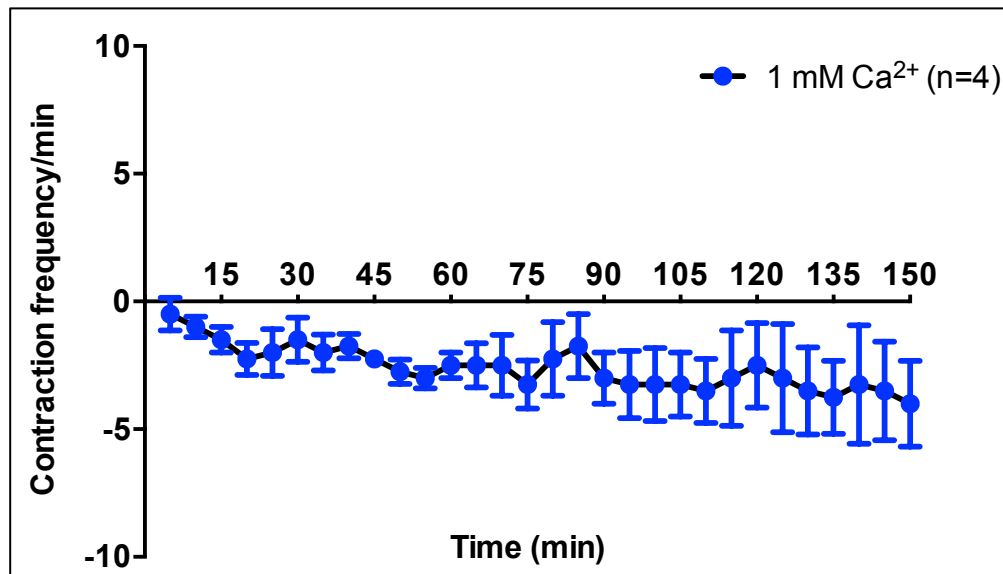
Figure 4.3 Change in frequency of contractions (mean ± SEM) in vessels maintained in APSS with Ca^{2+} added to media every 30 min. No significant differences were observed from baseline. A stable frequency was observed over 2.5 h. Baseline frequency= 10 ± 2.
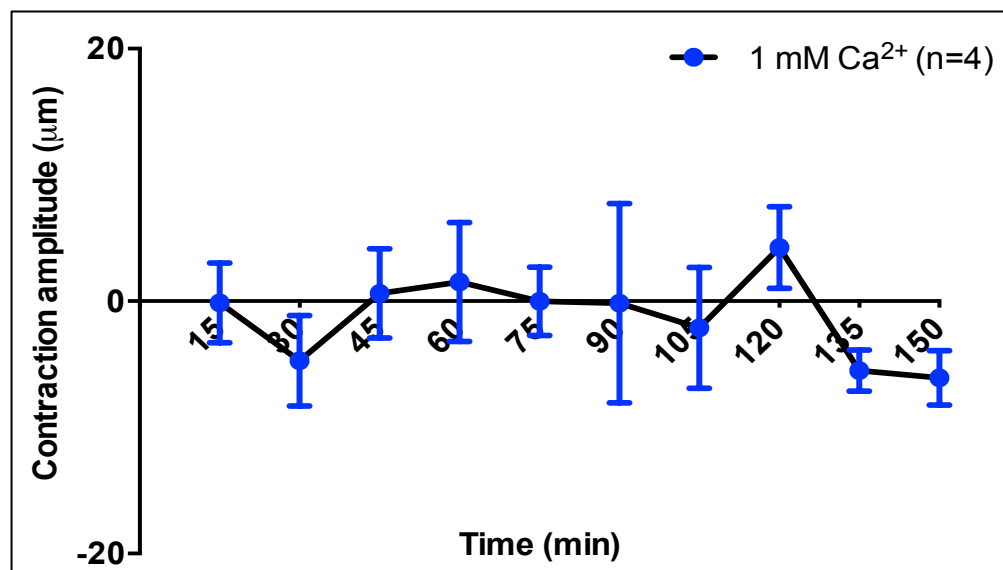
Figure 4.4 Change in amplitude of contractions (mean ± SEM) in vessels maintained in APSS with Ca^{2+} added to media every 30 min. No significant differences were observed from baseline. A stable amplitude was observed over 2.5 h. Baseline amplitude = 113.3 ± 7.7 μ.

4.3 Investigation into the role of NO

We first wanted to establish the role played by intrinsic and extrinsic NO in the contractility of lymphatic vessels in our experimental setting. L-NAME was used to globally inhibit intrinsic NO production. Effects of intrinsic NO were assessed by stimulation of vessels with Ach and Acetyl-β-methylcholine chloride (AMch). Extrinsic NO was provided by the NO-donor, SNP.

L-NAME

L-NAME was added to the bath at concentrations of 1mM and 10mM in separate groups of experiments to determine whether inhibition of basal NO altered frequency or amplitude of contraction in the vessels. Initially, 1mM L-NAME was used as *in vivo* effects have been observed at this concentration (Bohlen *et al* 2009). Application of 1mM L-NAME or its inactive isomer D-NAME did not alter the frequency (9 ± 2 vs 10 ± 4) (Figure 4.5) or amplitude (117.07 ± 11.35 vs 116.71 ± 2.24) (Figure 4.6). An irregular frequency was observed on treatment with 10mM L-NAME and this effect was not different compared to 10mM D-NAME treatment (Figure 4.7).
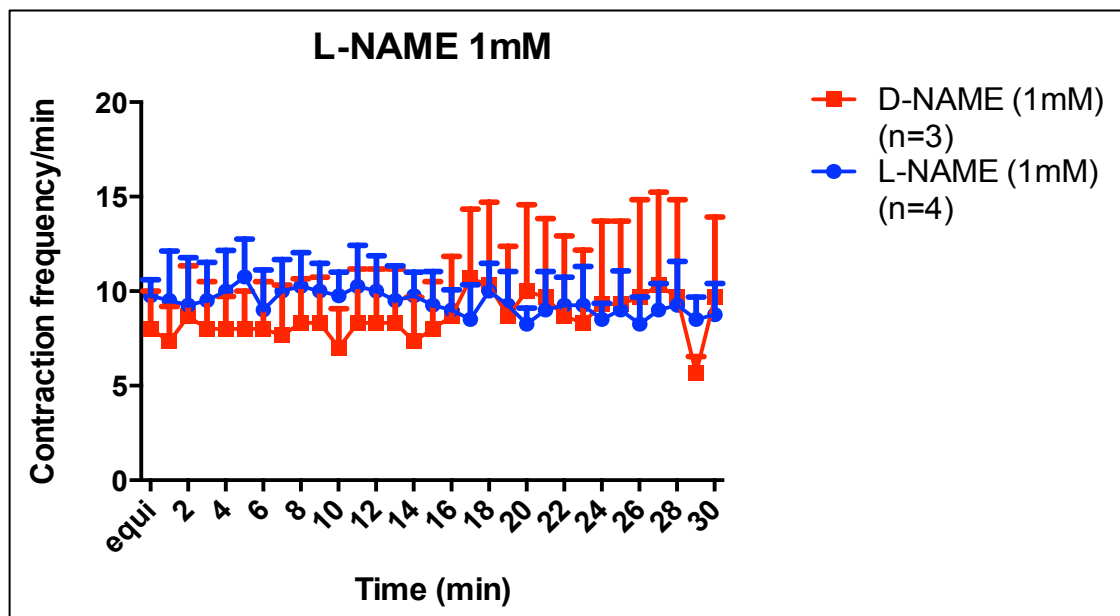
Figure 4.5 Frequency of contractions (mean ± SEM) in vessels treated with 1mM L-NAME and D-NAME. Minimal decrease in frequency (6 ± 13%) was observed over 30 min from baseline but differences within groups from baseline or between L-NAME and D-NAME were not significant at any time point. Baseline frequency for L-NAME=10 ± 1, D-NAME= 8 ± 2.
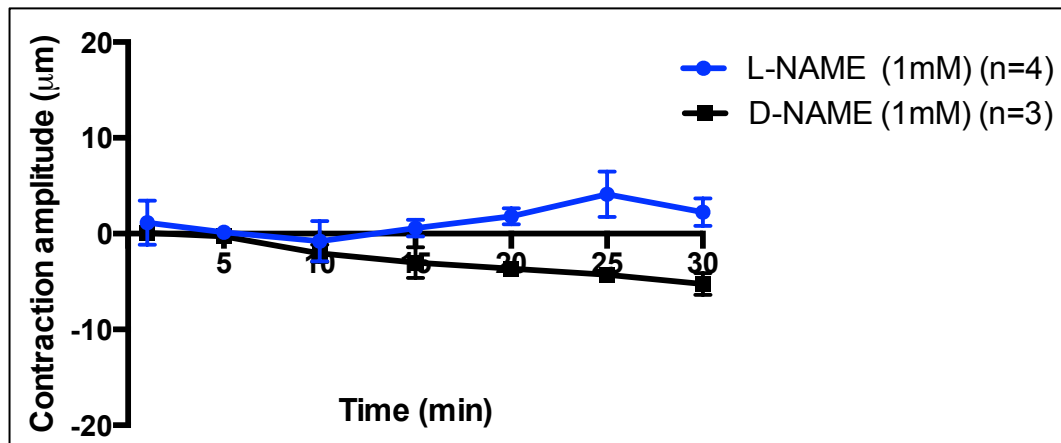
Figure 4.6 Amplitude of contractions (mean ± SEM) in vessels treated with 1mM L-NAME and 1mM D-NAME. No significant difference was observed in groups from baseline or between L-NAME and D-NAME. Baseline amplitude for L-NAME= 114.8 ± 11.7 μ, D-NAME= 121.9 ± 2.9 μ.
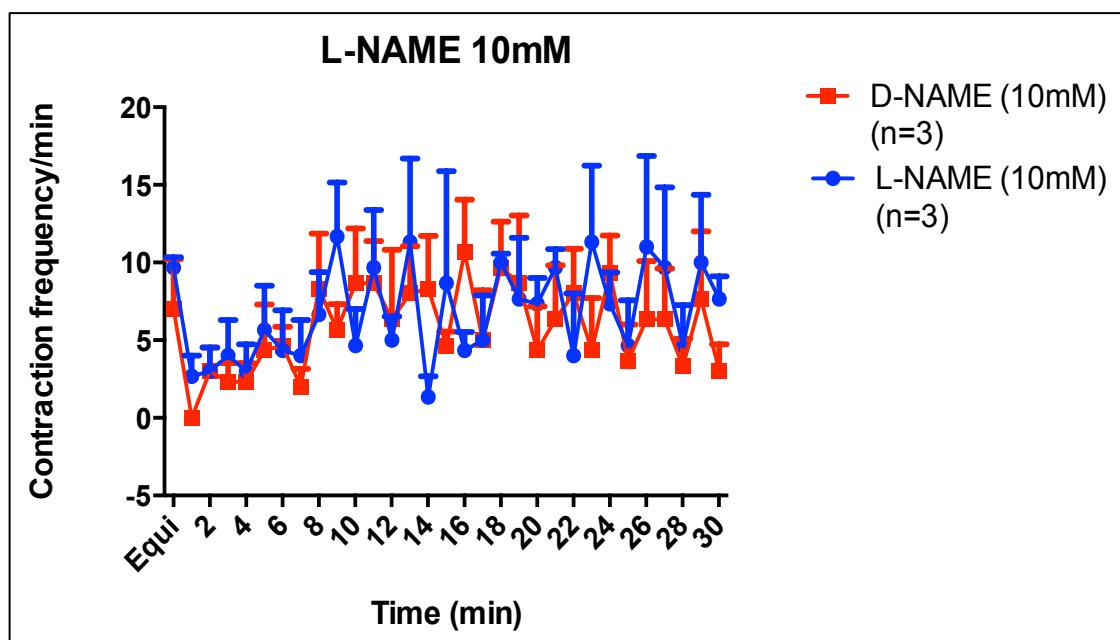
Figure 4.7 Frequency of contractions (mean ± SEM) in vessels treated with 10mM L-NAME and D-NAME. No significant difference was observed in groups from baseline or between L-NAME and D-NAME at any time point. Baseline frequency for L-NAME= 10 ± 1, D-NAME= 7 ± 3.

Acetylcholine chloride and Acetyl-β-methylcholine chloride

Vessels were stimulated with 10^{-5} M Ach to assess the effects of endogenous NO production on vessel frequency and amplitude of contraction. A considerable increase in frequency was observed in stimulated vessels compared to baseline after 10 min of application. Since this effect was in contrast with the previously published studies (Yokoyama and Ohhashi 1993), 10^{-5} M AMch, an analogue of Ach was used in the next experiment. Effects on frequency observed were similar to that of Ach (Figure 4.8). Both substances decreased amplitude after 10 min of application to vessels (Figure 4.9).
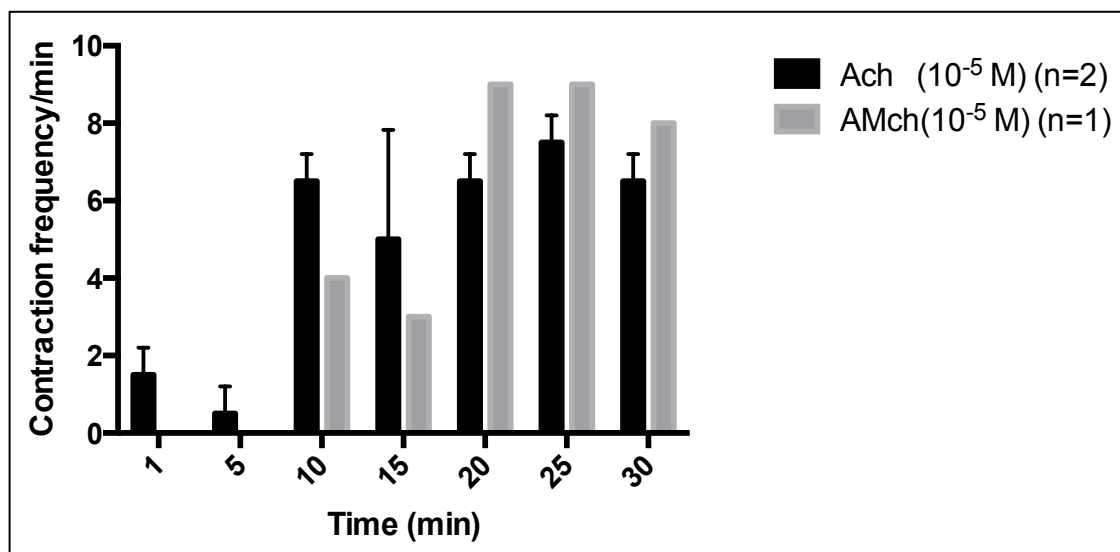
Figure 4.8 Change in frequency of contraction in vessels treated with acetylcholine chloride (10^{-5} M) and Acetyl-β-methylcholine chloride (10^{-5} M). A considerable increase in frequency was observed in stimulated vessels compared to baseline after 10 min of application of Ach and AMch. Baseline frequency with Ach= 6, AMch= 4.
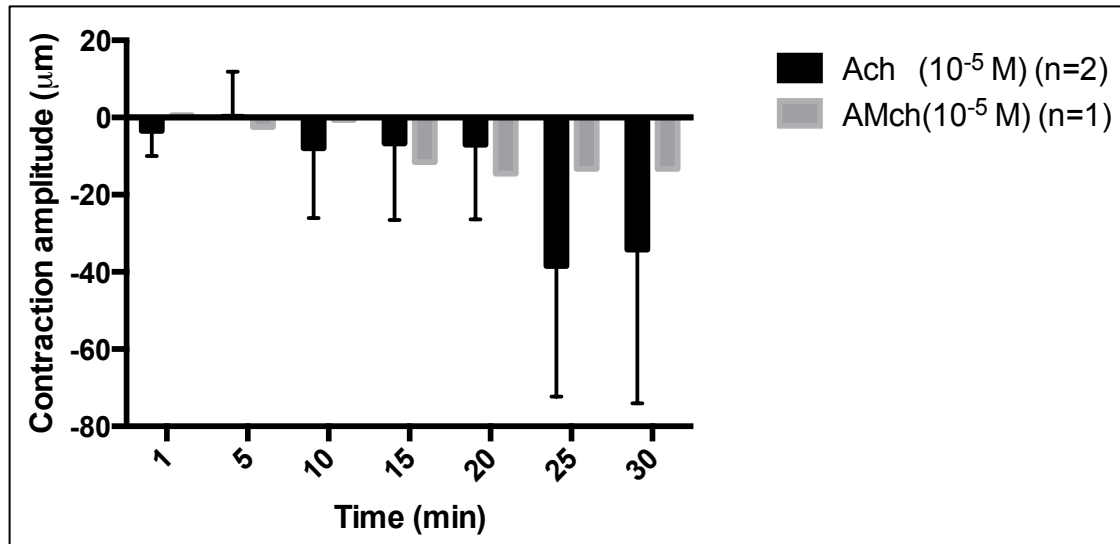
Figure 4.9 Change in amplitude of contraction in vessels treated with acetylcholine chloride (10^{-5} M) and Acetyl-β-methylcholine chloride (10^{-5} M). Stimulated vessels exhibited decreased amplitude after 10 min of application of Ach and AMch. Baseline amplitude with Ach= 147.2 ± 4.2 μ, AMch= 149.6 μ.

SNP

To determine the effects of external application of an NO donor on contractility, 1mM SNP was added to the bath. 1mM SNP was used in these experiments, but effects have also been observed with 10^{-4} M (von der Weid *et al* 2001). Treatment with 1mM SNP appeared to reduce frequency of contraction over 15 minutes when compared to baseline (44 ± 17 %), however this was not significant (Figure 4.10). Considerable reduction (13 ± 4 %) was observed in the amplitude of contractions within 5 min of treatment with SNP, which appeared minimal at subsequent time points (Figure 4.11).
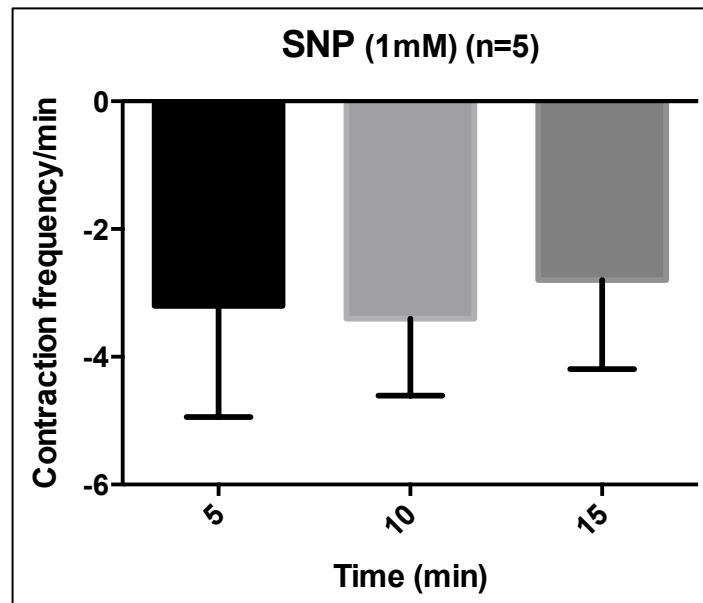
Figure 4.10 Change in frequency of contractions (mean ± SEM for 5 experiments) from baseline after addition of 1mM SNP. SNP induced a reduction in frequency over 15 min (44 ± 17 %). Reduction was not significantly different from baseline at any time point. Baseline frequency= 5 ± 1.
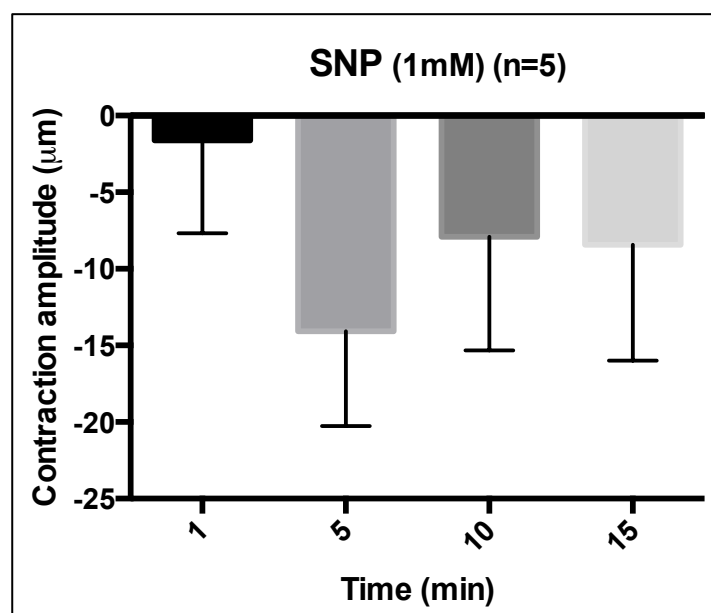
Figure 4.11 Change in amplitude of contractions (mean ± SEM for 5 experiments) from baseline after addition of 1mM SNP. Marked reduction in amplitude (13 ± 4%) was observed within 5 min of treatment with SNP. Reduction was not significantly different from baseline at any time point. Baseline amplitude= 122.9 ± 23.8 μ.

Whereas no significant role for basal NO in regulating contraction frequency and amplitude under normal pulsatile flow could be established from the results, exogenous NO caused a considerable reduction in contractility. Hence, we wanted to determine the effects of different inflammatory mediators on these parameters and if these effects were mediated by NO.

4.4 Effect of LPS

Figures 4.12 and 4.13 illustrate the effects of LPS on lymphatic contractile activity. These effects were assessed at a dose of 50 μg/ml LPS with and without 1% heat inactivated fetal calf serum (FCS) from Gibco® added to the media. FCS was added to the media as various reports have shown that serum provides LBP which accelerates the binding of the LPS–LBP complexes to CD14, thus enhancing cell activation (Ohki *et al* 1999). The number of contractions measured over 2.5 h revealed a potent inhibitory effect on phasic contractions in vessels treated with LPS (Batch 1). LPS (Batch 1) treated vessels appeared to reduce the frequency of contractions and amplitude at 45 min progressing to complete inhibition at 1 h. This effect however was not reproducible when a second set of experiments was performed with a different batch of LPS under the same conditions. No significant effect was observed with LPS treatment in the absence of FCS. In a different experimental setting (Texas A&M University), LPS reduced the frequency of contraction at 0 h and 1.5 h progressing to complete inhibition by 3 h (Figure 6.5, Appendix IV).
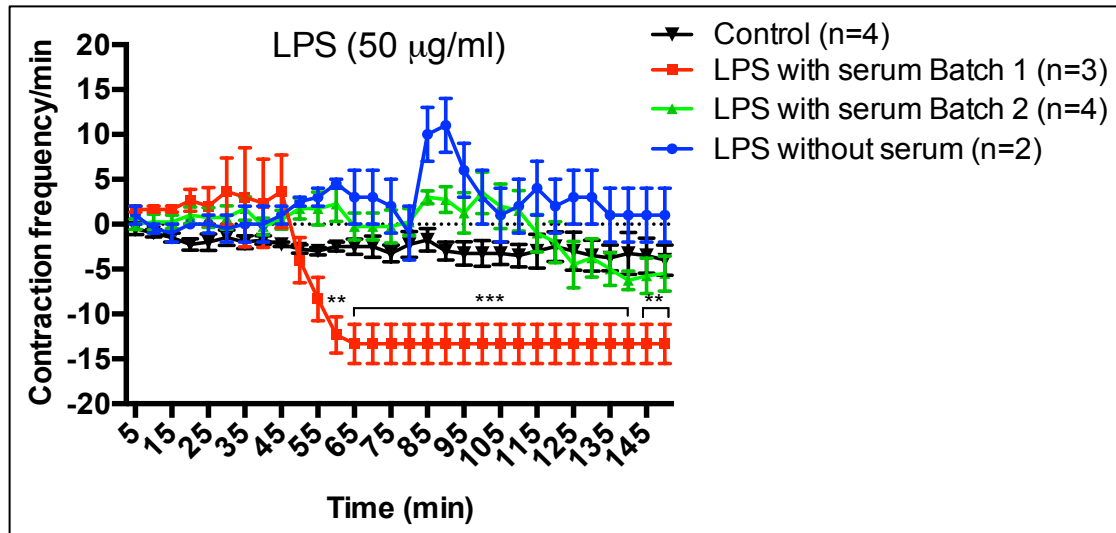
Figure 4.12 Change in frequency of contractions after addition of APSS containing 50 µg/ml LPS with and without serum. Decline in frequency was significant between 60-145 min in LPS treated with serum (batch 1) compared to baseline and control. **$p < 0.01$, ***$p < 0.001$ vs control. Baseline frequency for LPS with serum (batch 1)= 13 ± 2, LPS with serum (batch 2)= 11 ± 1, LPS without serum= 6 ± 1.
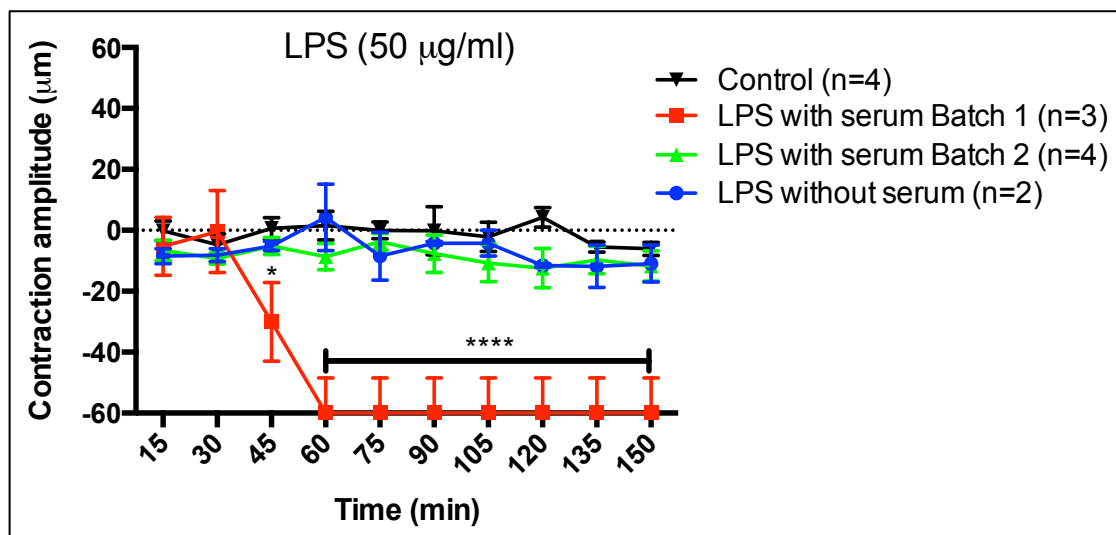
Figure 4.13 Change in amplitude of contractions after addition of APSS containing 50 µg/ml LPS with and without serum. Amplitude significantly dropped at 45 min in LPS with serum (batch 1) compared to control and maximum reduction in amplitude was observed at 60 min compared to baseline and control. *$p < 0.05$, ****$p < 0.0001$ vs control. Baseline amplitude for LPS with serum (batch 1)= 68.7 ± 15.5 µ, LPS with serum (batch 2)= 99.2 ± 12.1 µ, LPS without serum= 111.2 ± 50.6 µ.

4.5 Effect of TNF-α

Recombinant rat TNF-α was added to the bath in concentrations ranging from 10 – 500 ng/ml. Lower concentrations (10 and 30 ng/ml) reduced frequency of contractions consistently over the duration of the experiment. 100 ng/ml TNF-α increased frequency whereas 500 ng/ml resulted in an increase until 80 min after which a rapid decline was observed (Figure 4.14). A decline in amplitude observed at both concentrations reached significance over the last 15 min at 500 ng/ml (Figure 4.15). 10 ng/ml TNF-α was used for further studies as the response at higher concentrations was toxic as indicated by the biphasic response curve.
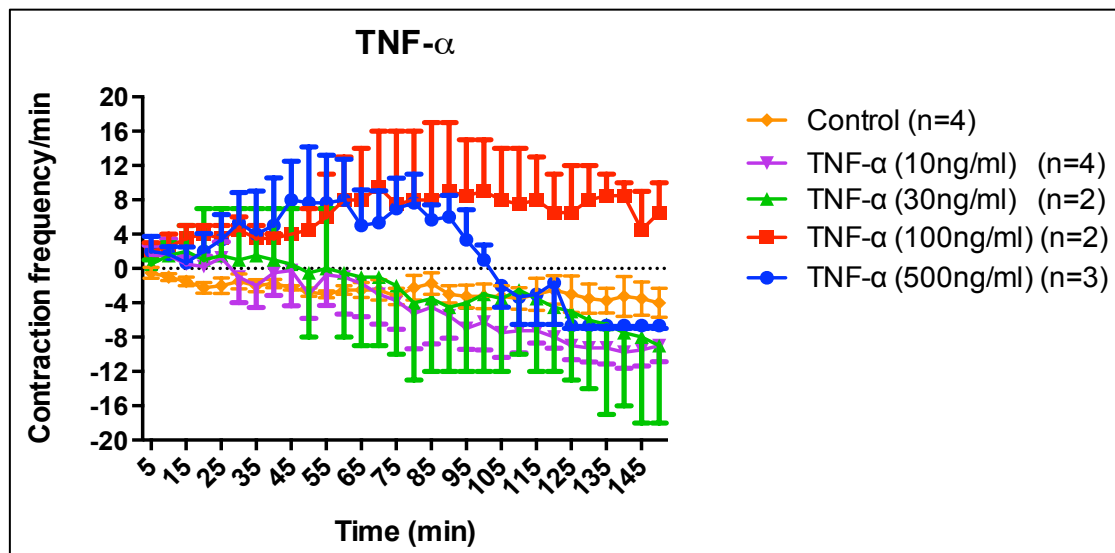
Figure 4.14 Change in frequency of contractions after addition of APSS containing TNF-α (10 – 500 ng/ml). Compared to the change in frequency in untreated vessels (control), 10 ng/ml and 30 ng/ml TNF-α depressed frequency gradually as evident from the consistently declining trend. An increase in frequency was observed with 100 ng/ml. Response with 500 ng/ml was more complicated with a marked increase in frequency for up to 80 min leading to complete inhibition at 120 min. Baseline frequency for TNF-α (10 ng/ml)= 14 ± 4, TNF-α (30 ng/ml)= 15 ± 3, TNF-α (100 ng/ml)= 7 ± 1, TNF-α (500 ng/ml)= 7.
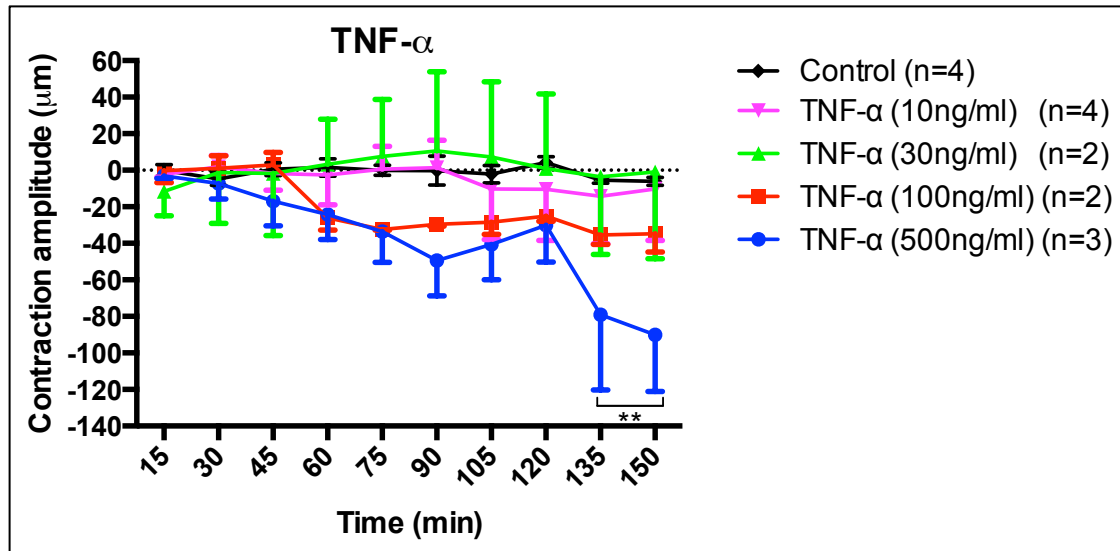
Figure 4.15 Change in amplitude of contractions after addition of APSS containing TNF-α (10 – 500 ng/ml). Amplitude was not significantly different from control in any group except between 135-150 min in the group treated with 500 ng/ml TNF-α and from baseline at 150 min. **p < 0.01 vs control. Baseline amplitude for TNF-α (10 ng/ml)= 72 ± 12.7 μ, TNF-α (30 ng/ml)= 92.4 ± 16 μ, TNF-α (100 ng/ml)= 103 ± 9 μ, TNF-α (500 ng/ml)= 109.2 ± 16.3 μ.

4.6 Effect of IL-1β

Recombinant rat IL-1β at 10 or 100 ng/ml did not effect change in the frequency of contractions (Figure 4.16). Higher concentration of IL-1β evoked a complicated response with a noticeable increase in frequency up to 60 min and a sharp decline at 65 min, which was consistent until the end of the experiment. In combination with 10 ng/ml TNF-α, the effects on frequency were relatively similar to 10 ng/ml TNF-α added alone (Figure 4.17). There was a significant reduction in amplitude between 75-90 min at 10 ng/ml IL-1β, which was not observed at a higher concentration or in combination with TNF-α (Figure 4.18).
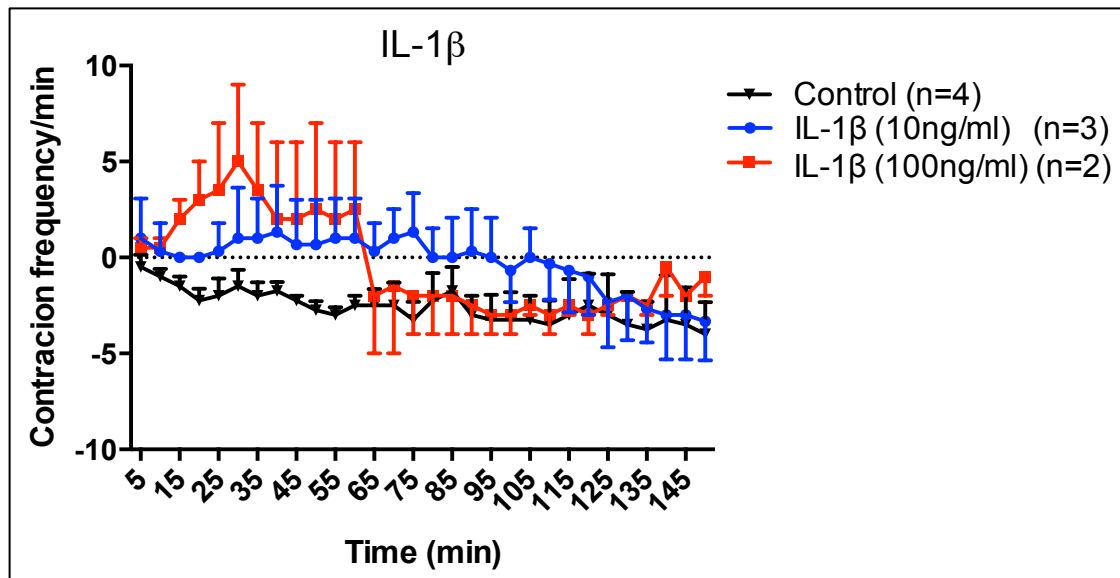
Figure 4.16 Change in frequency of contractions after addition of APSS containing IL-1β (10 – 100 ng/ml). No significant changes in frequency were observed in either group compared to control or baseline. 100 ng/ml IL-1β appeared to increase frequency up to 60 min with a rapid decline at 65 min that lasted until 150 min. Baseline frequency for IL-1β (10 ng/ml)= 7 ± 2, IL-1β (100 ng/ml)= 8 ± 5.
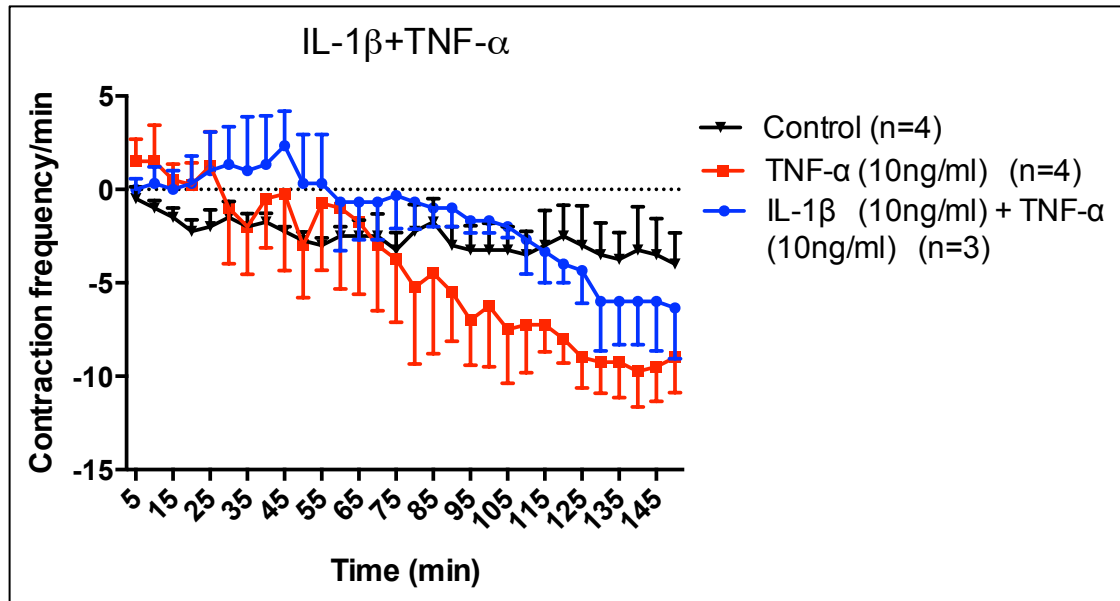
Figure 4.17 Change in frequency of contractions after addition of APSS containing TNF-α (10 ng/ml) alone and in combination with IL-1β (10 ng/ml). A gradual decrease in frequency was observed in vessels treated with TNF-α and IL-1β between 60-150 min. This trend was comparable to the reduction in frequency between 30-150 min induced by TNF-α alone. Differences were not significant in either group compared to control or baseline. Baseline frequency for IL-1β +TNF-α= 8 ± 2.
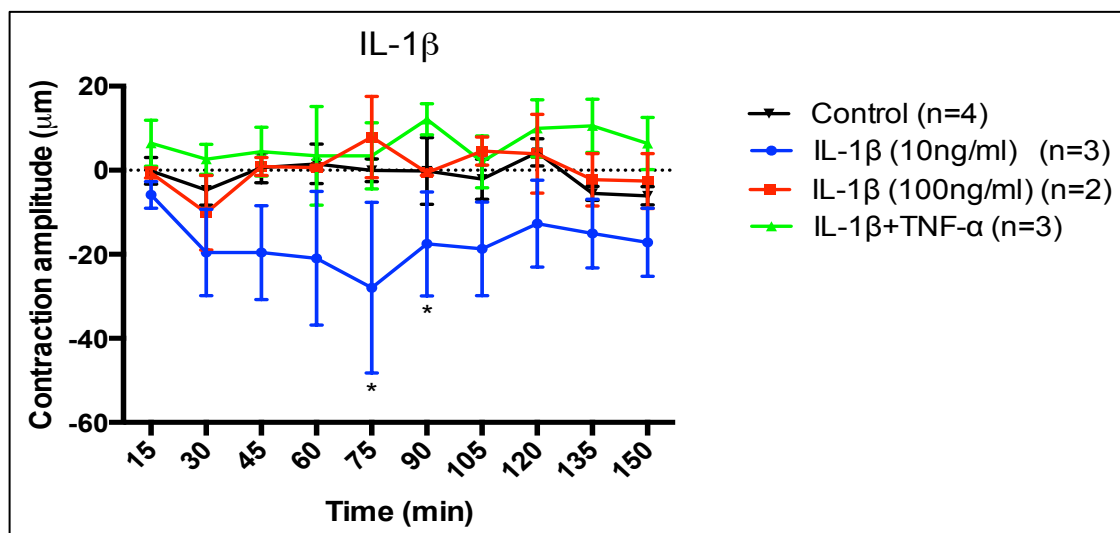
Figure 4.18 Change in amplitude of contractions after addition of APSS containing IL-1β (10 – 100 ng/ml) and IL-1β (10 ng/ml) with TNF-α (10 ng/ml). Amplitude decreased significantly between 75-90 min with 10 ng/ml IL-1β compared to control but not baseline. No changes were observed at 100 ng/ml or in combination with TNF-α. *$p < 0.05$ vs control. Baseline amplitude for IL-1β (10 ng/ml)= 115.3 ± 9.3 μ, IL-1β (100 ng/ml)= 127.8 ± 19.4 μ, IL-1β +TNF-α= 100.6 ± 20.3 μ.

Amongst the 3 different inflammatory mediators we tested, the most consistent effects on the frequency of contraction were demonstrated by 10 ng/ml TNF-α. We then investigated if these effects were NO mediated. L-NAME was added to the bath at 2 different concentrations of 0.1mM and 1mM. Both concentrations prevented the decline in frequency observed with TNF-α alone (Figure 4.19). Change in amplitude did not reach statistical significance in any group (Figure 4.20).
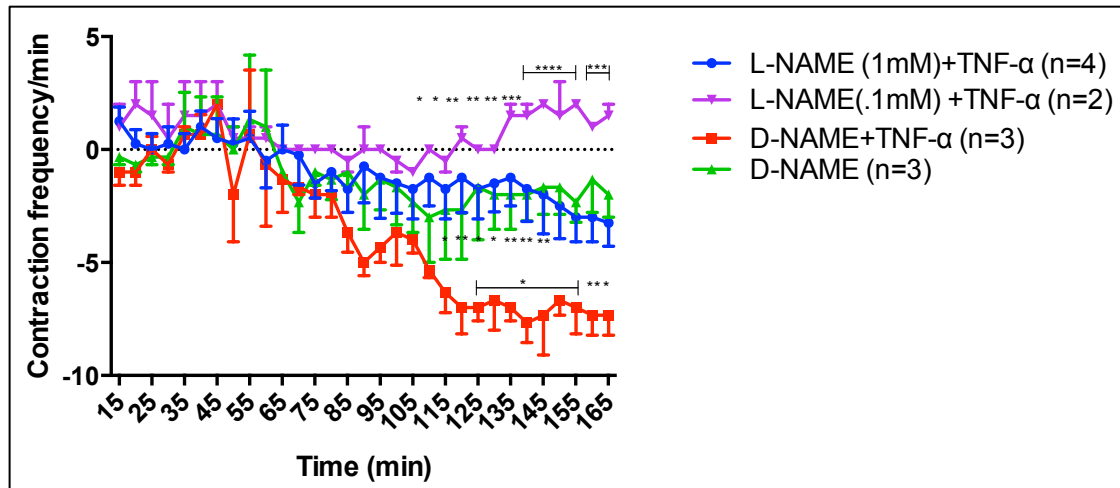
Figure 4.19 Change in frequency of contractions after addition of APSS containing 10 ng/ml TNF-α to vessels treated with L-NAME (0.1 – 1 mM) or D-NAME (1 mM). Frequency of contractions altered by TNF-α in presence of 0.1mM L-NAME between 105-165 min was significantly lower than frequency altered by TNF-α in presence of D-NAME. $*p < 0.05$, $***p < 0.001$, $****p < 0.0001$ vs D-NAME + TNF-α. Effect of TNF-α + 1mM L-NAME on frequency between 115-145 min was significantly lower than TNF-α + D-NAME. $*p < 0.05$, $**p < 0.01$ vs D-NAME + TNF-α. TNF-α + D-NAME significantly lowered frequency between 125-165 min compared to D-NAME alone. $*p < 0.05$, $**p < 0.01$ vs D-NAME. Baseline frequency for L-NAME (.1mM) + TNF-α= 9, D-NAME + TNF-α= 12 ± 2, L-NAME (1mM) + TNF-α= 10 ± 2.
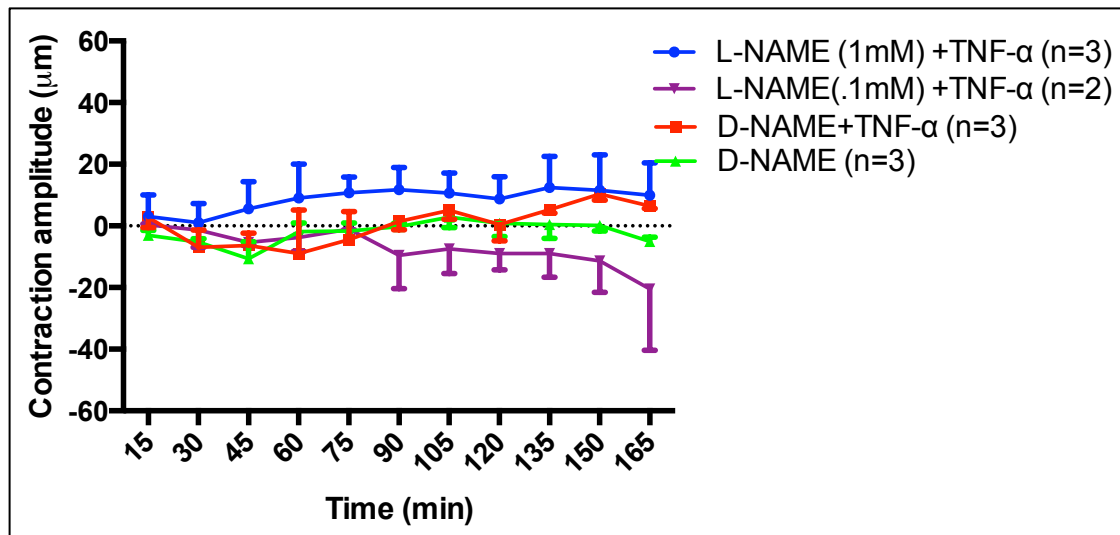
Figure 4.20 Change in amplitude of contractions after addition of APSS containing 10 ng/ml TNF-α to vessels treated with L-NAME (0.1 – 1 mM) or D-NAME (1mM). Amplitude remained unaltered in vessels treated with TNF-α with or without NO blockade. Baseline amplitude for L-NAME (.1mM) + TNF-α= 140.4 ± 13.8 μ, D-NAME + TNF-α= 102.6 ± 5.2 μ, L-NAME (1mM) + TNF-α= 94.8 ± 13.4 μ.

We then wanted to investigate if prostaglandins had a role in mediating the response resulting from exposure to TNF-α. Addition of 10μM indomethacin reverted the effects of TNF-α on frequency of contractions (Figure 4.21). Indomethacin induced a stable increase in amplitude for the duration of the experiment compared to TNF-α treated vessels (Figure 4.22).
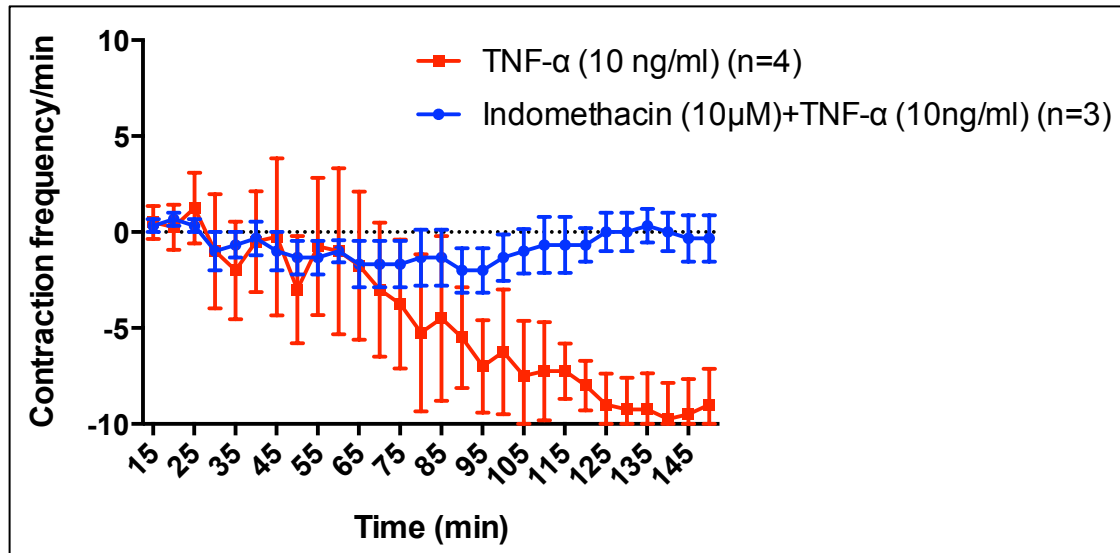
Figure 4.21 Change in frequency of contractions after treatment of vessels with 10 ng/ml TNF-α or Indomethacin (10μM) followed by 10 ng/ml TNF-α. Indomethacin appeared to prevent the reduction in frequency of contractions compared to frequency reduced by TNF-α. Baseline frequency for indomethacin + TNF-α= 6 ±1.
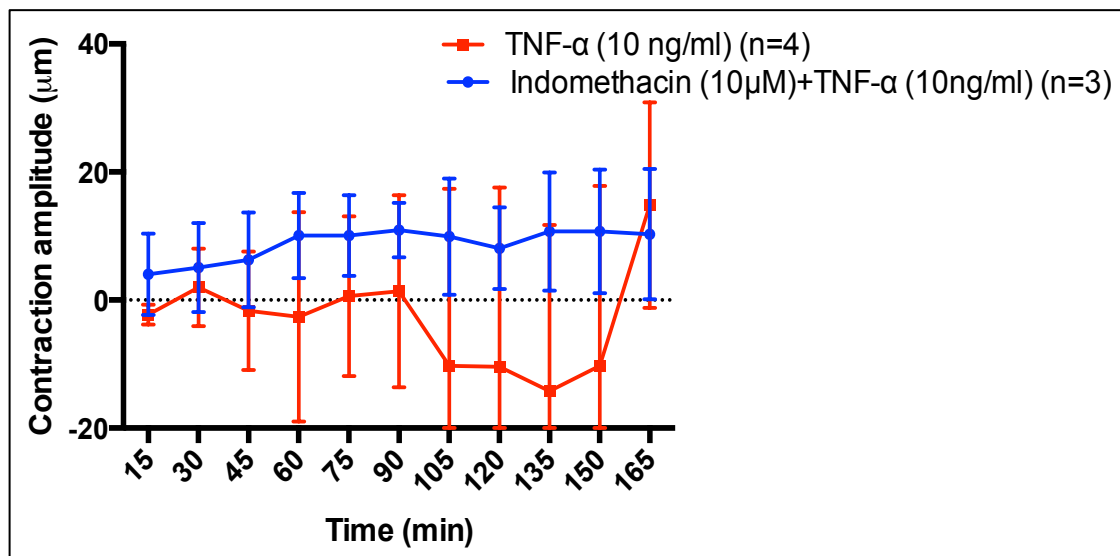
Figure 4.22 Change in amplitude of contractions after treatment of vessels with 10 ng/ml TNF-α or Indomethacin (10μM) followed by 10 ng/ml TNF-α. A decrease in amplitude was noticeable between 90-150 min with a rapid increase at 165 min in TNF-α treated vessels. Treatment with indomethacin maintained an increased amplitude between 15-165 min. Differences observed were not significant. Baseline amplitude for indomethacin + TNF-α= 118.5 ±10.5 μ.

Studies with inflammatory mediators showed that LPS and TNF-α have negative chronotropic effects on the vessels. LPS abolished contraction amplitude within 60 min whereas increased amplitude was observed with 10 ng/ml TNF-α at the end of 2.5 h. IL-1β alone did not alter frequency of contraction but decreased amplitude over a brief 15 min time period. Decline in frequency with TNF-α was prevented by L-NAME and indomethacin independently.

4.7 Effect of Ang-1

Following on from the response obtained with TNF-α treatment, we wanted to determine if Ang-1 attenuated or prevented this response. Vessels were treated with HR.Ang-1 (denoted as Ang-1) to investigate effects on the lymphatic vessel. The dose used was 250 ng/ml (Hall and Brookes 2005). Vessels incubated in 250 ng/ml Ang-1 15 min prior to addition of TNF-α maintained a stable frequency and amplitude throughout the experiment. There were no changes in frequency or amplitude when vessels were treated with Ang-1 alone. These data suggest that pre-treatment with Ang-1 abrogated the deleterious effects of TNF-α on lymphatic vessel function (Figures 4.23, 4.24). There was minimal change in frequency of contractions from baseline at the end of 2.5 h with Ang-1 alone (1.33 ± 0.66) and in combination with TNF-α (0.66 ± 1.76) compared to the reduced contractions induced by TNF-α alone (-9 ± 1.87), suggesting a protective effect of Ang-1. Ang-1 alone slightly decreased amplitude (-10 ± 16%) with minimal change in combination with TNF-α (2 ± 5%) compared to increased amplitude induced by TNF-α alone (15 ± 23%).

Response of vessels to 250 ng/ml MAT.Ang-1 alone was also investigated during studies performed at Texas A&M University (Figures 6.7, 6.8, Appendix IV). Additionally, one experiment using MAT.Ang-1 was performed in our lab but experiments could not be continued due to unavailability of MAT.Ang-1. Hence HR.Ang-1 was used for further experiments. Frequency remained unaltered in presence of MAT.Ang-1 over 3 h in experiments performed using set-ups in Texas and Sheffield (Figure 6.7, Appendix IV).
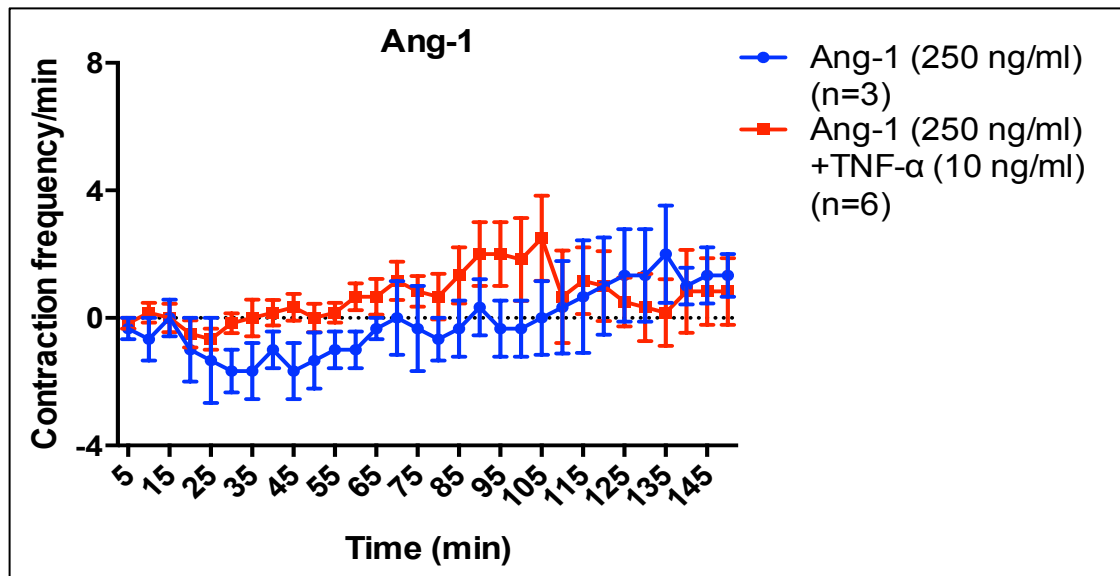
Figure 4.23 Change in frequency of contractions after treatment of vessels with Ang-1 alone (250 ng/ml) or Ang-1 followed by TNF-α (10 ng/ml). Contraction frequency changed minimally at the end of 2.5 h in vessels treated with Ang-1 alone (1.33 ± 0.66) or with TNF-α in presence of Ang-1 (0.66 ± 1.76). Baseline frequency for Ang-1= 6 ± 2, Ang-1 + TNF-α= 4 ±1.
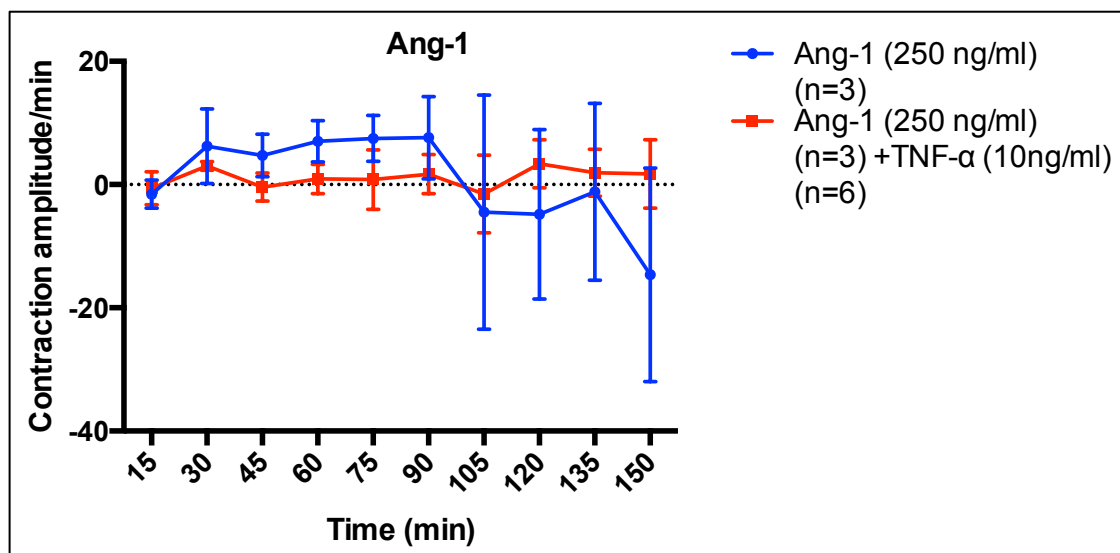
Figure 4.24 Change in amplitude of contractions after treatment of vessels with Ang-1 alone (250 ng/ml) or Ang-1 followed by TNF-α (10 ng/ml). Amplitude did not change significantly in vessels treated with Ang-1 alone (10 ± 16%) or with TNF-α in presence of Ang-1 (2 ± 5%) at the end of 2.5 h. Baseline amplitude for Ang-1= 110.2 ± 12 μ, Ang-1 + TNF-α= 115.2 ± 7.5 μ.

4.8 Molecular analysis of NOS levels

Our next objective was to investigate the levels of eNOS and iNOS expressed in unstimulated vessels and vessels treated with inflammatory mediators. Attempts to achieve this objective were made using routine RNA isolation methods and RT-PCR. Quantification of eNOS and iNOS levels in inflamed vessels would allow further evaluation of the effects of Ang-1 on eNOS/iNOS levels in inflamed RMLV.

4.8.1 RNA isolation

RNA isolation was attempted using different protocols described in chapter 2. The first kit used for isolation was Sigma's GenElute Mammalian Total RNA Miniprep Kit. Low yields of RNA were obtained from both the control and RMLV tissue. The protocol was repeated twice resulting in similar yield of RNA. The mirVana Paris RNA Isolation Kit was used for the next series of isolations (repeated four times). A standard amount of RNA was obtained from the lung tissue, however the amount of RNA extracted from RMLV was still low and insufficient for amplification. An organic extraction method (three repeats) was also used to compare yields with the previous methods. The last attempt was made using RNeasy Kit (three repeats) but there was no difference in the yield obtained from RMLV. The methods and the results obtained over a period of ~3 months are tabulated below:

Kit/Procedure	RNA yields		
	Lung (control) (ng/ul)	RMLV (ng/ul)	Blank (ng/ul)
RNeasy	232.53	20.17	0.01
Sigma GenElute Mammalian Total RNA Miniprep Kit	20.48	11.71	0.01
mirVana Paris RNA Isolation Kit	577.69	6.28	0.06
Organic extraction method	-	10.71	0.02

Table 4.2 RNA yields obtained from different kits used.

4.8.2 PCR

Semi-quantitative RT-PCR was carried out to detect mRNA expression of eNOS and iNOS genes in the lung sample. Oligonucleotide primer sequences used are as follows: rat eNOS sense: 5′-AAGACAAGGCAGCGGTGGAA-3′, antisense: 5′-GCAGGGGA CAGGAAATAGTT-3′, 292 bp; iNOS sense 5′-CCGGGCAGCCTGTGAGACG-3′, antisense: 5′-AGCTGGGTGGGAGGGGTAGTGATG-3′, 482 bp. Total RNA was extracted from isolated rat lung tissue. cDNA was synthesized from the total RNA. 1 μg of total RNA was used for the synthesis of 20 μl first strand cDNA. cDNA was detected in the lung sample but not in the RMLV sample. The resulting cDNA from lung sample was used as template for subsequent PCR. Following RT-PCR, 10 μl samples of amplified products were resolved by electrophoresis on agarose gel and stained with ethidium bromide. The level of each PCR product was semi-quantitatively evaluated using a gel image analysis system. Expected product size for eNOS was 292 bp and 482 bp for iNOS. Bands were observed in the sample indicating presence of eNOS (~200 bp) and iNOS (~400 bp) in the isolated lung RNA. The band intensities indicate a higher level of eNOS expression compared to iNOS (Figure 4.25).
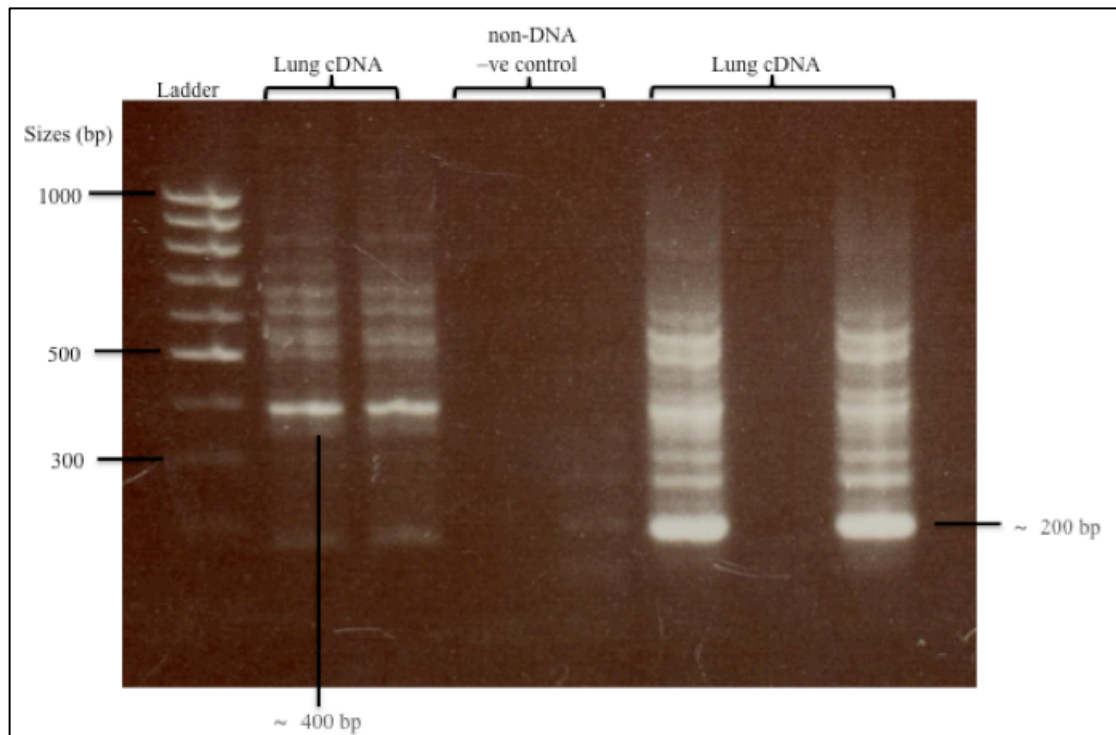
Figure 4.25 Evidence for iNOS and eNOS gene expression in lung tissue of male Sprague Dawley rats. Base-pair markers denoting DNA size are shown on the extreme left. From left to right, columns depict results for iNOS expression, non-DNA negative (−ve) control followed by eNOS expression. The band corresponding to iNOS is a ~400 bp product and a ~200 bp product for eNOS.

4.9 Confocal immunofluorescent microscopy

Lymphatic endothelium

RMLV was stained with anti-mouse LYVE-1 Alexa fluor 488 to confirm that an intact endothelium is maintained by lymphatic myography. Strong LYVE-1 staining was detectable in the lymphatic vessel indicating the presence of an intact endothelial layer (Figure 4.26).
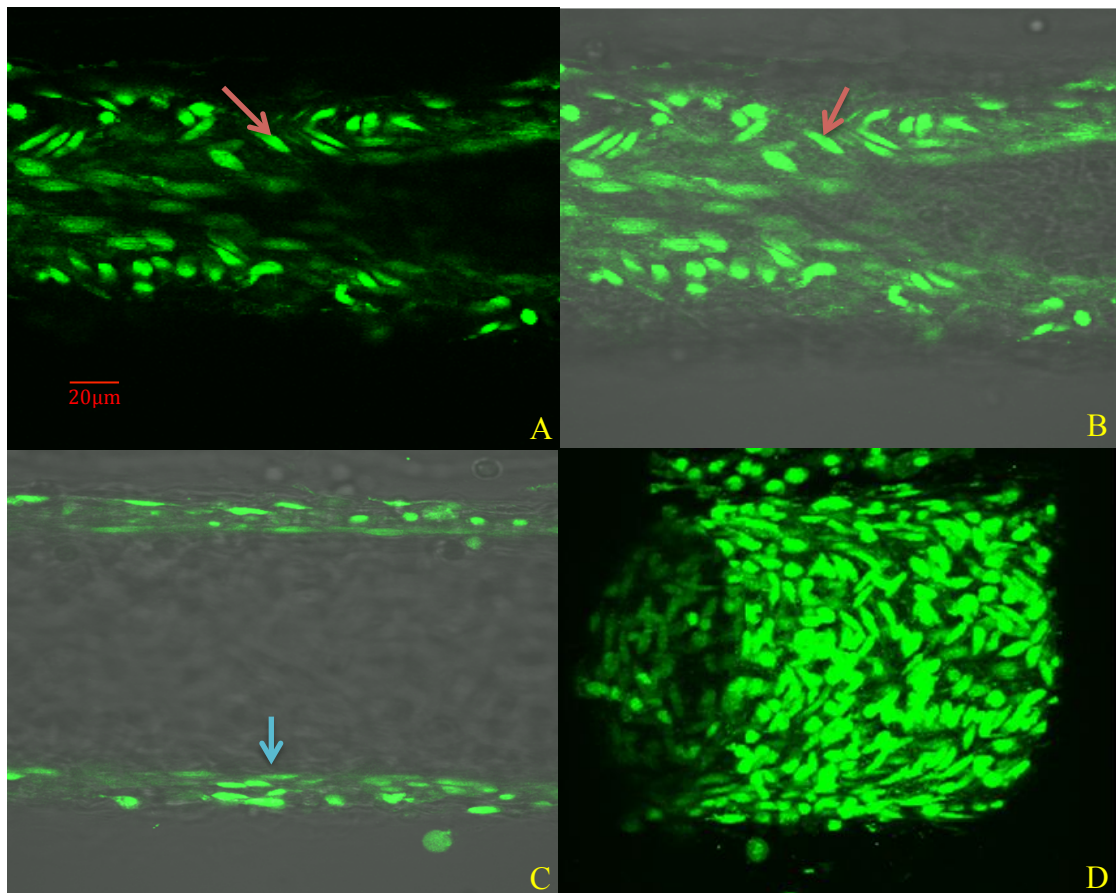
Figure 4.26 LYVE-1 staining in RMLV. Confocal immunofluorescent micrographs (x10) of isolated rat mesenteric lymphatic stained with anti-mouse LYVE-1 Alexa fluor 488. Strong LYVE-1 staining is detectable in LECs (indicated by red arrows in fig A and B). An intact endothelial layer is detectable in the wall of the vessel (indicated by blue arrow in fig C). Fig D shows a 3-D reconstruction of the vessel. Scale bar- 20 μm.

Tie-2

To our knowledge, expression of Tie-2 has not been shown in RMLV previously. RMLV were stained with a primary goat anti-mouse Tie-2 polyclonal antibody to detect the expression of Tie-2. A secondary anti-goat IgG antibody conjugated with Alexa-fluor 647 was used to observe immunofluorescence under a confocal microscope (Figure 4.27).
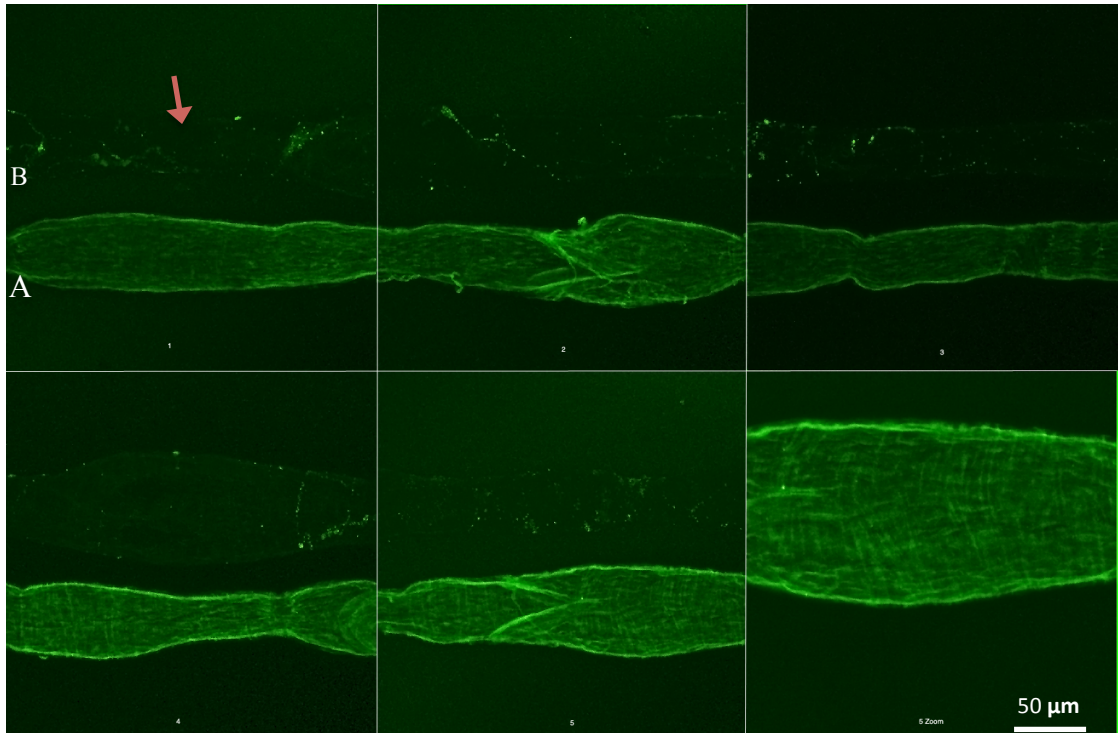
Figure 4.27 Tie-2 expression in rat mesenteric lymphatics. Multiple confocal immunofluorescent micrographs (x10) (pseudocoloured) of isolated mesenteric lymphatics stained with goat anti-mouse Tie-2 polyclonal antibody (A) or goat IgG (B) and Alexa-fluor 647 conjugated anti-goat IgG. Strong Tie-2 expression is detectable in SMCs in a circumferential pattern and ECs of the lymphatic vessel. Red arrow indicates unstained vessel.

4.10 Summary of results

Minimal decrease (6 ± 13%) in frequency of contractions with no change in amplitude was observed in presence of L-NAME (NOS inhibitor) over 30 min.

SNP (NO donor) reduced frequency of contractions by 44 ± 17 % over 15 min and decreased amplitude by 13 ± 4% within 5 min.

LPS (batch 1) abolished frequency and amplitude of contractions at 60 min whereas no changes in contractility were observed with LPS (batch 2).

TNF-α (10 ng/ml) decreased frequency of contractions (-9 ± 1.87) and increased amplitude (15 ± 23%) from baseline at the end of 2.5 h.

IL-1β (10 ng/ml) did not alter frequency alone but reduced frequency in combination with TNF-α (-6.3 ± 2.7) at the end of 2.5 h. Significant change in amplitude compared to control was observed between 75-90 min with IL-1β alone.

No considerable change was observed in frequency or amplitude with TNF-α (10 ng/ml) in presence of L-NAME or indomethacin (COX inhibitor).

There was minimal change in frequency of contractions from baseline at the end of 2.5 h with Ang-1 alone (1.33 ± 0.66) and in combination with TNF-α (0.66 ± 1.76).

Ang-1 alone slightly decreased amplitude (10 ± 16%) with minimal change in combination with TNF-α (2 ± 5%) from baseline at the end of 2.5 h.

LYVE-1 staining was detectable in the lymphatic vessel indicating the presence of an intact endothelial layer. Tie-2 expression on RMLV was confirmed using confocal microscopy.

4.11 Discussion

The aim of these experiments was to assess the effects of pro-inflammatory mediators on the functional parameters of collecting lymphatics, determine whether effects were mediated via NO and evaluate the anti-inflammatory potential of Ang-1 in protecting lymphatic vessel function during inflammation. The *ex vivo* model used for this series of investigations successfully allowed evaluation of vessel responses which are discussed in detail below. Our results provide preliminary evidence to support the hypothesis that lymphatic contractility is impaired during sepsis via regulation of NO and Ang-1 protects pump function in vessels exposed to inflammatory mediators.

4.11.1 Control optimisation

A number of problems were encountered whilst achieving a stable frequency of contraction for 3 h in untreated lymphatic vessels. With DMEM-F12, there were frequent changes in pH of the media, which were measured by submerging a pH probe in the organ bath. The media was changed to APSS in an attempt to achieve stable frequency throughout the protocol. The vessel required the media to be replenished at least every 45 min due to variable frequency of contractions and amplitude. Media was changed every 45 min in the same step-pressure protocol at each time point. Only 1 ml of the media (3 ml total in the bath) was changed to minimise changes in pH. Further, to reduce agitation to the vessel, the changes in pressure were eliminated. Indeed, the variability was observed to be reduced. However, in an experiment where LPS was added to the media and replaced every 45 min, unstable frequency was observed. There was an abnormal increase in frequency of contractions as soon as the media was replaced. Therefore, addition of 1mM Ca^{2+} dissolved in ultrapure water was added instead of media. The rationale behind this change was that Ca^{2+} is the single most important ion required to maintain the frequency of contractions and removal of extracellular Ca^{2+} from the media abolishes spontaneous contractions (Mizuno *et al* 1997). As evident from the results, the variation is frequency was reduced. Hence, further experiments were carried out with this adapted protocol.

4.11.2 Investigation into the role of NO

Negative chronotropic and inotropic effects of endothelium-derived NO were shown in bovine and rat collecting lymph vessels treated with Ach (Yokoyama and Ohhashi 1993; Mizuno *et al* 1998) and by continuous unidirectional flow (Gashev *et al* 2002).

Hence, stimulation of NO production by the lymphatic endothelium was originally shown to inhibit lymphatic contractile function. However, the role of lower levels of NO, due to the basal NO production in lymphatic function has been continuously questioned due to contrasting outcomes in a number of studies. Three studies performed prior to the current study, investigating of the role of basal NO in regulation of phasic contractions, demonstrated that basal NO either increased or induced no effect on the amplitude of contractions but reduced contraction frequency (Hagendoorn *et al* 2004; Gasheva *et al* 2006; Bohlen *et al* 2009). However, the study by Gasheva *et al* was performed in isolated rat thoracic duct, which possesses different contractile characteristics to that of the mesenteric lymphatic vessels we used in this study. The other two studies were performed under conditions where the intraluminal pressure and flow were not controlled. It is known that pressure and flow exert profound and opposite effects on lymphatic contractile function that may complicate the interpretation of *in vivo* observations (Scallan *et al* 2012). Hence, it was important to establish the function of basal NO in our experimental setting under constant transmural pressure and normal pulsatile flow. We investigated whether global inhibition of NO by L-NAME affected the frequency and amplitude of mesenteric lymphatic vessels in conditions where there was no continuous flow in the vessel. Though L-NAME is not a specific eNOS inhibitor, we assumed that it mainly inhibited NO production via eNOS since under physiological conditions, basal NO is mainly produced by eNOS (Yamashita *et al* 2000). The integrity of the endothelium was confirmed by LYVE-1 staining. As indicated by the results, L-NAME had no effect on either of these parameters. Though a slightly elevated amplitude in L-NAME treated vessels compared to D-NAME treated vessels was observed, the difference was not significant. Our results agree in part with a study performed by Scallan and Davis where popliteal collecting lymphatic vessels from WT and eNOS$^{-/-}$ mice were treated with L-NAME. Contractile parameters remained the same in vessels from mice of both genotypes after treatment with L-NAME; however, an increased contraction amplitude was observed in the eNOS$^{-/-}$ vessels when compared to WT (Scallan and Davis 2013). The authors concluded that basal NO production depresses contraction amplitude without increasing frequency. However, we cannot definitively make this conclusion from our results as the change in amplitude was not significant.

A number of studies performed more recently, support the initial hypothesis that basal NO increases lymphatic contraction amplitude by reducing the contraction frequency, thereby allowing more time for lymphangion filling to occur so that the next contraction becomes stronger (Bohlen *et al* 2011; Liao *et al* 2011; Kesler *et al* 2013). To address this discrepancy, Scallan and Davis proposed that in a complex *in vivo* setting, the elevated frequency and decreased contraction amplitude in response to eNOS ablation are best explained by an increase in intraluminal hydrostatic pressure, in agreement with their previous reports that increased lymphatic preload leads to an increase in EDD and frequency while reducing contraction amplitude in proportion to the pressure change (Davis *et al* 2012; Scallan and Davis 2013). They further proposed that a possible role for basal NO in collecting lymphatics might be to set contraction amplitude at a level that can be increased or decreased to modulate lymph flow. This current hypothesis may be further investigated in lymphatic vessels from different regions to determine whether basal NO indeed modulates lymph flow as proposed by authors. Differences in contractility of lymphatics such as the rat thoracic duct, mesenteric, cervical, and femoral lymphatics from different regions, in response to pressure and imposed flow have been shown previously. Imposed flow inhibited pumping activity by different degrees in different types of lymphatics and vessels exhibited optimal pumping activity at low levels of transmural pressure (Gashev *et al* 2004). Hence, an investigation into the effects of eNOS ablation on lymphatic vessels from different regions will corroborate the role of NO in modulating lymph flow under different hydrodynamic conditions.

We then investigated the role of exogenous NO on RMLV. Exogenous NO released by SNP has previously been shown to have inhibitory effects on lymphatic contractile function in guinea-pig mesenteric lymphatics (von der Weid *et al* 2001). It was proposed that NO inhibits contractile activity by production of cyclic GMP and cyclic-AMP-dependent protein kinase which affect the pacemaker activity by decreasing the synchronized release of underlying Ca^{2+} from intracellular stores. Though our results did not significantly alter the lymphatic contractile activity, considerable negative chronotropic and inotropic effects on the vessel were observed. These results combined with other studies mentioned previously clearly identify the role of exogenous NO (von der Weid *et al* 1996) or increased NO production stimulated by Ach (Mizuno *et al* 1998; Scallan and Davis 2013), as a regulator of spontaneous

contractions in pathophysiological conditions. The effect of endogenous NO stimulation was additionally assessed by treatment of vessels with Ach and AMch. Both substances appeared to increase frequency of contraction and caused a decrease in amplitude. Though effects on amplitude were in agreement with previous studies, the effects on frequency were contradictory (Yokoyama and Ohhashi 1993). This discordant data may be due to the intraluminal application of Ach and AMch after equilibration. This method was chosen instead of extraluminal application in order to achieve a dilatory response in the vessel. However, no changes were observed in vessel diameter, possibly due to loss of vessel tone (discussed in Appendix IV). Vessel agitation due to intraluminal application may have caused an increase in frequency thus disrupting the normal response of the vessel.

4.11.3 Effects of LPS

Next, we directed our attention to exploring the effects of LPS, TNF-α and IL-1β on lymphatic function. Previously, *in vivo* studies using intravenous administration of endotoxin in sheep, reduced lymph flow and suppressed contractile activity in the intestinal lymphatic vessels (Elias *et al* 1987). An *in vitro* study investigating lymphatic function in bovine mesenteric lymphatics (BML) treated with *E.Coli* endotoxin showed reduction in contractility and tone of the vessels. The latter was shown to be mediated by NO and prostacyclin released from ECs; however reduction in contractility was endothelium-dependent at higher concentrations of LPS (1 mg/l) (Lobov and Kubyshkina 2004). Indeed, in vessels isolated from live animals we observed an increase in diameter after treatment with LPS. The study by Elias *et al* also demonstrated that endotoxin exerts its effect on the lymph pump via interaction with cellular and/or humoral components *in vivo*. This could explain the lack of response in vessels in experiments where FCS was not added to the media. However, in groups where FCS was added, two different responses were observed with different batches of LPS. Whereas potent effects of LPS were observed on frequency and amplitude of contraction in one group, the second group did not demonstrate any changes in these parameters. These differences could be attributed to the variation in potency of LPS batches. A similar problem with LPS was encountered in *in vivo* experiments where we employed the low-dose infusion model of endotoxemia (discussed in section 3.3.1). Further experiments with LPS were not performed due to the inconsistency of effects observed between different groups. Future experiments

could be performed with LPS from the same lot to overcome any potential batch variation.

4.11.4 Effects of TNF-α

The production of pro-inflammatory cytokines is a prime marker of the inflammatory process. LECs, macrophages and other cells are a source of cytokine production in response to LPS (Sawa and Tsuruga 2008). We wanted to investigate if cytokines could affect lymphatic function directly. On treatment of vessels with TNF-α, we found a reduction in frequency of contractions consistently at lower concentrations and increased contraction amplitude. Effects at higher concentrations of TNF-α were inconsistent. 10 ng/ml concentration of TNF-α was chosen for our study as cultured human neonatal dermal LECs stimulated with 10 ng/ml TNF-α showed increased VCAM-1 and ICAM-1 expression suggesting inflammatory effects on the lymphatic endothelium (Sawa *et al* 2007). Responses at higher concentrations (100 – 500 ng/ml) were also investigated, as any effects at these concentrations have not been reported so far. This is the first study to demonstrate the chronotropic and inotropic effects of TNF-α on internal vessels such as mesenteric lymphatic vessels *ex vivo*. Increased amplitude of contractions suggests a compensatory response by the vessel to maintain pumping during acute inflammation as frequency of contraction decreases. The results we obtained with TNF-α are consistent with a recently published study, which demonstrated that TNF-α, IL-1β and IL-6 acutely and systemically decrease lymphatic frequency and lymph velocity in inguinal-to-axillary vessels after intradermal administration in mice (Aldrich and Sevick-Muraca 2013).

We further showed that effects induced by TNF-α were inhibited by L-NAME and indomethacin. Thus, our results implicate NO and a COX product as one of the main mediators of the effects of TNF-α. iNOS-driven NO production in LEC cultures stimulated with TNF-α alone has indeed been shown previously (Leak *et al* 1995). The study showed that TNF-α induced an increase in levels of NO, maximum at 4 h reverting to below normal levels by 24 h.

Arachidonic acid and its metabolites are also known to be important mediators of inflammatory reactions. These substances are important modulators of lymphatic function and have been shown to directly act on lymphatic vessels (Johnston, 1987). The response of lymphatics to arachidonic acid can be inhibitory or excitatory

response depending on the predominant metabolite to which it is converted (Johnston *et al* 1983). This was further substantiated by experiments in which the COX inhibitor indomethacin inhibited increases in the contraction frequency in microlymphatics of rat iliac lymphatics (Mizuno *et al* 1998). Further evidence of the critical role in pathophysiological events was reported from an animal model of intestinal inflammation in which impaired contractility in mesenteric lymphatics was attributed to PGE_2 and prostacyclin (Wu *et al* 2005). Indeed, *in vivo* studies demonstrated that the inhibition of lymphatic contraction frequency was reverted upon application of indomethacin or a combination of COX-1 and COX-2 selective inhibitors to inflamed mesenteric vessels in TNBS-induced ileitis in guinea pigs (Wu *et al* 2006). Increased expression of PGE_2 and prostacyclin in lymphatic tissues of TNBS-treated animals has recently been reported (Rehal and von der Weid 2015). An important role for prostanoids in inflammation-induced lymphatic contractile dysfunction surfaced with these findings.

In the experiments we performed, the TNF-α effects were inhibited by indomethacin suggesting that metabolites produced through COX, had an inhibitory effect on the frequency. These observations are supported by studies which showed that PGE_2 and prostacyclin decreased frequency of contraction without affecting the amplitude (Rehal *et al* 2009). Our results indicate that independent inhibition of NO and prostanoids prevents the decline in the frequency of contraction. This suggests a mechanism linking NO and prostanoids that modulates lymphatic frequency in a manner where the effects of one mediator are abrogated when the other is inhibited. These studies confirm the complicated mechanism through by which the lymphatic system, may respond to its modulators.

4.11.5 Effects of IL-1β

A study as early as 1989 showed that intraluminal application of IL-1α and IL-1β inhibits pressure-dependent increase in lymphatic pumping in BML (Hanley *et al* 1989). The effects in this study were observed at 10^{-8} M, however this concentration was chosen due to limited supplies. 10 ng/ml was chosen in our study as IL-1β at this concentration was shown to induce EC adhesion molecule expression and disrupt LEC barrier in mouse and human LEC cell lines (Chaitanya *et al* 2010). Our results showed that IL-1β did not have any effect on the frequency; however significant reduction in

amplitude of contractions was observed between 75-90 min after stimulation. Again, this is the first study to demonstrate inotropic effects of IL-1β on lymphatic vessels. Interestingly, observations of one group studying effects of IL-1β in isolated guinea pig mesenteric vessels were similar to our observations relating to frequency but authors did not report effects on amplitude (Liao and von der Weid 2014). However, two recent studies provide evidence in favour of our hypothesis that IL-1β directly impairs lymphatic pump function. The more recently published *in vitro* study demonstrated an IL-1β-induced decrease in tonic contractility of rat mesenteric lymphatic muscles cells at doses of 5, 10 and 20 ng/ml via upregulation of COX-2 levels leading to PGE_2 production (Al-Kofahi *et al* 2015). The other study investigating the effects of cytokines on lymphatic vessels *in vivo*, showed decreased pumping and reduced flow following intradermal administration of IL-1β in mice, which were abated by pre-treatment with an iNOS inhibitor. However, NO production by LECs in direct response to IL-1β, was not detected (Aldrich and Sevick-Muraca 2013). The former study directly demonstrates that the effects of IL-1β on tonic contraction are mediated by PGE_2, whereas the latter study shows that effects on phasic contractility are NO mediated. However, the absence of NO production in LECs in the latter study indicates that inhibitory effects on phasic contractions *in vivo* may be mediated via NO induced in other inflammatory cells such as macrophages. Further, drawing upon the results of Hanley *et al*, we postulated that IL-1β may also exert its actions on phasic contractility by interacting with other mediators such as PGE_2 in the inflammatory milieu. Authors showed that IL-1 requires PGE_2 for some of its actions, so we thought it is possible that production of various prostaglandins such as PGE_2 and prostacyclin via TNF-α application may stimulate IL-1β activity (Hanley *et al* 1989). Hence, we investigated if a combination of IL-1β and TNF-α would evoke a stronger vessel response. Our results indicated that the level of inhibition of frequency in response to a combination of both agents was not different from that stimulated by TNF-α administered alone. Future experiments using PGE_2 directly in combination with IL-1β could be performed to assess whether IL-1β requires a synergism with COX-2 products such as PGE_2, to mediate its effects on phasic contractility.

4.11.6 Effects of Ang-1

We then investigated the effects of Ang-1 on the lymphatic vessel function. No changes were observed in frequency and amplitude of contractions in vessel explants suggesting that Ang-1 does not have any effect on the contractile function of the lymphatic vessel. However, treatment of vessels with Ang-1 prior to application of TNF-α maintained stable contractility for the whole duration of the experiment indicating a protective effect of Ang-1. This effect of Ang-1 on inflamed lymphatic vessels is in agreement with previous studies (Alfieri *et al* 2012), establishing an anti-inflammatory effect of Ang-1 on blood endothelium (section 1.3.5). Furthermore, Ang-1-modified endothelial progenitor cells attenuated inflammatory responses induced by TNF-α *in vitro*, strengthening its potential to counteract cytokine-induced inflammation (Wang *et al* 2014).

As discussed in section 1.3.7, effects of Ang-1 are mediated via the downstream signaling cascade triggered by its binding to the Tie-2 receptor (Saharinen *et al* 2008). We confirmed the expression of Tie-2 in RMLV by confocal immunofluorescent microscopy (Figure 4.27). We speculate that the protective effect observed is mediated via the ability of Ang-1 to inhibit NF-κB activation triggered by TNF-α, which in turn prevents iNOS upregulation that promotes excessive NO production in the endothelium. The inflammatory response at the molecular level is mainly mediated by the transcription factors of the NF-κB family. NF-κB is constitutively active in the lymphatic vasculature (Saban *et al* 2004; Wang and Oliver 2010). Through association with the inhibitor proteins of the IκB family, it remains in an inactive state in the cytoplasm of quiescent cells. Activation of cells by pro-inflammatory factors leads to the phosphorylation and degradation of the IκBs, subsequently releasing NF-κB and its nuclear translocation. Studies demonstrated that phosphorylation of Tie-2 suppresses the activation of NF-κB via recruitment and activation of ABIN-2, which binds to and inhibits IKK, the upstream regulator of IκB (Simoes *et al* 2008; Gu *et al* 2010).

Moreover, Ang-1 may be a source of NOS beneficial to the vessel by upregulating eNOS expression via the PI3K/Akt pathway (Augustin *et al* 2009). While the total concentration of NO that the lymphatic is exposed to is critical, locally generated temporal and spatial gradients of NO due to its short half-life *in vivo* are integral to its action on vessels. As described earlier (section 1.2.2.1), elevated shear force resulting

from a contraction in the valvular region during the systolic phase triggers release of NO. The NO released causes vessel relaxation necessary for diastolic filling and starting the next cycle of contraction. eNOS activation by Ang-1 could maintain these temporal and spatial NO gradients, thus preventing the decrease in frequency due to TNF-α. This dual action of Ang-1 could prove beneficial in improving lymph flow during septic insult.

4.11.7 RNA isolation

RNA extraction from RMLV was attempted using different protocols, as the amplified cDNA was undetectable with low yields (≈20 ng/ml) of RNA. However, a PCR product was obtained after isolation of RNA from the lung sample using mirVana Paris RNA Isolation Kit. Though, the size of the amplified cDNA was smaller than expected, it may be due to the binding of primers to an internal hybridisation site in the template and could be resolved by using a different annealing temperature to enable specific primer binding. Nevertheless, obtaining a successful PCR product indicated that a different strategy was needed for isolating RNA from lymphatic vessels. Bridenbaugh described an organic extraction method to isolate RNA from lymphatic vessels due to the difficulties in obtaining a high RNA yield by standard procedures. The RNA isolation strategy in this study was particularly developed and optimized to isolate high-quality RNA from very small quantities of dissected rat vessel tissue (Bridenbaugh 2012). Due to time constraints, further experiments using this method could not be performed. However, this study reveals the reasons for our lack of success during several attempts to isolate RNA and clearly outlines a strategy for confidently approaching RNA isolation from lymphatic vessels in the future. An optimum RNA yield would allow detection and quantification of eNOS and iNOS levels in non-inflamed and inflamed vessels. Once successful isolation of RNA is achieved, inflamed vessels could be treated with Ang-1 to identify changes in levels of eNOS and iNOS. These experiments would be critical in establishing the role of Ang-1 in lymphatic vessel modulation during inflammation.

4.11.8 Summary and future directions

These series of studies have begun to characterise the effects of inflammatory mediators such as TNF-α and IL-1β on lymphatic function and demonstrated that effects of TNF-α may be mediated via NO and prostanoids during early sepsis. An

anti-inflammatory role of Ang-1 in ameliorating the effects of TNF-α on lymphatic contractile function has also been demonstrated. Since a fundamental role of basal and agonist-evoked NO in modulating lymphatic pump function has been identified by several studies (Bohlen *et al* 2011; Kesler *et al* 2013; Scallan and Davis 2013), further experiments were warranted to investigate the expression of NOS isoforms in inflamed vessels in order to delineate whether TNF-α mediates alterations via NOS modulation. Therefore, studies were performed to assess eNOS and iNOS expression in RMLV tissue. It was not possible to offer mechanistic insights into the modulation of lymphatic function in this study. Nevertheless, it offers useful insights into the challenges of RNA isolation from lymphatic vessels. Whether modulation of lymphatic contractility by cytokines occurs due to eNOS-iNOS imbalance and Ang-1 mediates a protective effect on contractile function via NOS regulation, needs further investigation. In our knowledge, there have been no reports on the mechanism of cytokine action on lymphatic contractility. Successful quantification of NOS transcripts in lymphatic tissue is needed to substantiate our hypothesis.

Chapter Five

General discussion

5.1 The lymphatic system in sepsis

The inflammatory response is a central component of sepsis driving the multiple physiological impairments that lead to its progression. A tight regulation of this response is crucial to maintain a balance between protective and host-damaging responses. However, a loss of this balance is a key feature that identifies the destructive nature of sepsis. Thus far, a large number of immunomodulatory agents have been investigated in pre-clinical models and clinical settings to find an effective therapeutic agent that reduces mortality in patients affected with severe sepsis. Particularly, increased attention has been directed towards strategies targeting the exaggerated pro-inflammatory response after the onset of sepsis (Marshall 2008; Rittirsch *et al* 2008). However, despite some success in experimental models, most of the clinical trials have shown little success in reducing mortality rates (Ulloa *et al* 2009; Angus and van der Poll 2013; Fink and Warren 2014). These poor clinical outcomes warrant further research into under-investigated inflammatory aspects of the pathophysiology and anti-inflammatory strategies to resolve particular pathological processes that contribute to disease progression.

Over the last decade, the importance of microcirculatory dysfunction resulting due to the ensuing inflammation has been increasingly recognised. As discussed in section 1.3.7, multiple derangements at the microcirculatory level drive the pathophysiology of sepsis (Vincent and De Backer 2005; De Backer *et al* 2014). While investigative research has mostly been focused on these derangements in the blood vasculature, there is an equally important involvement by its counterpart, the lymphatic vasculature. In this study, we have discussed the changes that occur in the lymphatic vasculature during an inflammatory state, focusing on that which follows a septic insult. A greater knowledge of changes in the lymphatic vasculature would inform the potential for future therapies that can be designed to ameliorate dysfunction at the microcirculatory level in sepsis.

The principal function of lymphatics in maintaining tissue fluid balance by adapting its pumping activity to changes in fluid load has been recognised historically (Gashev and Zawieja 2001). The role of the lymphatic circulatory system is sepsis was identified nearly three decades ago when authors suggested that impaired lymph propulsion may contribute to oedema by reducing the ability of the lymphatic vessel to remove

interstitial fluid from the extravascular tissue spaces (Elias *et al* 1987; Johnston *et al* 1987). Oedema, defined as the accumulation of excess interstitial fluid volume can be a cause and an effect of inflammation-induced organ failure. Endotoxin-induced oedema worsens with increased microvascular pressure due to increased microvascular filtration and reduced lymphatic function (Dongaonkar *et al* 2008). The biological role of lymphatic vessels in the pathogenesis of inflammation is not clearly established to date. Lymphatic vessels clear inflammation-associated oedema by active pumping activity removing immune cells and inflammatory cytokines from the site of infection in the process but in contrast they partake in mounting an immune response by transporting activated APCs from the site of infection to regional lymph nodes. Growing evidence (reviewed in section 1.2.5) suggests that lymphatic vessels play an active role in the inflammatory process (Cueni and Detmar 2008; Shields 2011). However, dysregulated inflammation, such as occurs in sepsis, causes lymphatic impairment and dysfunctional lymphatics may be a key contributing factor to its pathogenesis. Moreover, a recent study unravelled a protective role for lymphatics in maintaining intestinal tissue integrity, thus protecting us from sepsis. It showed that ablation of intestinal lymphatics leads to gut-derived sepsis (Jang *et al* 2013).

The lymphatic endothelial and smooth muscle cell layer, as active players in inflammatory conditions where oedema is a hallmark have only been the focus of research over the last decade (von der Weid and Muthuchamy 2010). The classical view of the function of LECs of the initial lymphatic vessels has been that of a passive barrier equipped with primary valves facilitating the convective diffusion of interstitial fluid into the lymphatic vessel. Over the years, a number of labs unravelled an active role of the lymphatic endothelium in regulating translymphatic flux of fluids and solutes (Ono *et al* 2005; Scallan and Huxley 2010). However, hyper-permeability of the lymphatic system in an inflammatory condition is a very recent area of investigation. It has been suggested that mesenteric lymphatics may be especially compromised, as they are rich in lipids and gut-derived antigens. Moreover, inflammation in the region may be aggravated by loss of compartmentalization of these factors (Deitch 2012; Cromer *et al* 2014).

5.2 Modulation of lymphatic endothelial barrier function by LPS

One of the objectives of our first study was to investigate whether mesenteric collecting lymphatic vessels become 'leaky' during an LPS-induced endotoxemic state. The *in vivo* model we chose complicated the interpretation of altered vessel leakage. However, recent *in vitro* studies have provided evidence of altered LEC permeability to LPS and cytokines thus warranting further investigation into vessel leakiness during inflammation (Cromer *et al* 2014; Kawai *et al* 2014). The model used by Ono *et al* would be useful to accurately measure the permeability of hydrophilic substance through the walls of collecting lymphatics in inflammatory conditions (Ono *et al* 2005). Further, we were also interested in examining the mechanisms of endothelial permeability, which is modulated by inter-endothelial junctional disruption and intracellular contraction of the cytoskeletal components (Bazzoni and Dejana 2004; Dejana *et al* 2008). We used confocal immunofluorescent microscopy to detect VE-cadherin expression as it plays a major role in regulating BEC permeability. We could not further this objective due to time constraints but determining whether sepsis-related factors such as TNF-α and LPS influence VE-cadherin expression or induce dissociation of the junctional complex via phosphorylation of VE-cadherin, is key to understanding if lymphatic permeability is regulated through mechanisms similar to those in blood vessels. The challenge, however, will be to visualize VE-cadherin clustering with other adhesion molecules and quantify expression in response to stimulation of receptors such as Tie-2 that control permeability. Molecular techniques combined with high-resolution confocal microscopy would be the next step to take the investigation forward. Identifying these mechanisms should reveal novel therapeutic targets that may be applicable in the treatment of many pathological situations where vascular permeability is adversely affected (Aghajanian *et al* 2008).

5.3 Modulation of lymphatic contractile function by inflammatory mediators

Striking alterations in lymphatic vessel pumping are linked to acute inflammation, such as that in sepsis (Alitalo 2011). The rapid release of mediators in tissue injury and inflammation during sepsis that increases vascular permeability, results in elevated interstitial fluid pressure and increased lymph flow. As lymphatic drainage changes rapidly and dramatically, augmented fluid flow serves as an early signal for inflammation (Miteva *et al* 2010). Moreover, lymph flow declines after a certain duration due to alterations in lymphatic contractility. Thus, we were interested in

assessing changes in flow during early sepsis and any correlation to changes in contractility (0-4 h). However, our observations were limited by the camera used for imaging lymph flow; moreover, *in vivo* measurement of contractility was difficult. With the advent of new agents such as NIR organic fluorophores or fluorescent nanoparticles such as upconverting nanocrystals conjugated with macromolecules these have been used to image lymphatic flow using advanced optical techniques; pathophysiological changes in flow can now be readily measured (Lucarelli *et al* 2009). Studies using *in vivo* photo thermal flow cytometry (PTFC) integrated with transmission digital microscopy (TDM) have demonstrated the potential of these techniques for real-time high-resolution monitoring of functional parameters such as diameter, phasic contraction frequency, lymph flow velocity, valve function, and cell behaviour in physiological and pathological states and under the influence of different therapeutic interventions (Galanzha *et al* 2007).

Due to the limitations posed by *in vivo* measurement of contractile characteristics, lymphatic myography was used to determine changes in lymphatic contractility, upon inflammatory stimulus *ex vivo*. The response to the effects of inflammatory mediators released in the vicinity of lymphatic vessels was investigated. LPS and the classical cytokines TNF-α and IL-1β were chosen to stimulate vessels, as reports on the direct effects of these mediators on lymphatic pumping are sparse. LPS and TNF-α decreased frequency of lymphatic contractions and reduction in amplitude was observed with LPS and IL-1β; however, due to the inconsistent vessel responses to LPS from different batches, mechanisms through which TNF-α mediates its effects were investigated further.

The role of NO in mediating the effects of TNF-α was further investigated. Since TNF-α is known to disrupt the physiological balance between eNOS and iNOS in blood vasculature (Zhang *et al* 2009), we hypothesised that downregulation of lymphatic contractility by TNF-α is mediated via alterations in NO production. Indeed, our results showed no reduction in frequency with TNF-α in the presence of L-NAME.

The role of NO in regulating lymphatic contractile function has been intensively studied over the past decade and a series of elegant studies demonstrate a key role for basal levels of NO in maintaining lymphatic function (Gashev *et al* 2002; Gasheva *et al* 2006; Bohlen *et al* 2011). The most recent hypothesis that has been proposed

regarding the role for endogenous NO in collecting lymphatics is that basal NO regulates the contraction amplitude at a level allowing either increased or decreased levels to modulate lymph flow without altering frequency (Scallan and Davis 2013). Whether the increase in strength of contraction is a consequence of reduced frequency by basal levels of endogenous NO, is a disputed hypothesis. Results from our investigation showed that endogenous may regulate amplitude but not frequency in physiological conditions, which is in support of the recent hypothesis proposed by Scallan and Davis. The effect in response to exogenous NO, is supportive of the current hypothesis that higher agonist-evoked concentrations of NO reduce contractile function (Chakraborty *et al* 2015).

Chronotropic effects of TNF-α were also blocked by indomethacin, which suggested a role for a COX product such as PGE_2 and/or prostacyclin in regulation of frequency (Rehal and von der Weid 2015). Our results demonstrate that multiple bioactive agents may modulate the frequency of lymphatic vessels in an inflammatory environment. The pathways involved in the mechanism of action of these agents, is an area of further research.

5.4 Modulation of lymphatic function by Ang-1

We then evaluated the potential of Ang-1 in restoring lymphatic contractility impaired by TNF-α. We chose Ang-1 because of its ability to provide beneficial eNOS and remove NO produced by iNOS (Augustin *et al* 2009). Recent studies have shown that temporal and spatial gradients of NO, in addition to the total concentration produced, are fundamental to its action on lymphatic pumping. Under physiological conditions, NO is produced in LECs via eNOS at specific sites and times during a contraction cycle, which facilitates lymphangion filling in the diastolic phase (Bohlen *et al* 2011). While suppression of NOS in activated lymph vessels disrupts the contraction/relaxation cycle to increase contraction frequency, NO production via eNOS is essential by an activated lymph vessel to facilitate diastolic filling and hence sustain elevated lymph pump flow (Kesler *et al* 2013). Hence, we speculated Ang-1 to be an ideal candidate to improve lymphatic contractile function. Indeed, Ang-1 prevented the decline in frequency observed with TNF-α.

We next wanted to determine if these effects were mediated via maintaining eNOS and preventing an increase in iNOS levels in the vessels. We observed Tie-2 expression in

RMLV suggesting that Ang-1 might exert direct effects on the lymphatic endothelium. Time constraints did not allow us to fully investigate these mechanisms underlying the action of Ang-1 on lymphatic pumping. Delineation of pathways involved in this phenomenon may facilitate the development of therapeutic strategies that restore the eNOS - iNOS balance.

Ang-1 may serve as a powerful therapeutic target in improving lymphatic function as it has the potential to redress lymphatic barrier dysfunction, another potential mechanism that may be underlying lymphatic vessel dysfunction during sepsis (Kajiya *et al* 2012; Kakei *et al* 2014). Again, we speculate a role for protective eNOS upregulating Ang-1. Our speculation that Ang-1 may improve lymphatic endothelial barrier function via NO regulation is supported by results from a recent *in vivo* study performed in our lab which suggests that both reduced eNOS and increased NO production via iNOS impair blood endothelial barrier function through reduction of VE-cadherin expression at the inter-endothelial junctions. This was restored to control levels by MAT.Ang-1. Furthermore, VE-cadherin phosphorylation, a mechanism that causes disassembly of the protein from the endothelial junction, was increased by L-NAME and restored to normal levels after MAT.Ang-1 administration (Alfieri *et al* 2014). As evident from this study, and shown previously, maintenance of the endothelial barrier requires a basal level of NO produced via eNOS (Predescu *et al* 2005). Both reduced NO levels and increased NO production, secondary to expression of iNOS during an inflammatory response, induce increases in endothelial permeability (Lucas *et al* 2013). iNOS expression activates IP$_3$, triggering intracellular release of Ca^{2+} and activation of myosin light chain kinase (MLCK). Increased amount of phosphorylated myosin light chain 20 is indicative of enhanced permeability (Giannotta *et al* 2013). NO production in response to shear stress, independent of NOS, also increases permeability (Vandenbroucke *et al* 2008). Though the permeability response at different concentrations of NO is likely to be mediated by different mechanisms, both NO deficiency as well as high NO levels destabilize inter-endothelial junctions. Ang-1 binding to Tie-2 receptors, initiates eNOS activation via Akt, thus providing the much-needed protective NOS for junctional stability. VE-cadherin is also a direct target of Tie-2 activation as sequestration of non-receptor tyrosine kinase Src through the RhoA downstream target mDia prevents internalization of VE-Cadherin (Gavard *et al* 2008). Thus, there is a current consensus that eNOS-derived NO regulates the integrity of

endothelial barrier by directly affecting the adhesive properties of AJs (Vandenbroucke *et al* 2008; Alfieri *et al* 2014). The ability of Ang-1 to regulate NOS levels and VE-cadherin, strengthen its potential to overcome lymphatic endothelial barrier dysfunction. It warrants an investigation into the mechanism of barrier disruption in LEC junctions and the potential of Ang-1 in protecting the lymphatic endothelial barrier. Ang-1 has been shown to bridge trans-interactions of Tie-2 on neighbouring cells, which support cell-cell adhesion. It also increases the availability of VE-PTP molecules at inter-endothelial junctions, which may strengthen the adhesive function of VE-cadherin (Fukuhara *et al* 2009). Whether Tie-2 can strengthen cell-cell contact in LECs is an interesting question for the future. A mechanism through which Ang-1 may mediate its protective effects in LECs in inflammatory conditions is proposed in figure 5.1.
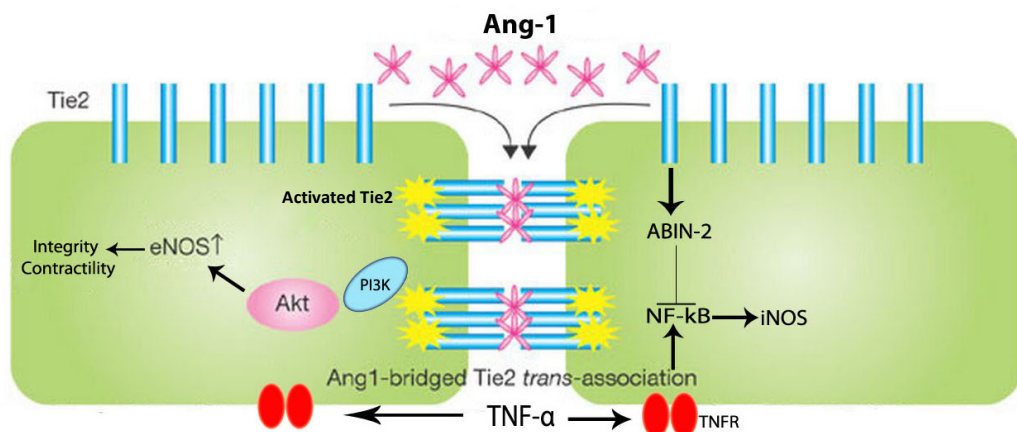
Figure 5.1 Proposed mechanism of action of Ang-1 in LECs in inflammatory conditions. Trans-association of Tie-2 may occur at cell-cell contacts in the presence of Ang-1 leading to the activation of PI3K/Akt pathway. Activated Akt may result in upregulation of eNOS contributing to vessel integrity and contractility. ABIN-2 recruited to Tie-2 by Ang-1 may prevent iNOS induction by inhibiting NF-κB activation. Adapted from (Fukuhara *et al* 2010)**.**

5.5 Conclusions and future directions

Our studies characterise the lymphatic vessel behaviour in inflammatory conditions such as sepsis and elucidate the potential mechanisms that may be involved. We established an *ex vivo* model of sepsis to investigate changes in mesenteric lymphatic

vessel function during early phase of sepsis. This model has allowed the exclusion of external influences such as flow, assess direct effects of inflammatory agents on vessel contractility and identify any modulation via NO, a key modulator of lymphatic contractility. Vessels stimulated with inflammatory cytokines such as TNF-α and IL-1β have shown a reduction in pump function, with protection from effects of TNF-α in vessels pre-treated with Ang-1.

Results from our study provide preliminary evidence that modulation of eNOS in sepsis may be a promising strategy. eNOS plays a crucial role not only in the control of blood flow at the microcirculatory level, but also lymphatic flow. Stimulation of eNOS leads to an increase in microcirculatory perfusion in the relevant vessels and maintains lymphatic pumping. In sepsis, inadequate production of eNOS, results in impaired perfusion and decreased clearance of interstitial fluid aggravating disease outcomes. Modulation of eNOS, enabling local generation of NO may thus be beneficial not only for microcirculatory perfusion but also for lymphatic function (De Backer *et al* 2014). Cumulatively, our data and results from *in vitro* and *in vivo* studies performed over a decade suggest that an Ang-1 mimetic might be an effective therapeutic tool for increasing microvascular perfusion, mitigating the effects of incomplete lymphatic drainage by improving lymphatic contraction and lymph flow (David *et al* 2013). *In vivo* studies using Ang-1 as a prophylatic agent could be designed to assess effects on lymphatic flow in acute and chronic models of endotoxemia. It is also necessary to assess whether the protective effects of Ang-1 are mediated via eNOS upregulation. IHC of vessels exposed to inflammatory mediators following pre-treatment with Ang-1 to detect eNOS expression could clarify the role of this NOS isoform in mediating effects of Ang-1.

As discussed in section 1.2.7, the inflammatory process triggers an increase in the permeability in post-capillary venules and evidence in now emerging that the lymphatic endothelial barrier may be compromised as well (Cromer *et al* 2014; Kawai *et al* 2014). The LECs of the collecting lymphatics, which transport lymph and immune cells into ducts, form continuous zipper-like junctions comprised of AJ protein VE-cadherin and TJ proteins claudin-5 and ZO-1, TJ-associated Ig-like transmembrane proteins ESAM, JAM-A, and PECAM-1/CD31(Kesler *et al* 2013). Destabilisation of endothelial AJs by TNF-α has been reported (Angelini *et al* 2006). Future experiments could be designed to investigate the effects of inflammatory

mediators on VE-cadherin in RMLV and assess differences in expression and organization of VE-cadherin and its binding partners pre- and post-treatment with Ang-1. We began the investigation of this objective with confocal immunofluorescent microscopy of VE-cadherin in Prof Zawieja's laboratory (Figure 6.9, Appendix IV). Studies were initiated in this lab due to the available expertise in confocal immunofluorescent microscopy of lymphatic vessels; however, time constraints did not allow us to continue the studies in our lab.

Our study also supports the role of NO and other inflammatory mediators in the vicinity of the lymphatics in regulating basic contractile parameters during sepsis. A better understanding of the signaling pathways and regulatory mechanisms involved is critical as insufficient lymphatic drainage or fluid stasis is the key underlying feature of several other inflammatory pathologies. An effective protocol developed for maintenance of isolated RMLV in culture up to 12 days without compromising contractile patterns and successful adenoviral/GFP transfection of LECs and lymphatic muscle cells, will aid investigation into the mechanisms during this response (Gashev *et al* 2009). Furthermore, the recent successful generation of an *in vivo* murine model of lymphatic contraction will further advance the research by allowing investigation into these underlying molecular mechanisms as molecular reagents, genetic knockouts, and disease models in mice are easily available (Liao *et al* 2011). Determining the mechanisms in this important response will answer critical questions, which will inform the future of developing potent clinically relevant agents as lymphatic disease interventions. Hence, future studies, would investigate:

1) mechanisms regulating lymphatic barrier integrity.
2) mechanisms mediating the effects of potent inflammatory mediators on lymphatic barrier and contractile function.
3) growth factors as a potential therapeutic target for modulating lymphatic function during inflammation.

Chapter Six

Appendices

APPENDIX I

Chapter 2- Materials and methods

Consumables

Item	Supplier
2.0 ml eppendorf tubes	Fisher Scientific UK Ltd
Aluminium foil	Terinex Ltd
BD Plastipak™ 1 ml, 2 ml, 5 ml, 20 ml, 50 ml syringes	BD Biosciences
Cellulose dialysis tubing (12, 400 MW) Lot# 10B040530	Sigma-Aldrich Ltd
Hospira Butterfly needles, 10 mm	Venisystems
Mersilk 5-0 Sutures	Ethicon
MICRO-MATE® Interchangeable hypodermic syringe	Popper & Sons Inc.
Portex fine bore polythene tubing 0.58mm x 0.96mm	Cole-Parmer Instrument Co. Ltd
Propax® 8-ply 5 x 5 cm sterile gauze	Shermond Surgical Supply Ltd
Saran wrap	SC Johnson
Scalpel blades Size 11	Paragon
Silastic® Laboratory polypropylene tubing 0.76mm x 1.65mm	Cole-Parmer Instrument Co. Ltd
Silclear™ silicone tubing size 0.020" x 0.037"	Degania Silicone Ltd
Terumo® 23G, 26G needles	Neolus
Trigene disinfectant, concentration diluted 1:50	Medichem International Ltd
Universal tubes	Scientific Laboratory Supplies Ltd

Drugs & Reagents

Acetyl-β-methylcholine chloride	Sigma-Aldrich
Acetylcholine chloride	Sigma-Aldrich
BSA	Sigma-Aldrich
Calcium chloride dihydrate Lot# BCBF6545V	Sigma
D-NAME	Sigma-Aldrich
DEPC-treated water	Ambion
Dextrose Lot# 060M0141V	Sigma
Donkey serum Product# D9663	Sigma
DPBS Product# D8862	Sigma
EDTA disodium salt dihydrate Batch# 067K01442	Sigma-Aldrich
Heparin sodium 5000 I.U./ml	Wockhardt UK Ltd
HEPES Batch# 030M5402	Sigma
HR.Ang-1 Lot# FHW17	R&D Systems
Indomethacin Lot# BCBF9122V	Sigma
Isoflo® Isoflurane 100%w/w	Abbott
L-NAME	Sigma-Aldrich
LPS (L2637) Pressure myography: Lot# 078K4067; 100M4061V (Shef) Lot# 067K4135; 038K4056 (Tx) IVM: Lot# 067K847; EU- 6 x 10^5 Lot# 127K4026; EU-1.2 x 10^6 Lot# 038K4056; EU-3 x 10^6	Sigma

Magnesium sulphate Lot# 031M01341V	Sigma
MOPS Batch# 098K0033	Sigma
Potassium chloride Lot# BCBF2693V	Sigma-Aldrich
Potassium phosphate monobasic Lot# 018K0128	Sigma
Recombinant rat IL-1β Lot# 100991-1	Peprotech
Recombinant rat TNF-α Lot # 070473	Peprotech
RNA*later*® stabilisation solution Cat No# AM7020	Ambion™
Saline	Fresenius Kabi Ltd
Sodium chloride Lot# BCBF8020V	Sigma-Aldrich
Sodium nitroprusside dihydrate	Sigma-Aldrich
Sodium phosphate monobasic Lot# BCBD2824V	Sigma
Thiopental sodium	Archimedes Pharma Ltd
TRI Reagent® Cat No. T9424	Sigma-Aldrich

Antibodies (Ab) and kits

Alexa fluor 647 donkey anti-goat IgG	Invitrogen
Anti-mouse LYVE-1 Alexa fluor 488	eBioscience
Mouse Tie-2 polyclonal Ab goat IgG 352588, Lot# EFK0208111	R&D systems
Mouse VE-Cadherin affinity polyclonal Ab goat IgG AF1002, Lot# FQI0109041	R&D systems
GenElute™ Mammalian TotalRNA	Sigma-Aldrich

Miniprep kit Product# RTN10	
mirVana PARIS Kit Product# AM1556	Applied Biosystems
RNeasy Mini Kit Cat. No. 74104	Qiagen
TURBO DNA-*free*™ Kit	Ambion
High capacity RNA-to-cDNA Kit	Applied Biosystems

Equipment

Anaesthesia syringe Pump (Graseby 3400)	Graseby Medical
Anaesthetic machine	Burtons Medical Equiment Ltd.
Angled forceps Product Code: 00649-11	Fine Science Tools
Artery clamp Product Code: 18055-04	Fine Science Tools
BIOPAC MP system	Biopac systems, Inc.
Black and white video monitor (Model: CMM1200N)	Costar video systems
C28 rechargeable cordless cautery	Warecrest Ltd
CH/2/M vessel chamber	Living Systems Instrumentation
Colour video camera	JVC; Sony Trinitron
Colour video monitor	Sony Trinitron
Curved forceps Product Code: 11051-10	Fine Science Tools
Dumont Forceps #5 Product Code: 11255-20	Fine Science Tools
Glass cannula pack	Living Systems Instrumentation
Optical Power Meter	Omega Universal Technologies Inc
Professional DVD recorder MP-6000 Mk2	Datavideo
Spectrophotometer (Nanodrop ND-1000)	Labtech International

Sphygmomanometer Model No. 605	Kenzmedico Co. Ltd.
Spring scissors Product Code: 15012-12	Fine Science Tools
Surgical scissors Product Code: 14559-11	Fine Science Tools
Temperature controller (Model TC-02)	Living Systems Instrumentation
Thermometer	Fluke Ltd
Video Dimension Analyser (V94)	Living Systems Instrumentation

APPENDIX II

Chapter 2- Materials and Methods

APSS was prepared from the following components:

Salt	Chemical MW	Molarity (mM)	Amount per 500 ml (g)
NaCl	58.44	145.000	4.235
KCl	74.56	4.700	0.175
$CaCl_2.2H_2O$	147.02	2.000	0.145
$MgSO_4$	120.37	1.170	0.07
NaH_2PO_4	119.98	1.200	0.07
Dextrose	180.16	5.000	0.45
Sodium Pyruvate	100mM solution	2.000	10ml
$EDTA.2H_2O$	372.2	0.020	0.0037
MOPS	209.2	3.000	0.628

To prepare APSS, 500ml glass bottle was filled with 0.4 l of ultrapure H_2O. The above ingredients were added while mixing until they dissolved. 10g/l BSA (96%, Sigma) was added to the solution until it completely dissolved. The volume was adjusted to 500 ml by ultrapure H_2O. The pH of the solution was adjusted to 7.4 at RT. It was filtered into a sterile polypropylene bottle using a bottle top filter unit (50 mm, Nalgene filtration product) and kept refrigerated. Prior to use in the experiment, the solution was warmed to $38^{o}C$ and the pH adjusted if needed.

Ca^{2+} -free solution was prepared in a manner similar to preparation of APSS using the same ingredients as above except $CaCl_2$ and EDTA. Prior to use in the experiment, 0.075g of EDTA was added to 50 ml of stock solution and mixed until all the EDTA dissolved. The pH was adjusted to 7.4 at $38^{o}C$.

HEPES was prepared from the following components:

Salt	MW	Amount per 500 ml
HEPES	237.3	11.915
RINGER		
NaCl	58.44	41.4915
KCl	74.56	1.752
KH_2PO_4	136.09	0.803
$MgSO_4$	120.4	1.442
$CaCl_2$	147.02	3.675

Stock solutions of $MgSO_4$, $CaCl_2$, HEPES, Ringer were stored for 1 month at 4°C. 500 ml of intermediate HEPES solution was prepared by mixing 50 ml of $MgSO_4$, HEPES, Ringer each (stock solutions), 16 ml of $CaCl_2$ (stock) and the volume was adjusted to 500 ml with distilled water. This was stored for 1 week at 4°C. Working HEPES was prepared on the day of the experiment by adding 0.99 g/L D(+) glucose (Fw: 180.16) to the required volume of intermediate HEPES and pH was adjusted to 7.4.

Results Chapter 1
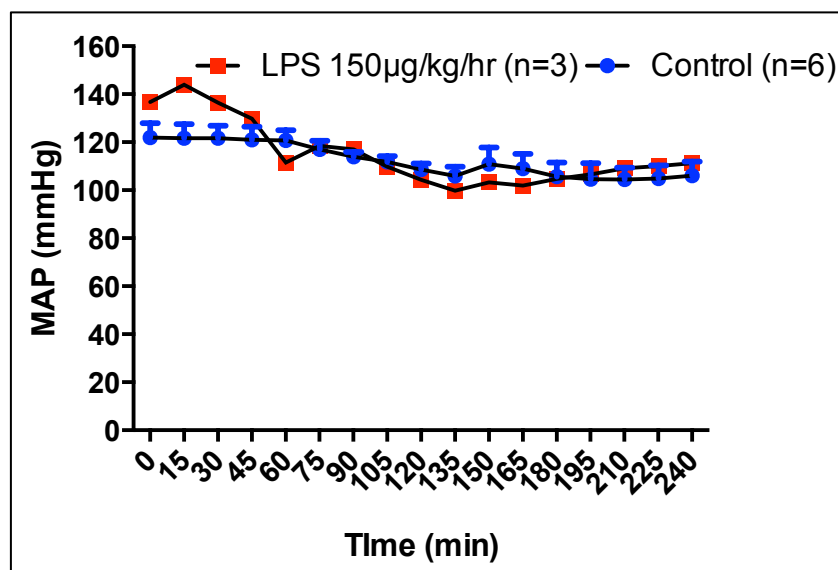
Figure 6.1 Mean arterial pressure (MAP) (mean ± SEM) in LPS (n=1) and control groups. No significant differences were observed between experimental and control groups.
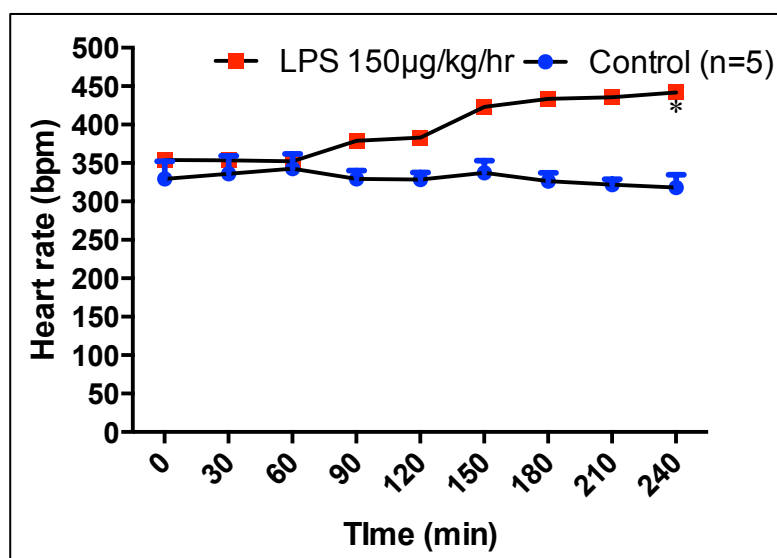
Figure 6.2 Heart rate (bpm; beats per minute) (mean ± SEM) in LPS (n=1) and control groups. LPS induced an increase in heart rate at 4 h. *$p < 0.05$ significantly different to saline.
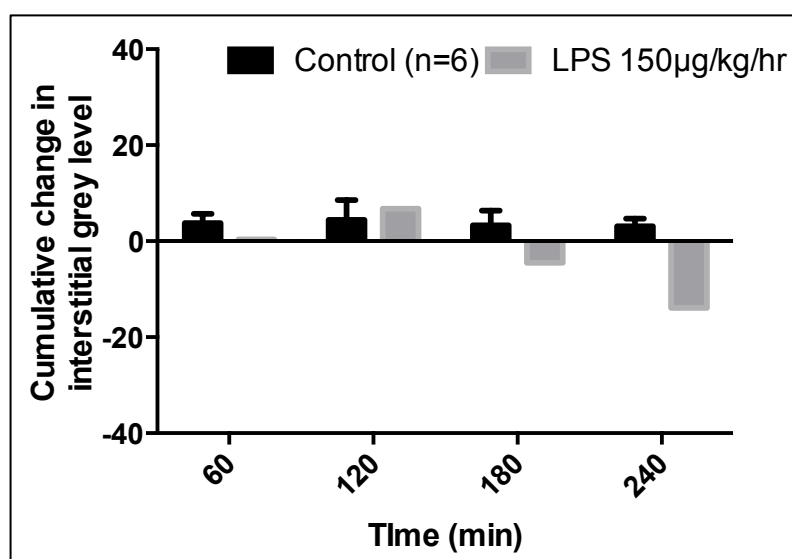
Figure 6.3 Effect of LPS (0127:B8) on macromolecular leak. Macromolecular leak is expressed as mean cumulative change in grey level (arbitrary units) (±SEM) in LPS (n=1) and control groups. No significant difference in leak was observed compared to control.
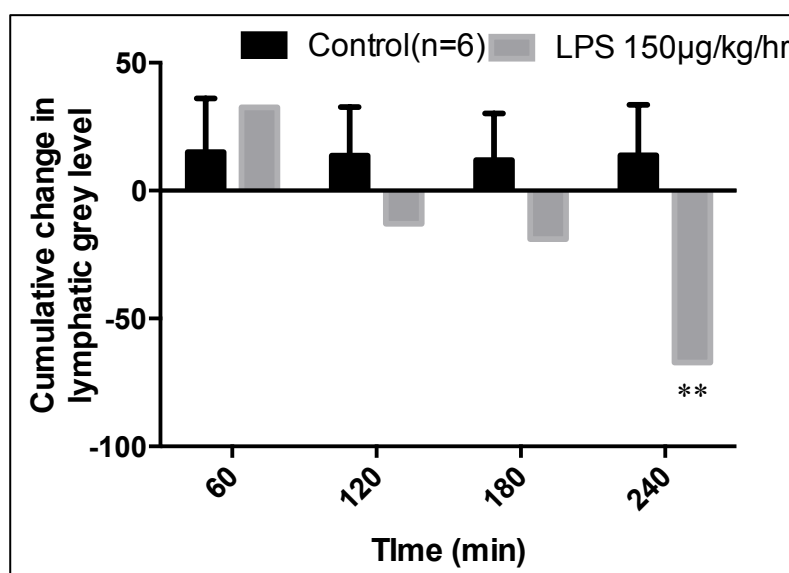
Figure 6.4 Effect of LPS (0127:B8) on level of FITC-BSA in lymphatic vessel. Change in protein concentration within the lymphatic vessel is expressed as mean cumulative change in grey level (arbitrary units) (±SEM) in LPS (n=1) and control groups. A significant decrease in grey levels is observed at 4 h after LPS administration. **$p < 0.01$ significantly different to control.

Results chapter 2

LPS
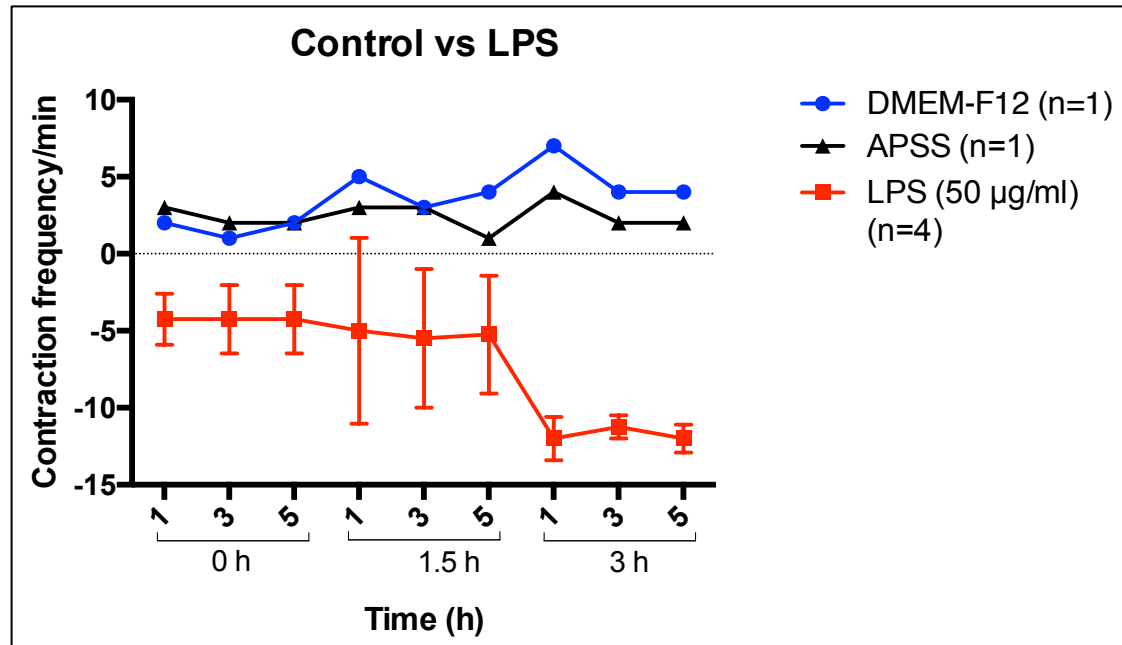
Figure 6.5 Change in frequency of contractions in vessels continuously suffused with DMEM-F12 containing LPS (50 μg/ml). Frequency declined markedly at 3 h in LPS treated vessels pressurised at 1, 3 and 5 cm H_2O compared to baseline and control.

There were significant changes in diameter at 3 h (3 cm H_2O) as indicated by % increase in diameter in LPS (3 x 10^6 EU, 1.2 x 10^6 EU) treated vessels compared to the control (Figure 6.6, Table 6.2).
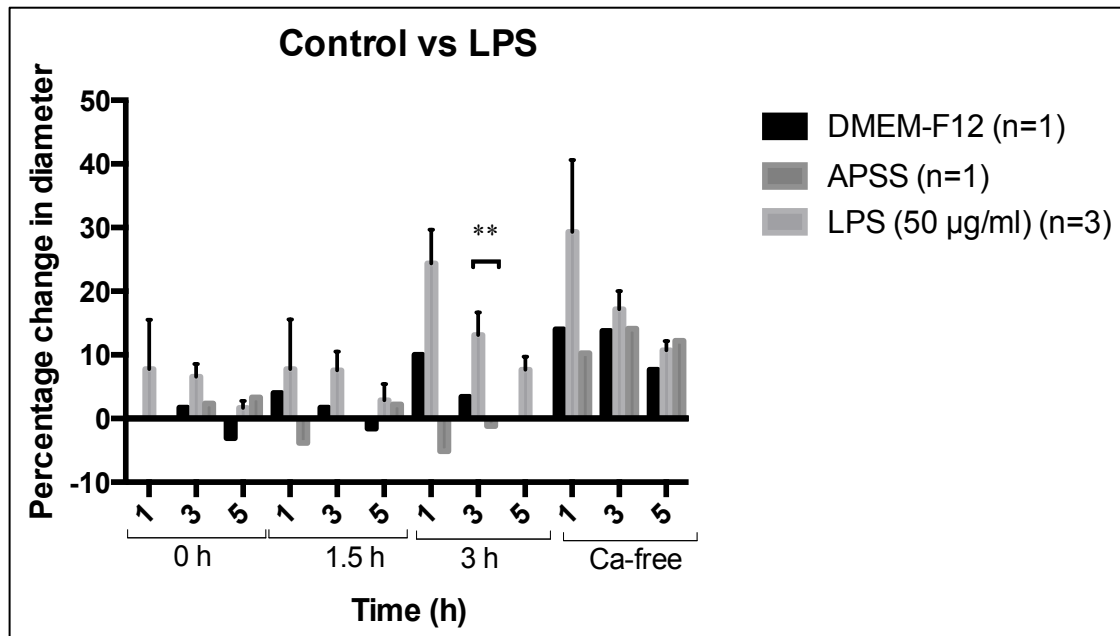
Figure 6.6 Percentage change in diameter of vessels continuously suffused with DMEM-F12 containing LPS (50 µg/ml). Increase in diameter was observed at all time points in LPS treated vessels pressurised at 1, 3 and 5 cm H_2O compared to baseline and control. Increase was significant at 3 h at a pressure of 3 cm H_2O compared to untreated vessels suffused with APSS. **p < 0.01 vs APSS. Vessels were maximally dilated in Ca-free APSS.

MAT.Ang-1
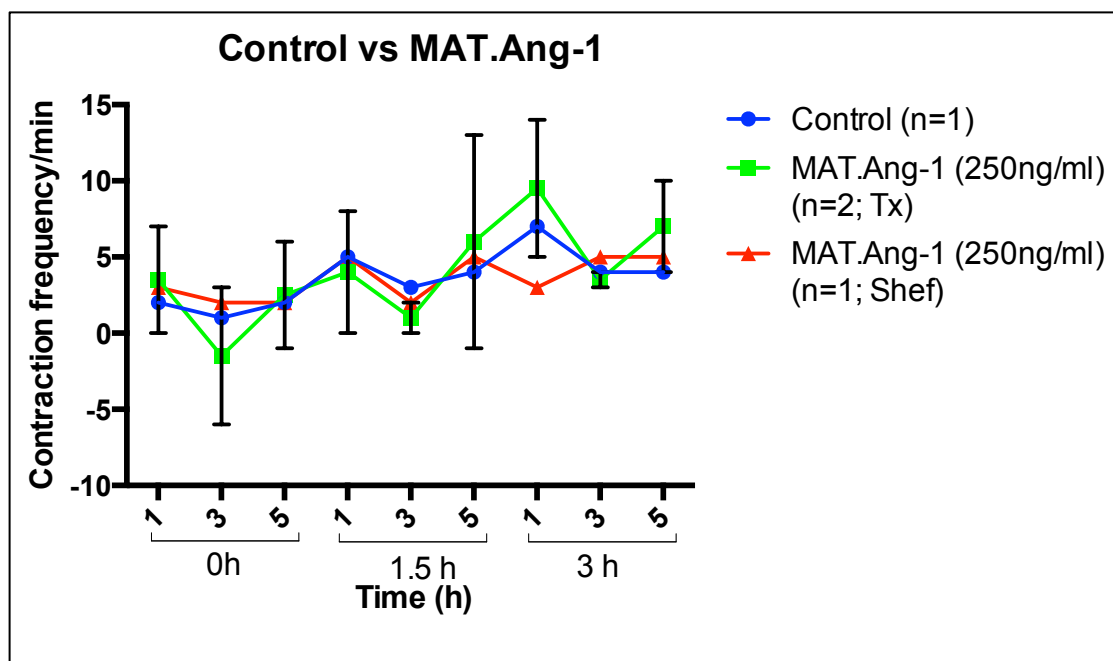
Figure 6.7 Change in frequency of contractions in presence of MAT.Ang-1.
Frequency remained unaltered in presence of MAT.Ang-1 in experiments performed using set-ups in Texas (Tx) and Sheffield (Shef) at 0, 1.5 and 3 h.
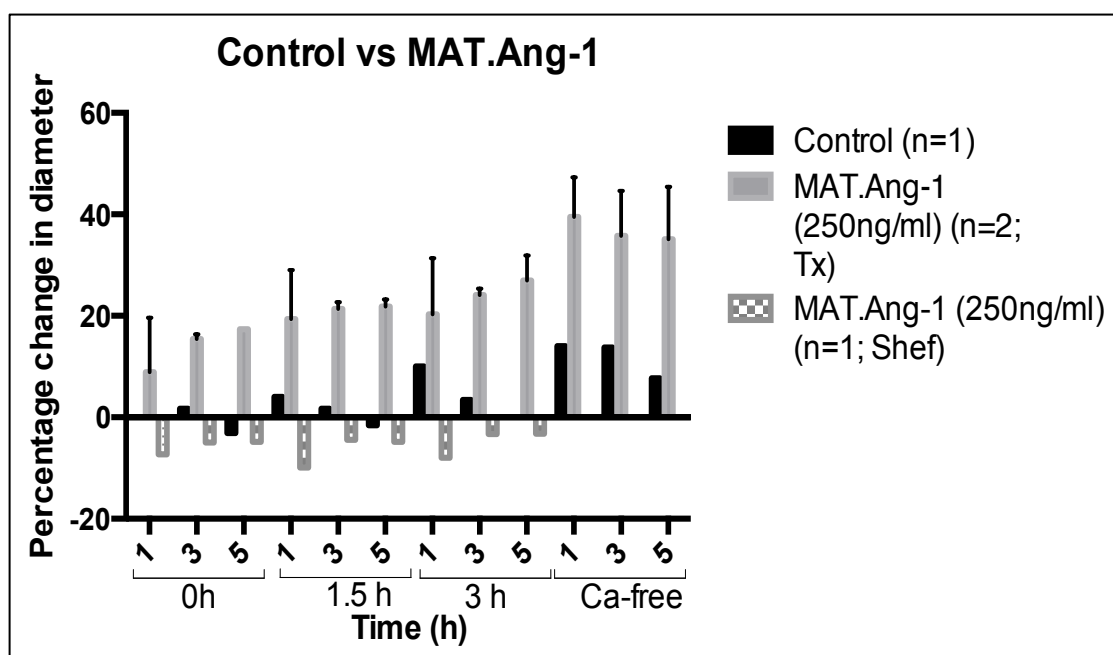
Figure 6.8 Percentage change in diameter of vessels in presence of MAT.Ang-1.
Increase in diameter was observed at all time points in vessels at 0, 1.5 and 3 h compared to baseline and control in experiments performed using the set-up in Tx. Vessels were maximally dilated in Ca-free APSS (35.75 ± 6.3 %). Minimal change in diameter was observed in the experiment performed using the set-up in Shef.

Tone of vessels

Vessels isolated from animals culled after Schedule 1 procedure exhibited much lesser tone than vessels isolated from anaesthetised animals. The tone, indicated by maximum percentage change in diameter of vessels in Ca-free solution using both methods is tabulated below (Table 6.1). The latter procedure, which was performed in Texas A&M University (Gashev *et al* 2002), could not be adopted at the Biological services in the University of Sheffield due to limitations imposed by Home Office ethics guidelines. Therefore, experiments were performed with the vessels obtained after schedule 1 procedure was performed on animals. Percentage change in diameter at the end of the experiment when compared to baseline in vessels isolated from anesthetised animals (maintained in APSS or DMEM-F12) or after animal was culled by Schedule 1 procedure and treated with different pharmacological or inflammatory agents is shown in table 6.2. Vessels isolated from live animals exhibited a higher increase in diameter after treatment with LPS and MAT.Ang-1 compared to vessels isolated from culled animals. The decreased tone of vessels maybe due to the stimulation of vessels by dilatory agents released during the schedule 1 procedure.

Treatment	Max % change in diameter (Ca-free)
Vessel isolated from live animal (maintained in DMEM-F12)(n=1)	**10%**
Vessel isolated from live animal (maintained in APSS)(n=1)	**14.11%**
Vessel isolated after animal culled by Schedule 1(maintained in APSS) (n=3)	**4.07 ± 1.09 %**
LPS treated vessel isolated from live animal	**17 ± 1.7 %**
MAT.Ang-1 treated vessel isolated from live animal	**35.75 ± 6.3 %**

Table 6.1 Percentage change in diameter of vessels in Ca-free solution. Percentage change in diameter in Ca-free solution when compared to baseline in vessels isolated from anesthetised animals (maintained in APSS or DMEM-F12) or after animal was culled by Schedule 1 procedure in control and experimental conditions.

Treatment	Max % change in diameter
Control (APSS; Tx)	2%
Control (DMEM-F12; Tx)	3%
LPS (DMEM-F12; Tx)	13 ± 2 %
LPS with serum batch 1 (APSS; Shef)	10.2 ± 3.6 %
LPS with serum batch 2 (APSS; Shef)	-0.8 ± 2.5 %
LPS without serum (APSS; Shef)	0.92 %
Ach	<1%
L-NAME (1mM)	0.8 ± 0.6 %
D-NAME (1mM)	-2.6 ± 1.7 %
SNP	4 ± 5 %
TNF-α	4 ± 5.9 %
L-NAME (1mM) + TNF-α	16 ± 8 %
L-NAME (.1mM) + TNF-α	-1.4 ± 1.2 %
D-NAME (1mM) + TNF-α	11 ± 4 %
Indomethacin + TNF-α	3.3 ± 0.7 %
IL-1β	-0.3 ± 3.1 %
TNF-α + IL-1β	-2.3 ± 3.8 %
MAT.Ang-1 (Tx)	24 ± 0.9 %
MAT.Ang-1 (Shef)	0 %
HR.Ang-1	4.2 ± 3.7 %
Ang-1+ TNF-α	5.4 ± 2.3 %

Table 6.2 Percentage change in diameter of treated vessels in Ca-free solution.
Percentage change in diameter at the end of the experiment when compared to baseline in vessels isolated from anesthetised animals (maintained in APSS or DMEM-F12) or after animal was culled by Schedule 1 procedure and treated with different pharmacological or inflammatory agents.

Confocal immunofluorescent microscopy

VE-cadherin

To detect expression of VE-cadherin, RMLV were treated with purified goat anti-mouse CD144 polyclonal antibody. Alexa-fluor 647 conjugated anti-goat IgG antibody was used to observe immunofluorescence under a confocal microscope (Figure 6.9). Specific VE-cadherin staining with the antibody concentrations used could not be achieved. Further optimisation was needed to obtain specific staining of VE-cadherin, however this was not possible due to time constraints. Detection and visualisation of VE-cadherin expression will enable assessment of AJ integrity in the lymphatic endothelium during sepsis.
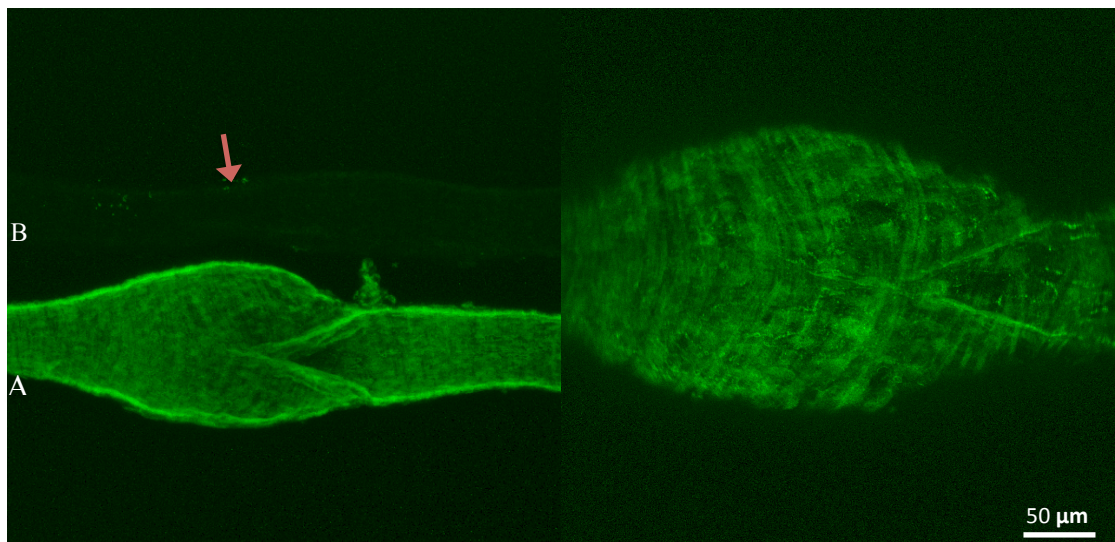
Figure 6.9 Non-specific staining in rat mesenteric lymphatics. Confocal immunofluorescent micrographs (x10) (pseudocoloured) of isolated mesenteric lymphatics stained with goat anti-mouse CD144 polyclonal antibody (A) (primary Ab) or goat IgG (B) and Alexa-fluor 647 conjugated anti-goat IgG (secondary Ab). Staining for VE-cadherin is non-specific and visible in non-endothelial cells present in the vessel. Red arrow indicates unstained vessel.

References

Abraham, E. (2005). "Alterations in cell signaling in sepsis." Clin Infect Dis **41 Suppl 7**: S459-464.

Aebischer, D., et al. (2014). "The inflammatory response of lymphatic endothelium." Angiogenesis **17**(2): 383-393.

Aghajanian, A., et al. (2008). "Endothelial cell junctions and the regulation of vascular permeability and leukocyte transmigration." J Thromb Haemost **6**(9): 1453-1460.

Al-Kofahi, M., et al. (2015). "Interleukin-1 beta Reduces Tonic Contraction of Mesenteric Lymphatic Muscle Cells: Involvement of Cyclooxygenase-2 / Prostaglandin E2." Br J Pharmacol.

Aldrich, M. B. and E. M. Sevick-Muraca (2013). "Cytokines are systemic effectors of lymphatic function in acute inflammation." Cytokine **64**(1): 362-369.

Alexander, J. S., et al. (2010). "Gastrointestinal lymphatics in health and disease." Pathophysiology **17**(4): 315-335.

Alexopoulou, L., et al. (2001). "Recognition of double-stranded RNA and activation of NF-kappaB by Toll-like receptor 3." Nature **413**(6857): 732-738.

Alfieri, A., et al. (2014). "Angiopoietin-1 regulates microvascular reactivity and protects the microcirculation during acute endothelial dysfunction: role of eNOS and VE-cadherin." Pharmacol Res **80**: 43-51.

Alfieri, A., et al. (2012). "Angiopoietin-1 variant reduces LPS-induced microvascular dysfunction in a murine model of sepsis." Crit Care **16**(5): R182.

Alitalo, K. (2011). "The lymphatic vasculature in disease." Nat Med **17**(11): 1371-1380.

Andrew, P. S. and S. Kaufman (2001). "Splenic denervation worsens lipopolysaccharide-induced hypotension, hemoconcentration, and hypovolemia." Am J Physiol Regul Integr Comp Physiol **280**(5): R1564-1572.

Angelini, D. J., et al. (2006). "TNF-alpha increases tyrosine phosphorylation of vascular endothelial cadherin and opens the paracellular pathway through fyn activation in human lung endothelia." Am J Physiol Lung Cell Mol Physiol **291**(6): L1232-1245.

Angus, D. C. and T. van der Poll (2013). "Severe sepsis and septic shock." N Engl J Med **369**(21): 2063.

Augustin, H. G., et al. (2009). "Control of vascular morphogenesis and homeostasis through the angiopoietin-Tie system." Nat Rev Mol Cell Biol **10**(3): 165-177.

Augustin, H.G. and Fiedler, U. 2008. Regulation of angiogenesis and vascular homeostasis through the Angiopoietin/Tie system. In: Marmé, D. and Fusenig, N.ed.

Tumor Angiogenesis: Basic Mechanisms and Cancer Therapy. Germany: Springer, pp.109-116.

Aziz, M., et al. (2013). "Current trends in inflammatory and immunomodulatory mediators in sepsis." J Leukoc Biol **93**(3): 329-342.

Baffert, F., et al. (2006). "Angiopoietin-1 decreases plasma leakage by reducing number and size of endothelial gaps in venules." Am J Physiol Heart Circ Physiol **290**(1): H107-118.

Baluk, P., et al. (2007). "Functionally specialized junctions between endothelial cells of lymphatic vessels." J Exp Med **204**(10): 2349-2362.

Bateman, R. M., et al. (2003). "Bench-to-bedside review: microvascular dysfunction in sepsis--hemodynamics, oxygen transport, and nitric oxide." Crit Care **7**(5): 359-373.

Bazzoni, G. and E. Dejana (2004). "Endothelial cell-to-cell junctions: molecular organization and role in vascular homeostasis." Physiol Rev **84**(3): 869-901.

Bellingan, G. (1999). "Inflammatory cell activation in sepsis." Br Med Bull **55**(1): 12-29.

Bennett, T., et al. (2004). "Regional and temporal changes in cardiovascular responses to norepinephrine and vasopressin during continuous infusion of lipopolysaccharide in conscious rats." Br J Anaesth **93**(3): 400-407.

Benoit, J. N. and D. C. Zawieja (1992). "Effects of f-Met-Leu-Phe-induced inflammation on intestinal lymph flow and lymphatic pump behavior." Am J Physiol **262**(2 Pt 1): G199-202.

Benoit, J. N., et al. (1989). "Characterization of intact mesenteric lymphatic pump and its responsiveness to acute edemagenic stress." Am J Physiol **257**(6 Pt 2): H2059-2069.

Bohlen, H. G., et al. (2011). "Nitric oxide formation by lymphatic bulb and valves is a major regulatory component of lymphatic pumping." Am J Physiol Heart Circ Physiol **301**(5): H1897-1906.

Bohlen, H. G., et al. (2009). "Phasic contractions of rat mesenteric lymphatics increase basal and phasic nitric oxide generation in vivo." Am J Physiol Heart Circ Physiol **297**(4): H1319-1328.

Bridenbaugh, E. A. (2012). "Isolation and preparation of RNA from rat blood and lymphatic microvessels for use in microarray analysis." Methods Mol Biol **843**: 265-289.

Brindle, N. P., et al. (2006). "Signaling and functions of angiopoietin-1 in vascular protection." Circ Res **98**(8): 1014-1023.

Brookes, Z. L., et al. (2000). "Intravenous anaesthesia and the rat microcirculation: the dorsal microcirculatory chamber." Br J Anaesth **85**(6): 901-903.

Brookes, Z. L. and S. Kaufman (2005). "Effects of atrial natriuretic peptide on the extrasplenic microvasculature and lymphatics in the rat in vivo." J Physiol **565**(Pt 1): 269-277.

Brookes, Z. L., et al. (2009). "Macromolecular leak from extrasplenic lymphatics during endotoxemia." Lymphat Res Biol **7**(3): 131-137.

Brown, G. T. and T. M. McIntyre (2011). "Lipopolysaccharide signaling without a nucleus: kinase cascades stimulate platelet shedding of proinflammatory IL-1beta-rich microparticles." J Immunol **186**(9): 5489-5496.

Bryant, C. E., et al. (2010). "The molecular basis of the host response to lipopolysaccharide." Nat Rev Microbiol **8**(1): 8-14.

Cepinskas, G. and J. X. Wilson (2008). "Inflammatory response in microvascular endothelium in sepsis: role of oxidants." J Clin Biochem Nutr **42**(3): 175-184.

Chaitanya, G. V., et al. (2010). "Differential cytokine responses in human and mouse lymphatic endothelial cells to cytokines in vitro." Lymphat Res Biol **8**(3): 155-164.

Chakraborty, S., et al. (2015). "Emerging trends in the pathophysiology of lymphatic contractile function." Semin Cell Dev Biol **38**: 55-66.

Chakraborty, S., et al. (2011). "Substance P activates both contractile and inflammatory pathways in lymphatics through the neurokinin receptors NK1R and NK3R." Microcirculation **18**(1): 24-35.

Childs, E. W., et al. (2008). "Angiopoietin-1 inhibits intrinsic apoptotic signaling and vascular hyperpermeability following hemorrhagic shock." Am J Physiol Heart Circ Physiol **294**(5): H2285-2295.

Cho, C. H., et al. (2004). "COMP-Ang1: a designed angiopoietin-1 variant with nonleaky angiogenic activity." Proc Natl Acad Sci U S A **101**(15): 5547-5552.

Cinel, I. and S. M. Opal (2009). "Molecular biology of inflammation and sepsis: a primer." Crit Care Med **37**(1): 291-304.

Cohen, J. (2002). "The immunopathogenesis of sepsis." Nature **420**(6917): 885-891.

Cromer, W. E., et al. (2014). "The effects of inflammatory cytokines on lymphatic endothelial barrier function." Angiogenesis **17**(2): 395-406.

Cueni, L. N. and M. Detmar (2008). "The lymphatic system in health and disease." Lymphat Res Biol **6**(3-4): 109-122.

Daniels, R. (2011). "Surviving the first hours in sepsis: getting the basics right (an intensivist's perspective)." J Antimicrob Chemother **66 Suppl 2**: ii11-23.

Daubeuf, B., et al. (2007). "TLR4/MD-2 monoclonal antibody therapy affords protection in experimental models of septic shock." J Immunol **179**(9): 6107-6114.

Dauphinee, S. M. and A. Karsan (2006). "Lipopolysaccharide signaling in endothelial cells." Lab Invest **86**(1): 9-22.

David, S., et al. (2013). "Mending leaky blood vessels: the angiopoietin-Tie2 pathway in sepsis." J Pharmacol Exp Ther **345**(1): 2-6.

Davis, M. J., et al. (2009). "Myogenic constriction and dilation of isolated lymphatic vessels." Am J Physiol Heart Circ Physiol **296**(2): H293-302.

Davis, M. J., et al. (1992). "Stretch-induced increases in intracellular calcium of isolated vascular smooth muscle cells." Am J Physiol **263**(4 Pt 2): H1292-1299.

Davis, M. J., et al. (2012). "Intrinsic increase in lymphangion muscle contractility in response to elevated afterload." Am J Physiol Heart Circ Physiol **303**(7): H795-808.

De Backer, D., et al. (2014). "Pathophysiology of microcirculatory dysfunction and the pathogenesis of septic shock." Virulence **5**(1): 73-79.

Deitch, E. A. (2010). "Gut lymph and lymphatics: a source of factors leading to organ injury and dysfunction." Ann N Y Acad Sci **1207 Suppl 1**: E103-111.

Deitch, E. A. (2012). "Gut-origin sepsis: evolution of a concept." Surgeon **10**(6): 350-356.

Deitch, E. A., et al. (2006). "Role of the gut in the development of injury- and shock induced SIRS and MODS: the gut-lymph hypothesis, a review." Front Biosci **11**: 520-528.

Dejana, E., et al. (2008). "The role of adherens junctions and VE-cadherin in the control of vascular permeability." J Cell Sci **121**(Pt 13): 2115-2122.

Dellinger, M., et al. (2008). "Defective remodeling and maturation of the lymphatic vasculature in Angiopoietin-2 deficient mice." Dev Biol **319**(2): 309-320.

Dixon, J. B., et al. (2006). "Lymph flow, shear stress, and lymphocyte velocity in rat mesenteric prenodal lymphatics." Microcirculation **13**(7): 597-610.

Dixon, J. B., et al. (2005). "Measuring microlymphatic flow using fast video microscopy." J Biomed Opt **10**(6): 064016.

Dongaonkar, R. M., et al. (2009). "Balance point characterization of interstitial fluid volume regulation." Am J Physiol Regul Integr Comp Physiol **297**(1): R6-16.

Dongaonkar, R. M., et al. (2013). "Adaptation of mesenteric lymphatic vessels to prolonged changes in transmural pressure." Am J Physiol Heart Circ Physiol **305**(2): H203-210.

Dongaonkar, R. M., et al. (2008). "Edemagenic gain and interstitial fluid volume regulation." Am J Physiol Regul Integr Comp Physiol **294**(2): R651-659.

Eklund, L. and B. R. Olsen (2006). "Tie receptors and their angiopoietin ligands are context-dependent regulators of vascular remodeling." Exp Cell Res **312**(5): 630-641.

Elias, R. M. and M. G. Johnston (1990). "Modulation of lymphatic pumping by lymph-borne factors after endotoxin administration in sheep." J Appl Physiol **68**(1): 199-208.

Elias, R. M., et al. (1987). "Decreased lymphatic pumping after intravenous endotoxin administration in sheep." Am J Physiol **253**(6 Pt 2): H1349-1357.

Ermert, M., et al. (2002). "Cell-specific nitric oxide synthase-isoenzyme expression and regulation in response to endotoxin in intact rat lungs." Lab Invest **82**(4): 425-441.

Fanous, M. Y., et al. (2007). "Mesenteric lymph: the bridge to future management of critical illness." JOP **8**(4): 374-399.

Fink, M. P. and H. S. Warren (2014). "Strategies to improve drug development for sepsis." Nat Rev Drug Discov **13**(10): 741-758.

Fleming, I., et al. (1992). "Endothelium-derived kinins account for the immediate response of endothelial cells to bacterial lipopolysaccharide." J Cardiovasc Pharmacol **20 Suppl 12**: S135-138.

Foldi, M. (2006). "Convincing evidence for the pumping activity of lymphatics." Acta Physiol (Oxf) **186**(4): 319; author reply 319.

Fukuhara, S., et al. (2008). "Differential function of Tie2 at cell-cell contacts and cell-substratum contacts regulated by angiopoietin-1." Nat Cell Biol **10**(5): 513-526.

Fukuhara, S., et al. (2009). "Tie2 is tied at the cell-cell contacts and to extracellular matrix by angiopoietin-1." Exp Mol Med **41**(3): 133-139.

Fukuhara, S., et al. (2010). "Angiopoietin-1/Tie2 receptor signaling in vascular quiescence and angiogenesis." Histol Histopathol **25**(3): 387-396.

Galanzha, E. I., et al. (2005). "In vivo integrated flow image cytometry and lymph/blood vessels dynamic microscopy." J Biomed Opt **10**(5): 054018.

Galanzha, E. I., et al. (2007). "Advances in small animal mesentery models for in vivo flow cytometry, dynamic microscopy, and drug screening." World J Gastroenterol **13**(2): 192-218.

Gale, N. W., et al. (2002). "Angiopoietin-2 is required for postnatal angiogenesis and lymphatic patterning, and only the latter role is rescued by Angiopoietin-1." Dev Cell **3**(3): 411-423.

Gamble, J. R., et al. (2000). "Angiopoietin-1 is an antipermeability and anti-inflammatory agent in vitro and targets cell junctions." Circ Res **87**(7): 603-607.

Gardiner, S. M., et al. (2005). "Involvement of CB1-receptors and beta-adrenoceptors in the regional hemodynamic responses to lipopolysaccharide infusion in conscious rats." Am J Physiol Heart Circ Physiol **288**(5): H2280-2288.

Gashev, A. A. (2008). "Lymphatic vessels: pressure- and flow-dependent regulatory reactions." Ann N Y Acad Sci **1131**: 100-109.

Gashev, A. A., et al. (2004). "Regional variations of contractile activity in isolated rat lymphatics." Microcirculation **11**(6): 477-492.

Gashev, A. A., et al. (2009). "Methods for lymphatic vessel culture and gene transfection." Microcirculation **16**(7): 615-628.

Gashev, A. A., et al. (2002). "Inhibition of the active lymph pump by flow in rat mesenteric lymphatics and thoracic duct." J Physiol **540**(Pt 3): 1023-1037.

Gashev, A. A. and D. C. Zawieja (2001). "Physiology of human lymphatic contractility: a historical perspective." Lymphology **34**(3): 124-134.

Gasheva, O. Y., et al. (2013). "Cyclic guanosine monophosphate and the dependent protein kinase regulate lymphatic contractility in rat thoracic duct." J Physiol **591**(Pt 18): 4549-4565.

Gasheva, O. Y., et al. (2006). "Contraction-initiated NO-dependent lymphatic relaxation: a self-regulatory mechanism in rat thoracic duct." J Physiol **575**(Pt 3): 821-832.

Gavard, J. and J. S. Gutkind (2006). "VEGF controls endothelial-cell permeability by promoting the beta-arrestin-dependent endocytosis of VE-cadherin." Nat Cell Biol **8**(11): 1223-1234.

Gavard, J., et al. (2008). "Angiopoietin-1 prevents VEGF-induced endothelial permeability by sequestering Src through mDia." Dev Cell **14**(1): 25-36.

Gessani, S., et al. (1993). "Enhanced production of LPS-induced cytokines during differentiation of human monocytes to macrophages. Role of LPS receptors." J Immunol **151**(7): 3758-3766.

Giannotta, M., et al. (2013). "VE-cadherin and endothelial adherens junctions: active guardians of vascular integrity." Dev Cell **26**(5): 441-454.

Gong, P., et al. (2008). "TLR4 signaling is coupled to SRC family kinase activation, tyrosine phosphorylation of zonula adherens proteins, and opening of the paracellular pathway in human lung microvascular endothelia." J Biol Chem **283**(19): 13437-13449.

Gu, H., et al. (2010). "Angiopoietin-1/Tie2 signaling pathway inhibits lipopolysaccharide-induced activation of RAW264.7 macrophage cells." Biochem Biophys Res Commun **392**(2): 178-182.

Hack, C. E. and S. Zeerleder (2001). "The endothelium in sepsis: source of and a target for inflammation." Crit Care Med **29**(7 Suppl): S21-27.

Hagendoorn, J., et al. (2004). "Endothelial nitric oxide synthase regulates microlymphatic flow via collecting lymphatics." Circ Res **95**(2): 204-209.

Hall, E. and Z. L. Brookes (2005). "Angiopoietin-1 increases arteriolar vasoconstriction to phenylephrine during sepsis." Regul Pept **131**(1-3): 34-37.

Hama, S., et al. (2008). "Nitric oxide attenuates vascular endothelial cadherin-mediated vascular integrity in human chronic inflammation." Clin Exp Immunol **154**(3): 384-390.

Hanley, C. A., et al. (1989). "Suppression of fluid pumping in isolated bovine mesenteric lymphatics by interleukin-1: interaction with prostaglandin E2." Microvasc Res **37**(2): 218-229.

Hansen, T. M., et al. (2010). "Effects of angiopoietins-1 and -2 on the receptor tyrosine kinase Tie2 are differentially regulated at the endothelial cell surface." Cell Signal **22**(3): 527-532.

Hargens, A. R. and B. W. Zweifach (1977). "Contractile stimuli in collecting lymph vessels." Am J Physiol **233**(1): H57-65.

Hauser, B., et al. (2008). "Nitric oxide, leukocytes and microvascular permeability: causality or bystanders?" Crit Care **12**(1): 104.

Hoesel, L. M., et al. (2006). "New insights into cellular mechanisms during sepsis." Immunol Res **34**(2): 133-141.

Hofmann, S., et al. (2002). "The tumour necrosis factor-alpha induced vascular permeability is associated with a reduction of VE-cadherin expression." Eur J Med Res **7**(4): 171-176.

Hong, Y. K. (2013). "Protective role of the lymphatics from sepsis." Blood **122**(13): 2143-2144.

Hranova, M. and Halin, C. (2014). "Lymphatic vessels in inflammation." J Clin Cell Immunol **5**: 250.

Huang, L., et al. (1994). "Platelet-activating factor and endotoxin induce tumour necrosis factor gene expression in rat intestine and liver." Immunology **83**(1): 65-69.

Huang, Y. Q., et al. (2008). "Angiopoietin-1 increases survival and reduces the development of lung edema induced by endotoxin administration in a murine model of acute lung injury." Crit Care Med **36**(1): 262-267.

Hwang, J. A., et al. (2009). "COMP-Ang1 ameliorates leukocyte adhesion and reinforces endothelial tight junctions during endotoxemia." Biochem Biophys Res Commun **381**(4): 592-596.

Ince, C. (2005). "The microcirculation is the motor of sepsis." <u>Crit Care</u> **9 Suppl 4**: S13-19.

Jang, J. Y., et al. (2013). "Conditional ablation of LYVE-1+ cells unveils defensive roles of lymphatic vessels in intestine and lymph nodes." <u>Blood</u> **122**(13): 2151-2161.

Jean-Baptiste, E. (2007). "Cellular mechanisms in sepsis." <u>J Intensive Care Med</u> **22**(2): 63-72.

Johnston, M. G., et al. (1987). "Role of the lymphatic circulatory system in shock." <u>J Burn Care Rehabil</u> **8**(6): 469-474.

Johnston, M. G., et al. (1983). "Effects of arachidonic acid and its cyclo-oxygenase and lipoxygenase products on lymphatic vessel contractility in vitro." <u>Prostaglandins</u> **25**(1): 85-98.

Jurisic, G. and M. Detmar (2009). "Lymphatic endothelium in health and disease." <u>Cell Tissue Res</u> **335**(1): 97-108.

Kajiya, K., et al. (2012). "Promotion of lymphatic integrity by angiopoietin-1/Tie2 signaling during inflammation." <u>Am J Pathol</u> **180**(3): 1273-1282.

Kakei, Y., et al. (2014). "Alteration of cell-cell junctions in cultured human lymphatic endothelial cells with inflammatory cytokine stimulation." <u>Lymphat Res Biol</u> **12**(3): 136-143.

Kalia, N., et al. (1997). "Studies on gastric mucosal microcirculation. 1. The nature of regional variations induced by ethanol injury." <u>Gut</u> **40**(1): 31-35.

Kawai, Y., et al. (2014). "Pivotal roles of lymphatic endothelial cell layers in the permeability to hydrophilic substances through collecting lymph vessel walls: effects of inflammatory cytokines." <u>Lymphat Res Biol</u> **12**(3): 124-135.

Kellum, J. A. and J. M. Decker (1996). "The immune system: relation to sepsis and multiple organ failure." <u>AACN Clin Issues</u> **7**(3): 339-350; quiz 459-360.

Kesler, C. T., et al. (2013). "Lymphatic vessels in health and disease." <u>Wiley Interdiscip Rev Syst Biol Med</u> **5**(1): 111-124.

Kim, I., et al. (2001). "Angiopoietin-1 reduces VEGF-stimulated leukocyte adhesion to endothelial cells by reducing ICAM-1, VCAM-1, and E-selectin expression." <u>Circ Res</u> **89**(6): 477-479.

Kobayashi, H. and P. C. Lin (2005). "Angiopoietin/Tie2 signaling, tumor angiogenesis and inflammatory diseases." <u>Front Biosci</u> **10**: 666-674.

Koller, A., et al. (1999). "Flow reduces the amplitude and increases the frequency of lymphatic vasomotion: role of endothelial prostanoids." <u>Am J Physiol</u> **277**(6 Pt 2): R1683-1689.

Kotsovolis, G. and K. Kallaras (2010). "The role of endothelium and endogenous vasoactive substances in sepsis." Hippokratia **14**(2): 88-93.

Kriehuber, E., et al. (2001). "Isolation and characterization of dermal lymphatic and blood endothelial cells reveal stable and functionally specialized cell lineages." J Exp Med **194**(6): 797-808.

Kumar, P., et al. (2009). "Molecular mechanisms of endothelial hyperpermeability: implications in inflammation." Expert Rev Mol Med **11**: e19.

Kumar, V. and A. Sharma (2008). "Innate immunity in sepsis pathogenesis and its modulation: new immunomodulatory targets revealed." J Chemother **20**(6): 672-683.

Kumar, V. 2008. Innate Immune System in Sepsis Immunopathogenesis and Its Modulation as a Future Therapeutic Approach. In: Khatami, M. ed. Immunopathology, Clinical and Pharmacological Bases. InTech, Available from: http://www.intechopen.com/books/inflammatory-diseases-immunopathology-clinical-and-pharmacological-bases/innate-immune-system-in-sepsis-immunopathogenesis-and-its-modulation-as-future-therapeutic-approach.

Lachance, P. A., et al. (2013). "Lymphatic vascular response to acute inflammation." PLoS One **8**(9): e76078.

Lattuada, M. and G. Hedenstierna (2006). "Abdominal lymph flow in an endotoxin sepsis model: influence of spontaneous breathing and mechanical ventilation." Crit Care Med **34**(11): 2792-2798.

Lauweryns, J. M. and L. Boussauw (1973). "The ultrastructure of lymphatic valves in the adult rabbit lung." Z Zellforsch Mikrosk Anat **143**(2): 149-168.

Leak, L. V., et al. (1995). "Nitric oxide production by lymphatic endothelial cells in vitro." Biochem Biophys Res Commun **217**(1): 96-105.

Lee, S., et al. (2014). "Distinct roles of L- and T-type voltage-dependent Ca2+ channels in regulation of lymphatic vessel contractile activity." J Physiol **592**(Pt 24): 5409-5427.

Legrand, M., et al. (2010). "The response of the host microcirculation to bacterial sepsis: does the pathogen matter?" J Mol Med (Berl) **88**(2): 127-133.

Liao, S., et al. (2011). "Impaired lymphatic contraction associated with immunosuppression." Proc Natl Acad Sci U S A **108**(46): 18784-18789.

Liao, S. and P. Y. von der Weid (2014). "Inflammation-induced lymphangiogenesis and lymphatic dysfunction." Angiogenesis **17**(2): 325-334.

Lobov, G. I. and N. A. Kubyshkina (2004). "Mechanisms underlying the effect of E. coli endotoxin on contractile function of lymphatic vessels." Bull Exp Biol Med **137**(2): 114-116.

London, N. R., et al. (2009). "Endogenous endothelial cell signaling systems maintain vascular stability." Angiogenesis **12**(2): 149-158.

Lucarelli, R. T., et al. (2009). "New approaches to lymphatic imaging." Lymphat Res Biol **7**(4): 205-214.

Lucas, R., et al. (2013). "Arginase 1: an unexpected mediator of pulmonary capillary barrier dysfunction in models of acute lung injury." Front Immunol **4**: 228.

Lynch, P. M., et al. (2007). "The primary valves in the initial lymphatics during inflammation." Lymphat Res Biol **5**(1): 3-10.

Magnotti, L. J., et al. (1998). "Gut-derived mesenteric lymph but not portal blood increases endothelial cell permeability and promotes lung injury after hemorrhagic shock." Ann Surg **228**(4): 518-527.

Mailman, D., et al. (1999). "Time- and surgery-dependent effects of lipopolysaccharide on gut, cardiovascular and nitric oxide functions." Shock **12**(3): 208-214.

Makinen, T., et al. (2001). "Isolated lymphatic endothelial cells transduce growth, survival and migratory signals via the VEGF-C/D receptor VEGFR-3." EMBO J **20**(17): 4762-4773.

Mammoto, T., et al. (2007). "Angiopoietin-1 requires p190 RhoGAP to protect against vascular leakage in vivo." J Biol Chem **282**(33): 23910-23918.

Marshall, J. C. (2008). "Sepsis: rethinking the approach to clinical research." J Leukoc Biol **83**(3): 471-482.

Matsuda, N. and Y. Hattori (2007). "Vascular biology in sepsis: pathophysiological and therapeutic significance of vascular dysfunction." J Smooth Muscle Res **43**(4): 117-137.

McGown, C. C. and Z. L. Brookes (2007). "Beneficial effects of statins on the microcirculation during sepsis: the role of nitric oxide." Br J Anaesth **98**(2): 163-175.

McGown, C. C., et al. (2010). "Beneficial microvascular and anti-inflammatory effects of pravastatin during sepsis involve nitric oxide synthase III." Br J Anaesth **104**(2): 183-190.

McHale, N. G. and K. D. Thornbury (1989). "The effect of anesthetics on lymphatic contractility." Microvasc Res **37**(1): 70-76.

McPherson, D., et al. (2013). "Sepsis-associated mortality in England: an analysis of multiple cause of death data from 2001 to 2010." BMJ Open **3**(8).

Mehta, D. and A. B. Malik (2006). "Signaling mechanisms regulating endothelial permeability." Physiol Rev **86**(1): 279-367.

Michel, C. C. (2004). "Fluid exchange in the microcirculation." J Physiol **557**(Pt 3): 701-702.

Miteva, D. O., et al. (2010). "Transmural flow modulates cell and fluid transport functions of lymphatic endothelium." Circ Res **106**(5): 920-931.

Mizuno, R., et al. (1997). "Myogenic responses of isolated lymphatics: modulation by endothelium." Microcirculation **4**(4): 413-420.

Mizuno, R., et al. (1998). "Regulation of the vasomotor activity of lymph microvessels by nitric oxide and prostaglandins." Am J Physiol **274**(3 Pt 2): R790-796.

Mofarrahi, M., et al. (2008). "Regulation of angiopoietin expression by bacterial lipopolysaccharide." Am J Physiol Lung Cell Mol Physiol **294**(5): L955-963.

Morisada, T., et al. (2005). "Angiopoietin-1 promotes LYVE-1-positive lymphatic vessel formation." Blood **105**(12): 4649-4656.

Munn, L. L. (2015). "Mechanobiology of lymphatic contractions." Semin Cell Dev Biol **38**: 67-74.

Muthuchamy, M., et al. (2003). "Molecular and functional analyses of the contractile apparatus in lymphatic muscle." FASEB J **17**(8): 920-922.

Nathens, A. B. and J. C. Marshall (1996). "Sepsis, SIRS, and MODS: what's in a name?" World J Surg **20**(4): 386-391.

Nawroth, R., et al. (2002). "VE-PTP and VE-cadherin ectodomains interact to facilitate regulation of phosphorylation and cell contacts." EMBO J **21**(18): 4885-4895.

Nemoto, K., et al. (2011). "Mesenteric lymph flow in endotoxemic guinea pigs." Lymphat Res Biol **9**(3): 129-134.

Nencioni, A., et al. (2009). "The microcirculation as a diagnostic and therapeutic target in sepsis." Intern Emerg Med **4**(5): 413-418.

Nottebaum, A. F., et al. (2008). "VE-PTP maintains the endothelial barrier via plakoglobin and becomes dissociated from VE-cadherin by leukocytes and by VEGF." J Exp Med **205**(12): 2929-2945.

Novotny, N. M., et al. (2009). "Angiopoietin-1 in the treatment of ischemia and sepsis." Shock **31**(4): 335-341.

Ohhashi, T., et al. (1980). "Active and passive mechanical characteristics of bovine mesenteric lymphatics." Am J Physiol **239**(1): H88-95.

Ohhashi, T., et al. (1977). "Vasa vasorum within the media of bovine mesenteric lymphatics." Proc Soc Exp Biol Med **154**(4): 582-586.

Ohhashi, T., et al. (2005). "Current topics of physiology and pharmacology in the lymphatic system." Pharmacol Ther **105**(2): 165-188.

Ohhashi, T. and S. Yokoyama (1994). "Nitric oxide and the lymphatic system." Jpn J Physiol **44**(4): 327-342.

Ohki, K., et al. (1999). "Suppressive effects of serum on the LPS-induced production of nitric oxide and TNF-alpha by a macrophage-like cell line, WEHI-3, are dependent on the structure of polysaccharide chains in LPS." Immunol Cell Biol **77**(2): 143-152.

Oliver, G. (2004). "Lymphatic vasculature development." Nat Rev Immunol **4**(1): 35-45.

Ono, N., et al. (2005). "Effective permeability of hydrophilic substances through walls of lymph vessels: roles of endothelial barrier." Am J Physiol Heart Circ Physiol **289**(4): H1676-1682.

Pegu, A., et al. (2008). "Human lymphatic endothelial cells express multiple functional TLRs." J Immunol **180**(5): 3399-3405.

Pepper, M. S. and M. Skobe (2003). "Lymphatic endothelium: morphological, molecular and functional properties." J Cell Biol **163**(2): 209-213.

Peters, K., et al. (2003). "Molecular basis of endothelial dysfunction in sepsis." Cardiovasc Res **60**(1): 49-57.

Pinheiro da Silva, F. and V. Nizet (2009). "Cell death during sepsis: integration of disintegration in the inflammatory response to overwhelming infection." Apoptosis **14**(4): 509-521.

Plaku, K. J. and P. Y. von der Weid (2006). "Mast cell degranulation alters lymphatic contractile activity through action of histamine." Microcirculation **13**(3): 219-227.

Predescu, D., et al. (2005). "Constitutive eNOS-derived nitric oxide is a determinant of endothelial junctional integrity." Am J Physiol Lung Cell Mol Physiol **289**(3): L371-381.

Reeves, K. J., et al. (2012). "Evaluation of fluorescent plasma markers for in vivo microscopy of the microcirculation." J Vasc Res **49**(2): 132-143.

Rehal, S., et al. (2009). "Characterization of biosynthesis and modes of action of prostaglandin E2 and prostacyclin in guinea pig mesenteric lymphatic vessels." Br J Pharmacol **158**(8): 1961-1970.

Rehal, S. and P. Y. von der Weid (2015). "Experimental ileitis alters prostaglandin biosynthesis in mesenteric lymphatic and blood vessels." Prostaglandins Other Lipid Mediat **116-117**: 37-48.

Remick, D. G. (1995). "Applied molecular biology of sepsis." J Crit Care **10**(4): 198-212.

Remick, D. G. (2007). "Pathophysiology of sepsis." <u>Am J Pathol</u> **170**(5): 1435-1444.

Riedemann, N. C., et al. (2003). "The enigma of sepsis." <u>J Clin Invest</u> **112**(4): 460-467.

Rittirsch, D., et al. (2008). "Harmful molecular mechanisms in sepsis." <u>Nat Rev Immunol</u> **8**(10): 776-787.

Rittirsch, D., et al. (2007). "The disconnect between animal models of sepsis and human sepsis." <u>J Leukoc Biol</u> **81**(1): 137-143.

Robertson, D. A., et al. (2004). "Expression of inducible nitric oxide synthase in cultured smooth muscle cells from rat mesenteric lymphatic vessels." <u>Microcirculation</u> **11**(6): 503-515.

Roger, T., et al. (2009). "Protection from lethal gram-negative bacterial sepsis by targeting Toll-like receptor 4." <u>Proc Natl Acad Sci U S A</u> **106**(7): 2348-2352.

Saban, M. R., et al. (2004). "Visualization of lymphatic vessels through NF-kappaB activity." <u>Blood</u> **104**(10): 3228-3230.

Saharinen, P., et al. (2008). "Angiopoietins assemble distinct Tie2 signalling complexes in endothelial cell-cell and cell-matrix contacts." <u>Nat Cell Biol</u> **10**(5): 527-537.

Sawa, Y., et al. (2007). "Effects of TNF-alpha on leukocyte adhesion molecule expressions in cultured human lymphatic endothelium." <u>J Histochem Cytochem</u> **55**(7): 721-733.

Sawa, Y. and E. Tsuruga (2008). "The expression of E-selectin and chemokines in the cultured human lymphatic endothelium with lipopolysaccharides." <u>J Anat</u> **212**(5): 654-663.

Sawa, Y., et al. (2008). "LPS-induced IL-6, IL-8, VCAM-1, and ICAM-1 expression in human lymphatic endothelium." <u>J Histochem Cytochem</u> **56**(2): 97-109.

Scallan, J. P. and M. J. Davis (2013). "Genetic removal of basal nitric oxide enhances contractile activity in isolated murine collecting lymphatic vessels." <u>J Physiol</u> **591**(Pt 8): 2139-2156.

Scallan, J. P. and V. H. Huxley (2010). "In vivo determination of collecting lymphatic vessel permeability to albumin: a role for lymphatics in exchange." <u>J Physiol</u> **588**(Pt 1): 243-254.

Scallan, J. P., et al. (2012). "Independent and interactive effects of preload and afterload on the pump function of the isolated lymphangion." <u>Am J Physiol Heart Circ Physiol</u> **303**(7): H809-824.

Schmid-Schonbein, G. W. (1990). "Microlymphatics and lymph flow." <u>Physiol Rev</u> **70**(4): 987-1028.

Schmidt, H., et al. (1996). "Effect of endotoxemia on intestinal villus microcirculation in rats." J Surg Res **61**(2): 521-526.

Schmidt, W., et al. (1998). "Influence of N-acetylcysteine treatment on endotoxin-induced microcirculatory disturbances." Intensive Care Med **24**(9): 967-972.

Schouten, M., et al. (2008). "Inflammation, endothelium, and coagulation in sepsis." J Leukoc Biol **83**(3): 536-545.

Schulte, W., et al. (2013). "Cytokines in sepsis: potent immunoregulators and potential therapeutic targets--an updated view." Mediators Inflamm **2013**: 165974.

Shields, J. D. (2011). "Lymphatics: at the interface of immunity, tolerance, and tumor metastasis." Microcirculation **18**(7): 517-531.

Shimaoka, M. and E. J. Park (2008). "Advances in understanding sepsis." Eur J Anaesthesiol Suppl **42**: 146-153.

Shirasawa, Y., et al. (2000). "Physiological roles of endogenous nitric oxide in lymphatic pump activity of rat mesentery in vivo." Am J Physiol Gastrointest Liver Physiol **278**(4): G551-556.

Silva, E., et al. (2008). "Sepsis: from bench to bedside." Clinics (Sao Paulo) **63**(1): 109-120.

Simoes, D. C., et al. (2008). "Angiopoietin-1 protects against airway inflammation and hyperreactivity in asthma." Am J Respir Crit Care Med **177**(12): 1314-1321.

Spanos, A., et al. (2010). "Early microvascular changes in sepsis and severe sepsis." Shock **33**(4): 387-391.

Sriskandan, S. and D. M. Altmann (2008). "The immunology of sepsis." J Pathol **214**(2): 211-223.

Steyers, C. M., 3rd and F. J. Miller, Jr. (2014). "Endothelial dysfunction in chronic inflammatory diseases." Int J Mol Sci **15**(7): 11324-11349.

Stücker, O., et al. (2008). "Towards a better understanding of lymph circulation." Phlebolymphology 15 (1): 31-36.

Swartz, M. A. (2001). "The physiology of the lymphatic system." Adv Drug Deliv Rev **50**(1-2): 3-20.

Tammela, T. and K. Alitalo (2010). "Lymphangiogenesis: Molecular mechanisms and future promise." Cell **140**(4): 460-476.

Tammela, T., et al. (2005). "Angiopoietin-1 promotes lymphatic sprouting and hyperplasia." Blood **105**(12): 4642-4648.

Thurston, G. (2003). "Role of Angiopoietins and Tie receptor tyrosine kinases in angiogenesis and lymphangiogenesis." Cell Tissue Res **314**(1): 61-68.

Thurston, G., et al. (2000). "Angiopoietin-1 protects the adult vasculature against plasma leakage." Nat Med **6**(4): 460-463.

Thurston, G., et al. (1999). "Leakage-resistant blood vessels in mice transgenically overexpressing angiopoietin-1." Science **286**(5449): 2511-2514.

Thurston, G., et al. (2005). "Angiopoietin 1 causes vessel enlargement, without angiogenic sprouting, during a critical developmental period." Development **132**(14): 3317-3326.

Tidswell, M., et al. (2010). "Phase 2 trial of eritoran tetrasodium (E5564), a toll-like receptor 4 antagonist, in patients with severe sepsis." Crit Care Med **38**(1): 72-83.

Triantafilou, M. and K. Triantafilou (2004). "Sepsis: molecular mechanisms underlying lipopolysaccharide recognition." Expert Rev Mol Med **6**(4): 1-18.

Trzewik, J., et al. (2001). "Evidence for a second valve system in lymphatics: endothelial microvalves." FASEB J **15**(10): 1711-1717.

Tsunemoto, H., et al. (2003). "Flow-mediated release of nitric oxide from lymphatic endothelial cells of pressurized canine thoracic duct." Jpn J Physiol **53**(3): 157-163.

Ulloa, L., et al. (2009). "Scientific and clinical challenges in sepsis." Curr Pharm Des **15**(16): 1918-1935.

Umarova, B. A., et al. (2006). "The role of protective effects of proline-containing peptides (PGP, PG, and GP) in contractile dysfunction of mesenteric lymphatic vessels in rats with experimental acute peritonitis." Bull Exp Biol Med **142**(3): 279-282.

van der Poll, T. and S. M. Opal (2008). "Host-pathogen interactions in sepsis." Lancet Infect Dis **8**(1): 32-43.

Vandenbroucke, E., et al. (2008). "Regulation of endothelial junctional permeability." Ann N Y Acad Sci **1123**: 134-145.

Vincent, J. L. and D. De Backer (2005). "Microvascular dysfunction as a cause of organ dysfunction in severe sepsis." Crit Care **9 Suppl 4**: S9-12.

von der Weid, P. Y. (1998). "ATP-sensitive K+ channels in smooth muscle cells of guinea-pig mesenteric lymphatics: role in nitric oxide and beta-adrenoceptor agonist-induced hyperpolarizations." Br J Pharmacol **125**(1): 17-22.

von der Weid, P. Y. (2001). "Review article: lymphatic vessel pumping and inflammation--the role of spontaneous constrictions and underlying electrical pacemaker potentials." Aliment Pharmacol Ther **15**(8): 1115-1129.

von der Weid, P. Y., et al. (1996). "Endothelium-dependent modulation of pacemaking in lymphatic vessels of the guinea-pig mesentery." J Physiol **493 (Pt 2)**: 563-575.

von der Weid, P. Y., et al. (2014). "Electrophysiological properties of rat mesenteric lymphatic vessels and their regulation by stretch." Lymphat Res Biol **12**(2): 66-75.

von der Weid, P. Y. and M. Muthuchamy (2010). "Regulatory mechanisms in lymphatic vessel contraction under normal and inflammatory conditions." Pathophysiology **17**(4): 263-276.

von der Weid, P. Y. and D. C. Zawieja (2004). "Lymphatic smooth muscle: the motor unit of lymph drainage." Int J Biochem Cell Biol **36**(7): 1147-1153.

von der Weid, P. Y., et al. (2001). "Nitric oxide decreases pacemaker activity in lymphatic vessels of guinea pig mesentery." Am J Physiol Heart Circ Physiol **280**(6): H2707-2716.

Walther, A., et al. (2003). "Role of nitric oxide in leukocyte-independent endothelial damage during experimental endotoxemia." Shock **20**(3): 286-291.

Wang, Y. and G. Oliver (2010). "Current views on the function of the lymphatic vasculature in health and disease." Genes Dev **24**(19): 2115-2126.

Wang, Y. Q., et al. (2014). "Effects of angiopoietin-1 on inflammatory injury in endothelial progenitor cells and blood vessels." Curr Gene Ther **14**(2): 128-135.

Weber, G. F. and F. K. Swirski (2014). "Immunopathogenesis of abdominal sepsis." Langenbecks Arch Surg **399**(1): 1-9.

Wigle, J. T. and G. Oliver (1999). "Prox1 function is required for the development of the murine lymphatic system." Cell **98**(6): 769-778.

Witte, C.L. and Witte, M.H. 1985. Lymphatics in pathophysiology of edema. In: Johnston, M.G. ed. Experimental biology of the lymphatic curculation. Amsterdam: Elsevier Science Publishers B.V., pp.167.

Witzenbichler, B., et al. (2005). "Protective role of angiopoietin-1 in endotoxic shock." Circulation **111**(1): 97-105.

Wu, T. F., et al. (2006). "Contractile activity of lymphatic vessels is altered in the TNBS model of guinea pig ileitis." Am J Physiol Gastrointest Liver Physiol **291**(4): G566-574.

Wu, T. F., et al. (2005). "Lymphatic vessel contractile activity and intestinal inflammation." Mem Inst Oswaldo Cruz **100 Suppl 1**: 107-110.

Wu, X. and N. Liu (2010). "The role of Ang/Tie signaling in lymphangiogenesis." Lymphology **43**(2): 59-72.

Xu, J., et al. (2012). "Angiopoietins regulate vascular reactivity after haemorrhagic shock in rats through the Tie2-nitric oxide pathway." Cardiovasc Res **96**(2): 308-319.

Yamashita, T., et al. (2000). "Mechanisms of reduced nitric oxide/cGMP-mediated vasorelaxation in transgenic mice overexpressing endothelial nitric oxide synthase." Hypertension **36**(1): 97-102.

Yang, D., et al. (2009). "Alarmins link neutrophils and dendritic cells." Trends Immunol **30**(11): 531-537.

Ye, L., et al. (2007). "Angiopoietin-1 for myocardial angiogenesis: a comparison between delivery strategies." Eur J Heart Fail **9**(5): 458-465.

Yokoyama, S. and T. Ohhashi (1993). "Effects of acetylcholine on spontaneous contractions in isolated bovine mesenteric lymphatics." Am J Physiol **264**(5 Pt 2): H1460-1464.

Zawieja, D. (2005). "Lymphatic biology and the microcirculation: past, present and future." Microcirculation **12**(1): 141-150.

Zawieja, D. C. (2009). "Contractile physiology of lymphatics." Lymphat Res Biol **7**(2): 87-96.

Zawieja, D. C., et al. (1993). "Distribution, propagation, and coordination of contractile activity in lymphatics." Am J Physiol **264**(4 Pt 2): H1283-1291.

Zhang, H., et al. (2009). "Role of TNF-alpha in vascular dysfunction." Clin Sci (Lond) **116**(3): 219-230.

Zhang, J. L., et al. (1997). "Inhibitory effects of fluorescein isothiocyanate photoactivation on lymphatic pump activity." Microvasc Res **54**(2): 99-107.

Zweifach, B. W. (1948). "Microscopic observations of circulation in rat mesoappendix and dog omentum; use in study of vasotropic substances." Methods Med Res **1**: 131-139.